

1933

Phylogenetic Implications of Tetrasporangial Ultrastructure in Coralline Red Algae with Reference to *Bossiella orbigniana* (Corallinales, Rhodophyta)

Christina Wilson
College of William & Mary - Arts & Sciences

Follow this and additional works at: <https://scholarworks.wm.edu/etd>



Recommended Citation

Wilson, Christina, "Phylogenetic Implications of Tetrasporangial Ultrastructure in Coralline Red Algae with Reference to *Bossiella orbigniana* (Corallinales, Rhodophyta)" (1933). *Dissertations, Theses, and Masters Projects*. Paper 1539624407.

<https://dx.doi.org/doi:10.21220/s2-pbyj-r021>

This Thesis is brought to you for free and open access by the Theses, Dissertations, & Master Projects at W&M ScholarWorks. It has been accepted for inclusion in Dissertations, Theses, and Masters Projects by an authorized administrator of W&M ScholarWorks. For more information, please contact scholarworks@wm.edu.

PHYLOGENETIC IMPLICATIONS OF TETRASPORANGIAL
ULTRASTRUCTURE IN CORALLINE RED ALGAE
WITH REFERENCE TO BOSSIELLA ORBIGNIANA
(CORALLINALES, RHODOPHYTA)

A Thesis
Presented to
The Faculty of the Department of Biology
The College of William and Mary in Virginia

In Partial Fulfillment
Of Requirements for the Degree of
Master of Arts

by
Christina Wilson
1993

APPROVAL SHEET

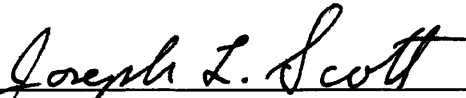
This Thesis is submitted in partial fulfillment of
the requirements for the degree of

Master of Arts

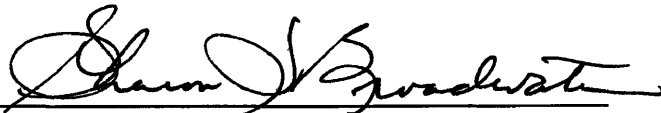


Christina Wilson

Approved, July 1993



Joseph L. Scott



Sharon T. Broadwater



Stanton F. Hoegerman

DEDICATION

For Sheila and Wesley Wilson

TABLE OF CONTENTS

	Page
ACKNOWLEDGEMENTS.....	v
LIST OF TABLES AND DIAGRAMS.....	vi
LIST OF FIGURES.....	vii
ABSTRACT.....	ix
INTRODUCTION.....	2
MATERIALS AND METHODS.....	9
RESULTS.....	11
DISCUSSION.....	27
APPENDIX.....	48
BIBLIOGRAPHY.....	51
TABLES AND DIAGRAMS.....	56
KEY TO ABBREVIATIONS.....	62
FIGURES.....	63
VITA.....	102

ACKNOWLEDGEMENTS

The author wishes to acknowledge the following group of individuals for their special contributions to this study. Dr. Joseph L. Scott introduced me to the world of coralline red algae. As my primary mentor, he patiently guided me through the technical and theoretical aspects of the project. Dr. Sharon T. Broadwater and Dr. Stanton F. Hoegerman both played crucial roles in the preparation of the final manuscript. Finally, this study could not have been completed without the expert technical assistance of William Saunders and Jewel Thomas.

LIST OF TABLES AND DIAGRAMS

FIGURE	PAGE
1. Summary of coralline taxonomic schemes.....	56
2. Tetrasporogenesis in <u>Bossiella orbigniana</u>	57
3. Survey summary.....	58
4. Coralline classification <i>sensu</i> Cabioch.....	59
5. Coralline tetrasporangial nuclear development.	60

LIST OF FIGURES

Figure		Page
1.	SEM of conceptacle-bearing intergenicula in <u>Bossiella orbigniana</u>	63
2-3.	SEM of longitudinal sections through <u>Bossiella</u> tetrasporangial conceptacles..	63
4.	DAPI stained tetrasporocyte.....	64
5-6.	DAPI stained stage 4 tetrasporangium....	64
7.	DAPI stained tetrasporangial conceptacle	65
8.	Toluidine blue stained tetrasporangial conceptacle.....	65
9.	DAPI stained stage 3 tetrasporangium....	65
10.	Toluidine blue stained stage 3 tetrasporangium.....	65
11-13.	PAS stained tetrasporangia.....	66
14-15.	PAS/Toluidine blue stained tetrasporangium.....	67
16-19.	Early stage 1 tetrasporocyte.....	68
20-23.	Stage 1 tetrasporocyte exhibiting elongation.....	69
24-30.	Details of late stage 1 pre-meiotic tetrasporocytes.....	70-71
31-32.	Stage 2 meiotic nuclei.....	72
33-36.	Details of early cleavage furrow formation during stage 2.....	73
37.	Stage 3 vacuolate tetrasporangia.....	74
38-39.	Localization of cleavage furrows-stage 3	74

40-44.	Stage 3 vacuolate nuclei	75-76
45.	Starch-flanked stage 3 vacuoles.....	76
46.	Stage 3 chloroplast division.....	76
47-49.	Stage 3 mucilage secretion.....	77
50-56.	Stage 3 post-vacuolate tetrasporangia...	78-81
57-68.	Stage 3 post-vacuolate tetrasporangia showing EDM dispersal.....	82-84
69-77.	Stage 4 fully cleaved tetrasporangia....	85-87
78.	Bisporangial conceptacle.....	88
79-82.	Stage 3 vacuolate bisporangia.....	89
83-87.	Stage 3 post-vacuolate bisporangia....	90
88-89.	Stage 4 bisporangial nucleus.....	91
90-92.	<u>Amphiroa</u>	92
93-95.	<u>Lithothrix</u>	93
96-97.	<u>Titanoderma</u>	94
98-102.	<u>Fosliella</u>	95-102
103-105.	<u>Metamastophora</u>	97
106-108.	<u>Haliptilon</u>	98
109-112.	<u>Jania</u>	99
113-116.	<u>Corallina</u>	100
117.	<u>Calliarthron</u>	101
118.	<u>Bossiella</u>	101

ABSTRACT

The red algal order Corallinales is most commonly divided into seven subfamilies primarily on the basis of the presence or absence of genicula (articulations). This classification scheme has been criticized as phenetic rather than phylogenetic. Ultrastructural details of tetrasporogenesis documented in this study further challenge this dichotomy.

Previous ultrastructural studies noted distinct perinuclear patterns in tetrasporangia of the coralline red algal genera Corallina, Jania, and Halitilon (Peel et al 1973, Duckett and Peel 1978, Vesik and Borowitzka 1984). Each investigation documented various stages of a single pattern of perinuclear ER (PER) with an associated electron-dense material (EDM). This pattern is believed to be unique to the order Corallinales.

The present study was conducted with two primary objectives. First, a detailed ultrastructural account of tetrasporogenesis in Bossiella orbigniana was completed. This work not only documented a previously undescribed PER/EDM pattern in a coralline alga, but also established the developmental framework for the second aspect of the study. Three non-geniculate and seven geniculate genera were surveyed to examine the extent of PER/EDM associations in coralline algae. A cursory phylogenetic analysis suggests that the classification of coralline red algae, with an emphasis on the presence or absence of genicula as a primary defining feature, may not be correct.

PHYLOGENETIC IMPLICATIONS OF TETRASPORANGIAL
ULTRASTRUCTURE IN CORALLINE RED ALGAE
WITH REFERENCE TO BOSSIELLA ORBIGNIANA
(CORALLINALES, RHODOPHYTA)

INTRODUCTION

The algal phylum Rhodophyta consists of a single class of organisms which range in structural complexity from unicells through psuedoparenchymatous upright thalli (Gabrielson *et al* 1991). The Rhodophyta are distinguished from other phyla of photosynthetic eukaryotes by the presence of chloroplasts with single, unstacked thylakoids, phycobilin pigments attached to thylakoids as phycobilisomes, floridean starch, and by a lack of flagellated structures at any life history stage (Gabrielson *et al* 1985; Gabrielson and Garbary 1986, 1987; Gabrielson *et al* 1991). Traditionally, taxonomists recognized two classes of red algae. The Bangiophyceae, considered the most primitive of the red algae, have been shown to lack shared, derived characteristics (synapormorphies) (Gabrielson *et al* 1985, Garbary and Gabrielson 1990). The Florideophyceae, which consisted of the more morphologically advanced red algae, were, in contrast, united by at least two synapormorphic reproductive features (Gabrielson *et al* 1991). Although, arguably, neither represents a valid taxonomic epithet, the terms "bangiophyte" and "florideophyte" continue to pervade systematic discussions of "primitive" and "advanced" red algal forms, respectively.

Taxonomic schemes elucidating ordinal relationships

within the Rhodophyta have been proposed, but none has been unanimously accepted (Garbary and Gabrielson 1990, Gabrielson *et al* 1991). The first ordinal classification schemes were principally derived from light microscopic studies on pre- and post-fertilization changes associated with female reproductive anatomy. Ongoing taxonomic revisions have stemmed from a new suite of traits revealed largely at the ultrastructural level. New knowledge of variations in the mitotic process, distinct organelle associations, and the fine structure of pit connections (unique regions of cytoplasmic continuity between cells) prompted a reevaluation of existing ordinal classification (Gabrielson and Garbary 1986). While molecular biology will undoubtedly generate further reevaluations of red algal systematics, morphological details of reproductive anatomy will likely continue to yield important classification information.

Sporangia and spores can be considered evolutionarily conserved within the phylum Rhodophyta. Spores of various types are found in every rhodophycean order (Guiry 1990). Important features which serve to distinguish sporangia/spores include the number of nuclei in each spore, the number and arrangement of spores in a given sporangium, the position of a sporangium on the thallus, the presence or absence of a generative mother cell and the role of the spore in the algal life history. Of primary importance is the presence or absence of meiosis (Guiry 1978). Mitospores germinate to form

thalli of the same ploidy level as the parent organism, while meiospores give rise to the gametophytic generation (Guiry 1978). More primitive spore types are likely non-meiotic and include endosporangia, monosporangia, conchosporangia, and zygotosporangia. Tetrasporangia, unique to marine forms of advanced red algal genera, typically arise on diploid thalli and represent the principal though not exclusive sites of meiosis in the Rhodophyta (Guiry 1978, 1990; Guiry and Irvine 1989). Tetraspores chiefly give rise to the haploid gametophyte generation, though in a few genera they have been shown to regenerate the diploid tetrasporophyte, indicating an apparent absence of meiosis.

Features of developing tetraspores have proved important in the revision of red algal taxonomy. There are two examples of rhodophytan families elevated to ordinal rank based on details of tetrasporogenesis. The first example involves the nature of the sporangium connection with the subtending stalk cell and the second, from the mechanism of sporangium cleavage.

The process of tetrasporogenesis may commence with the formation of a tetrasporangial stalk cell, sometimes also referred to as a tetrasporangial mother cell (TMC), which can generate one to many sporangia and sometimes also successive sporangia, depending on the organism (Guiry 1978). In Palmaria palmata, the stalk cell is formed within the sporangium wall. This feature led Guiry and Irvine (1978) to

propose the elevation of the family Palmariaceae to ordinal rank.

The Corallinales is a monophyletic taxon consisting of the single family Corallinaceae. This morphologically distinguished group of organisms, once classified as animals, currently comprises one of the best defined rhodophytan orders (Johansen 1981, Woelkerling 1988). The nature and timing of tetrasporangial cleavage proved important in defining the order Corallinales.

Three tetrasporiangial cleavage patterns have been demonstrated within the Rhodophyta (Guiry 1978, 1990). Cruciate division is found in all orders bearing tetrasporangia and is considered the most primitive cleavage pattern. Tetrahedral and zonate cleavage patterns are believed to be derived from the cruciate condition (Searles 1968). Cleavage initiation may be successive or simultaneous (Guiry 1978). The Corallinales is the only red algal order which exhibits simultaneous zonate cleavage of tetrasporangia (Guiry 1990). This feature, combined with the presence of both apical and intercalary meristems, pit connections with two-layered caps lacking cap membranes, and the deposition of calcite in cell walls, led Silva and Johansen (1986) to posit a separate order for the corallines, removing them from their previous inclusion in the Cryptonemiales.

Infraordinal classification of Corallinales, however, remains less clear. Diagnostic features relevant to

infraordinal classification have included the presence or absence and organization of genicula (specialized, non-calcified articulations), morphology of reproductive conceptacles, spore germination patterns, and the presence or absence of lateral cell fusions and secondary pit connections (Chamberlain 1978, Silva and Johansen 1986).

Taxonomists are divided over the degree of emphasis to be placed on thallus organization as a diagnostic feature (Gabrielson *et al* 1991). Two taxonomic schemes have resulted from the debate. The first scheme promotes the separation of the Corallinaceae into six subfamilies based primarily on the presence or absence of genicula (Table 1). Some investigators argue that genicula unequivocally distinguish articulated coralline growth forms from non-geniculate varieties (Adey and Johansen 1972, Johansen 1969, 1972, 1976, 1981). An alternative scheme, put forth by Cabioch (1971 a,b, 1972) suggests that separation based on genicula alone is invalid. With an emphasis on the presence of intercellular fusions and certain reproductive structures, Cabioch places select geniculate and non-geniculate growth forms in the same subfamily (Table 1). The issue remains unresolved and neither scheme has gained exclusive acceptance. This comparative study of tetrasporogenesis was initiated to help resolve the coralline dispute.

The developmental stages of tetrasporogenesis in coralline red algae are summarized by Johansen (1981). First,

sporangial initials divide to produce a young tetrasporocyte cell (TC) and a subtending tetrasporangial mother cell (TMC). The TC undergoes a period of elongation and maturation, prior to meiosis. Meiotic division is followed by positioning of resulting nuclei in the sporangium. Cytokinesis marks the final steps in sporangial maturation. The accumulation of cytoplasmic reserves may occur throughout sporangium development. Aspects of this generalized process are conserved in all red algal orders which undergo tetrasporogenesis. Features that may vary are the following: the presence of small vacuoles in youngest tetrasporocytes, the position of the pre-meiotic nucleus, the nature and timing of tetrasporangial initial/tetrasporocyte cell wall formation, the fine structure of nucleus associations, the nature and mechanism of starch deposition, and the mechanism and timing of cytokinesis.

Tetrasporogenesis was previously studied in two coralline genera, Corallina officinalis (Peel et al 1973) and Haliptilon cuvierii (Vesk and Borowitzka 1984). Peel et al (1973) focused primarily on the ultrastructure of post-meiotic nuclei, whereas Vesk and Borowitzka (1984) presented the only thorough documentation of tetrasporogenesis in a coralline genus. Both studies note elaborate organization of perinuclear endoplasmic reticulum (PER) and an associated electron dense material (EDM). These patterns are believed to be unique to coralline red algae.

The present study provides detailed ultrastructural documentation of tetrasporogenesis for a third coralline genus, Bossiella orbigniana. An additional unique pattern of PER and associated EDM is described and analyzed with light microscopic cytochemistry. Also, a comparative survey of post-meiotic tetraspore nuclei of select geniculate and non-geniculate genera is compiled and discussed in terms of the current coralline taxonomic schemes.

MATERIALS AND METHODS

Electron Microscopy

Bisporangial/tetrasporangial specimens of Bossiella orbigniana (Decaisne) Silva ssp. orbigniana (Corallinoideae) were collected from Laguna Beach, California, in the rocky lower intertidal-upper subtidal regions at mid-morning on November 13, 1992. Genera examined in the survey study were collected from the same site in March 1990, with the exception of epiphytic specimens of Fosliella, collected from Thalassia beds at a depth of 1 m, at mid-morning in Discovery Bay, Jamaica in June 1993, Metamastophora sp., obtained and fixed by Richard Wetherbee at the Univeristy of Melbourne in Australia in October 1990 and Titanoderma sp., from Cape Charles, VA. Conceptacle-bearing thalli were fixed in the field for 3 h on ice in 4% glutaraldehyde in 0.1 M phosphate buffer with 0.25 M sucrose and 2.5% EDTA at pH 6.8. Specimens were rinsed and stored for 12 h on ice in 2.5% EDTA, post-fixed in 1% OsO₄ in 0.05M phosphate buffer and 0.25M sucrose with 2.5% EDTA, briefly rinsed in the same buffer followed by a 30 min rinse in 50% acetone and 9 h in 70% methanol with 2% uranyl acetate. Samples were dehydrated in an ascending series of 30 min acetone washes and infiltrated with Embed 812. Serial sections were cut on an RMC MT 6000X

ultramicrotome, stained with lead citrate, and viewed on a Zeiss EM 109 transmission electron microscope.

Light and Fluorescence Microscopy

Conceptacle-bearing intergenicula fixed in glutaraldehyde as described above were stored at 4 C in 0.05M phosphate buffer with 0.25 M sucrose and 2.5% EDTA. Dehydration was carried out in a graded series of 30-45 min ethanol rinses. Samples were infiltrated in LKB Histo-resin, and 3 um thick sections were cut with glass knives using a Sorvall JB-4 microtome.

Cytochemical techniques applied to determine the nature of PER-EDM included the DNA/RNA specific stains methyl Green/pyronin Y and azure B. Stains were applied to Histo-resin-embedded tissue sections treated with RNase (Coleman 1978, Goff and Coleman 1984, 1990) or with 1 N HCl, and to control sections incubated in a variety of buffer solutions, over a pH and temperature range. PAS and PAS/toluidine blue were used to determine polysaccharide content of developing sporangia. The DNA fluorochrome 4'-6 diamidino-2-phenolindole (DAPI) (Coleman 1978, Goff and Coleman 1984, 1990) was applied directly to embedded tissue sections and viewed with an Olympus BH-2 microscope equipped with a high pressure mercury vapor lamp (HBO, 100W). All staining protocols are presented in the Appendix.

RESULTS

This study addresses tetrasporogenesis in coralline red algae with two primary objectives. First, a detailed documentation of tetrasporangial development in Bossiella orbigniana is presented. The developmental sequence established for Bossiella provides the framework for a subsequent comparative analysis of tetrasporangial nuclei in several coralline algal genera. Tetrasporogenesis in Bossiella and the results of the survey are thus presented under separate subheadings.

Tetrasporogenesis

Tetrasporangial conceptacles of Bossiella orbigniana ssp. orbigniana originate in cortical tissue of subterminal intergenicula. Two to four conceptacles typically form on a single intergenicular surface (Figs. 1-3) (Johansen 1971). Conceptacles examined were either exclusively tetrasporangial or bisporangial. Although bisporangial conceptacles are reported to outnumber tetrasporangial conceptacles in B. orbigniana (Johansen 1971), only one bisporangial specimen was observed in this study (Fig. 78).

The four discrete stages of tetrasporogenesis presented incorporate aspects of sequences proposed in previous studies (Kugrens and West 1972, Scott and Dixon 1973, Vesik and Borowitzka 1984), with modification based on personal observations (Table 2). The scheme is based on the meiotic

status of the sporangium along with the accumulation of perinuclear electron dense material (EDM) and starch, the initiation, arrest, and completion of cytokinesis, and the overall secretory activity of the developing sporangium. Stage 1 encompasses pre-meiotic sporangial development. Stage 2 delimits meiosis. Stage 3 post-meiotic tetrasporangia exhibit two primary phases of development, which can be summarized as vacuolate and non-vacuolate. Mature tetrasporangia complete cleavage in stage 4. For the sake of clarity, the term tetraspore mother cell (TMC) will denote the stalk cell, whereas tetrasporocyte (TC) will specify the pre-meiotic tetrasporangium (TS).

Light and Fluorescence Microscopy

DAPI treated tetrasporangia stain differently, depending on developmental stage (Fig. 4). Oddly, DAPI, which is reported to intercalate between A-T base pairs of double stranded DNA (Coleman 1978, Goff and Coleman 1990), binds strongly to nucleoli at all developmental stages (Figs. 6, 8, 10).

Young plastids in the earliest tetrasporocytes occupy the cell periphery and are visible in DAPI preparations as a lightly staining ring adjacent to the plasmalemma (Fig. 8). Chloroplasts are interspersed throughout the cytoplasm of the fully cleaved tetrasporangium. These mature plastids stain more intensely with DAPI than the young plastids (Compare Figs. 8 and 9-10). The chromatin in the fully cleaved

sporangium is diffuse within the nucleus and the small nucleoli lack "vacuolate" regions often seen in young or pre-meiotic tetrasporocytes (Fig. 10).

Attempts to cytochemically determine the nature of the perinuclear electron dense material (EDM) observed in some coralline algae yielded inconclusive results. RNase treatments failed to consistently reduce subsequent staining with the nucleic acid-specific stains, methyl green-pyronin Y and azure B. Although the staining affinity of the perinuclear zone was consistently reduced following acid hydrolysis, non-specific staining remained high. Attempts to vary pH within the range of RNA staining failed to reduce this problem satisfactorily.

Golgi derived cytoplasmic inclusions accumulate in Bossiella during two separate secretory phases, documented extensively in the EM portion of this study. The first resulting vesicle type is faintly electron dense, associates in clusters in the cytoplasm, and likely contributes to muclilage formation (Figs. 47-49). The second vesicle type forms aggregations flanked by starch grains, is strongly electron dense and persists in fully cleaved tetrasporangia (Figs. 51-53, 55, 59, 68, 70, 72-73, 75). Starch grains give the strongest positive result with PAS of any inclusion in Bossiella tetrasporangia (Figs. 11-13). The accumulation of starch can be followed through sporangial development, by comparing the relative staining of sporangia within a given

conceptacle (Figs. 12, 15). The second vesicle type stains less strongly than starch with the PAS reaction (Figs. 11-13), indicating that the contents may not be exclusively polysaccharide in nature (Fig. 13). PAS counterstained with toluidine blue shows perinuclear-EDM (Figs. 14, 15).

Electron Microscopy

Stage 1

Development of the tetrasporocyte (TC) involves elongation, progressive vacuolation, the beginning of starch accumulation, and TC wall formation. Prior to meiosis, a perinuclear RER membrane system and associated EDM begin to accumulate. Figures 16, 20, and 24 depict tetrasporocytes undergoing stage 1 pre-meiotic development.

The youngest tetrasporocytes are distinguished by a single, large tonoplast-delimited vacuole, most often located in the apical region of the cell (not shown). A single, large vacuole is also occasionally seen in stalk cells attached to young tetrasporocytes (Fig. 20).

Organelles such as Golgi and mitochondria, rare in the youngest tetrasporocytes, increase in number during elongation. Small Golgi with flat, straight cisternae appear during stage 1 (Fig. 26) and persist through meiosis. The mitochondrion-Golgi association, typical of nearly all red algae, is not always present in the tetrasporocyte (Figs. 16, 25). Interestingly, the mitochondrion-Golgi association is absent in the stalk cell during all developmental stages

(Figs. 18-19, 58). Stalk cell Golgi are usually organized in pairs, with an ER tract running between them (Figs. 19, 58, 60).

The maturing tetrasporocyte progressively accumulates smaller vacuoles (Figs. 16, 20, 24). The vacuolate condition of the cytoplasm becomes most pronounced immediately prior to meiosis (Fig. 24). Small starch grains at the vacuolar periphery (Figs. 24, 27, 30) distinguish these late stage 1 vacuoles from earlier Stage 1 vacuoles (Figs. 16, 20). The late stage 1 vacuoles frequently contain reticulate membranous material with electron dense regions (Fig. 30). Large, moderately-electron dense globular accumulations may be present in the cytoplasm beginning at the time of vacuolar accumulation (Figs. 16, 20, 23). This material, apparently characteristic of Stage 1 development, does not appear bounded by a unit membrane and is therefore likely lipid in nature.

Rough endoplasmic reticulum (ER) accumulates along the longitudinal axis of the cell, especially in the region of the nucleus (Figs. 16, 20, 22). The large tetrasporocyte nucleus initially occupies the basal region of the cell (Fig. 16) and migrates to the midregion as elongation progresses (Figs. 20, 24). The pre-meiotic sporangium shown in Fig. 20 is 35 x 8 μm . In sporangia undergoing elongation, a glancing section of the nucleus often reveals abundant nuclear pores and sometimes also adjacent microtubules (not shown). The stage 1 nucleus shown in Fig. 21 has the dimensions 6.5 x 3.7 μm . Prior to

meiosis, the dimensions show signs of increase; the nucleus shown in Fig. 27 is 15.3 x 7.9 μm . As the nucleus enlarges, a vacuole-free zone is maintained in the nuclear region (Figs. 16, 20, 24). Electron transparent nucleolar "vacuoles" are occasionally seen at this time (Fig. 27).

The tetrasporocyte undergoes several dramatic changes which indicate the approach of meiosis. The nucleus elongates (Figs. 16-17, 20-21, 27) and becomes surrounded by a massive accumulation of convoluted membranes and an associated electron dense material (EDM) (Figs. 24-25, 27-28). The nuclear poles remain free of the membranes and material, with the exception of a few ER cisternae (Fig. 27). Mitochondria abut the outermost edge of the membrane system (Fig. 28).

Layered peripheral ER is present in late stage 1 tetrasporocytes, but does not appear continuous (Fig. 29). A dark, extracellular region at the sporangial periphery (Figs. 21, 24, 30) indicates the forming tetrasporocyte (TC) wall. A dark, thickening at the tetrasporocyte plasmalemma (Fig. 29) represents initial stages of tetrasporangial (TS) wall formation. The tetrasporangial (TS) wall matures post-meiotically.

Stage 2

Observations of meiotic division were limited to two sporangia in what appears to be late anaphase II. Vacuoles are numerous at this stage of the developmental sequence. The

nucleus has an irregular profile, and the nuclear envelope is not resolvable at the division poles with this fixation (Figs. 31-32). ER cisternae organized in parallel arrays at the nuclear envelope (NE) comprise the perinuclear ER (PER) common in dividing red algal nuclei (Fig. 31). The region to the outside of the PER is occupied by an extensive, apparently ER-derived membrane system (Fig. 31). The membranes, similar to those described for tetrasporocytes just prior to meiosis, are coated with EDM. Non-EDM associated membranes, abundant at the poles with occasional extensions into the nucleoplasm (Fig. 32) may be derived from the extensive system described above. Microtubules and poorly defined kinetochores are visible in some planes. It was not, however, possible to resolve microtubules at the kinetochores. Golgi and Golgi derived vesicles are common in the nuclear vicinity (Figs. 31-32). The young tetrasporangial (TS) wall shows signs of detachment from the sporangial plasmalemma (Fig. 33-36). Tetrasporocyte (TC) wall material is visible to the outside of the tetrasporangium (TS) wall (Figs. 33, 35). In discrete regions, starch-flanked vacuoles can be seen closely juxtaposed with the TS wall (Figs. 33, 35). The starch free region of contact is marked by layered ER (Figs. 34, 36). This close association of vacuole with sporangial periphery was also observed in the non-geniculate coralline alga, Fosliella, and may represent a mechanism of delineating the site of cleavage initiation (Fig. 98).

Stage 3

The third stage comprises post-meiotic tetrasporangial development. The majority of tetrasporangia observed in a given mature conceptacle at one time exhibited a post-meiotic/pre-cleavage condition. Stage 3 tetrasporangia can be further segregated by the presence or absence of vacuoles. Starch flanked vacuoles characterize one group of stage 3 tetrasporangia, while starch flanked aggregations of electron dense vesicles characterize the second group. There does not appear to be a direct relationship between vacuoles and vesicle accumulation, as Golgi derived vesicles are clearly released directly into cytoplasmic aggregations and do not appear to be targeted to vacuoles. An intermediate, partially vacuolate condition, with electron dense vesicles present, was never observed. Thus, it is likely that vacuolar disappearance within a sporangium is synchronized and that this process must precede the second phase of Golgi secretion.

Post-meiotic sporangia undergo a transition to a non-vacuolate condition with a progressive reduction in vacuole size and number and a corresponding increase in the size of flanking starch grains. Figure 37 shows two post-meiotic vacuolate sporangia at different stages of maturity. The sporangium on the left illustrates the immediate post-meiotic condition in which starch-flanked vacuoles are large and irregular in profile. The delimitation of cleavage sites at the sporangial periphery by vacuoles, first noted during

meiosis (Figs. 33-35), appears to have progressed in the early stage 3 sporangium (Figs. 37-39). The thin layer of cytoplasm at the region of contact with the TS wall noted during meiosis (Figs. 33, 35) is no longer visible (Figs. 38-39). Thin strands of a lightly electron dense material remain in contact with the TS wall (Fig. 39).

In glancing section, Golgi, similar in appearance to those seen during meiosis, are common in the nuclear region (Fig. 42). Each of the four resulting nuclei are separated by approximately equal distances (Fig. 37). Post-meiotic nuclei are reduced in size from the pre-meiotic condition. Both vacuolate sporangia in Figure 37 exhibit a very close association between mitochondria and the nuclear envelope (Figs. 37, 40-41, 43-44). The distortion of the nuclear envelope may result from appressed mitochondria. This represents the first major change in organization of the nuclear region. The perinuclear membrane system and associated EDM persists but is distinctly less abundant than in previous stages (Figs. 40-41, 43-44).

The vacuoles in the sporangium on the right side of Fig. 37 have undergone a significant reduction in size (Figs. 37, 45). As starch-flanked vacuoles decrease in size, cytoplasmic inclusions increase. While abundant starch grains form concentric layers around the vacuoles (Fig. 45), there is a concurrent increase in free starch grains in the cytoplasm. Whether at vacuole periphery or free in the cytoplasm, each

starch grain is closely associated with a single layer of ER (Fig. 45).

Peripheral ER is not visible in vacuolate stage 3 tetrasporangia. By late stage 3, the sporangial plasma membrane has become highly convoluted (Figs. 37, 47, 49). Golgi are present throughout the cytoplasm of vacuolate stage 3 sporangia. Mitochondria are present and can be seen in association with Golgi at the nuclear periphery and throughout the cytoplasm (Figs. 43, 47). The lightly electron dense Golgi-derived vesicles first observed during meiosis II are especially notable at the sporangium periphery (Figs. 47-49). The vesicles associate in regular clusters in the cytoplasm (Fig. 47, 48). The region surrounding the innermost vesicle in a cluster is strongly electron dense (Fig. 48). Elongate, flattened membranes, which resemble attenuated Golgi in some planes of sectioning, are present throughout the cytoplasm (Figs. 47, 49, 82). The outermost membrane commonly maintains an ER association at the midregion.

As non-vacuolate stage 3 tetrasporangia prepare for cleavage, a second major phase of Golgi secretion begins. Golgi derived vesicles form aggregations which are flanked by concentric layers of starch grains (Figs. 50-51, 53, 55, 66, 68). The vesicles form as the entire outermost Golgi cisternum leaves the trans-Golgi region (Figs. 52, 85). The vesicle contents likely undergo chemical modification, since the vesicles in an aggregation are more strongly electron-

dense than those just released (Fig. 52). Flanking and cytoplasmic starch grains regularly associate in pairs, assuming curious "lip-like" formations (Figs. 50, 53, 55).

The mitochondrion-Golgi association is most prominent in mature non-vacuolate stage 3 sporangia. Mitochondria appressed to the NE are commonly juxtaposed with Golgi (Figs. 53-54). Annulate lamellae appear in nuclei at this time (Fig. 61, 84). ER cisternae originating in the nucleus associated membranes radiate out into the cytoplasm (Fig. 53) and occasionally terminate at a Golgi structure.

Post-meiotic nuclei are frequently observed in close proximity, prior to completion of cleavage (Fig. 55). Thick, multi-layered ER tracts surround and extend between the nuclei in a pair (Fig. 56). Each pair of nuclei lies in a different plane along the longitudinal axis of the sporangium (Fig. 55). A glancing section similarly reveals that the two nuclei in a pair may lie in different post-divisional planes (Fig. 56). A later section through the same paired nuclei shows an intermingling of the EDM (not shown).

The dispersal of the nucleus associated membrane system and EDM marks the final series of changes preceding cleavage completion. Mitochondria at the nuclear periphery are no longer as closely appressed to the NE, and only remnants of the EDM and membrane system can be seen (Figs. 57, 61-63). A glancing section of the nucleus reveals the extent of EDM dispersal (Fig. 64). The development of an electron-dense,

punctate border, which will later characterize the periphery of the mature sporangium, is visible for the first time and is especially notable in the region of the cleavage furrow, where layered PER is prominent (Figs. 66-67). The sporangial plasmalemma is connected to the TS wall via attachment sites, marked by plugs of electron dense material (Fig. 65). Aggregations of vesicles are common at the cleavage furrows, though exclusive localization does not occur (Figs. 57, 66-67, 70). ER tracts, possibly remnants of the extensive internuclear ER observed previously, are visible near the nuclear region (Fig. 63). Various-sized starch grains, as well as both aggregated and free electron dense vesicles, inclusions characteristic of the mature fully cleaved sporangium, are clearly visible in the cytoplasm (Fig. 68). The sporangium shown in Fig. 57 is 83 x 27 um in size.

Stalk cell pit connections persist throughout the developmental sequence and can be seen in mature Stage 3 tetrasporangia. At stage 3, however, the pit connection is attached to the sporangium wall and lacks continuity with the sporangial cytoplasm. Moreover, Stage 3 pit connections show signs of degradation (Fig. 59).

Stage 4

Nuclei of fully cleaved tetrasporangia lack the PER-EDM association (Figs. 71-72). The nuclear envelope is distorted, perhaps due to the abundance of small SER-like membranes and vesicles at the nuclear periphery (Figs. 69, 71-72). The

immediate region of the nucleus is also occupied by electron-dense vesicles which appear to have dispersed from the aggregations, as well as small, rounded starch grains (Fig. 73).

A comparison of the periphery of a mature post-meiotic, pre-cleaved sporangium with that of the fully cleaved sporangium reveals extensive modification (Fig. 70). A tubule system extends throughout the peripheral cytoplasm of the mature sporangium (Figs. 74-77). A punctate, electron dense border characterizes the wall region adjacent to the sporangium plasmalemma (Figs. 70, 74-77). Mature chloroplasts are abundant, but Golgi are no longer detectable in the cytoplasm.

Bisporangia

Bisporangia examined do not exhibit major deviations from the developmental progression described for tetrasporangia. The total volume of a bisporangium appears equivalent to that of a tetrasporangium, only the number and placement of cleavage furrows and the number of nuclei are obviously different (Fig. 78). Young tetrasporocytes and young bisporangia exhibit similar cytoplasmic features, especially the small vacuoles. The mechanism of starch deposition is likely similar, since starch-flanked vacuoles are present (Figs. 79-80). Bisporangia exhibit the same pattern of nucleus associated membranes and EDM noted in tetrasporangial specimens (Figs. 81-82, 84). Bisporangia with electron-dense

aggregations of Golgi derived vesicles (Figs. 83-85) do not differ in any detectable fashion from tetrasporangia at a comparable developmental stage. Electron-dense plugs of material are associated with the sporangial periphery (Figs. 86-87). Nuclei of mature fully cleaved tetrasporangia lack membranes and EDM and in fact are indistinguishable from nuclei of mature fully cleaved tetrasporangia (Figs. 78, 88-89).

Post-meiotic Tetrasporangial Nuclei Survey

Ultrastructural details of post-meiotic tetrasporangial nuclei (stage 3) were examined in 7 geniculate and 3 non-geniculate coralline genera. A nucleus associated ER-membrane system with corresponding electron dense material was absent at the defined stage in three of the examined genera (Table 3). The patterns of EDM and ER observed likely correspond with two primary modes of organization (Diagram 2).

Amphiroideae

The nuclei of post-meiotic tetrasporangia in Amphiroa (Figs. 90-91) and Lithothrix (Figs. 93-94) lack EDM. Lithothrix exhibits a perinuclear ER network, with a corresponding association with forming starch grains (Figs. 93, 95). Both organisms share a common pattern of starch deposition. Multiple RER cisternae, organized in parallel layers, surround forming starch grains (Figs. 92, 95).

Lithophylloideae

Titanoderma, like Lithothrix and Amphiroa, lacks EDM at

the defined stage (Figs. 96-97). Starch accumulation in the region of the nucleus is evident, but no starch-ER association was noted (Fig. 96).

Mastophoroideae

Fosliella (Figs. 98-102), though apparently lacking EDM, exhibits extensive PER. The ER closest to the NE in a mature Fosliella sporangium is densely studded with ribosomes (Fig. 102). EDM within nuclear envelope invaginations is prominent in post-meiotic nuclei of Metamastophora (Figs. 103-104). The cleavage furrow of this organism differs in organization from that seen in any other coralline genus surveyed in this study (Fig. 105). The poor quality of the Metamastophora fixation renders detailed analysis of the membranes at the nucleus difficult.

Corallinoideae

Post-meiotic nuclei of all examined genera within the Corallinoideae possess EDM. Haliptilon exhibits a pattern similar to that seen in Metamastophora, with EDM-filled nuclear envelope invaginations (Figs. 106-107). Haliptilon and Jania share similar conceptacle organization (Figs. 108, 112). Two similar EDM patterns, likely representing stage-specific variation, were observed in Jania (Figs. 109-111) and Corallina (Figs. 113-116). One pattern consists of concentric ER cisternae oriented parallel to the nuclear envelope with EDM diffuse in the ER region (Figs. 109-110, 113-114). The second pattern consists of tightly organized ER, oriented

perpendicular to the nuclear envelope, with EDM coating ER cisternae in highest concentration at the NE periphery (Figs. 111, 115-116). In Corallina, the PER can be seen radiating away from the NE, possibly reflecting a transition from the looser concentric PER organization (Fig. 114) to the tight perpendicular arrangement (Fig. 115-116). The post-meiotic nuclei of Calliarthron (Fig. 117) and Bossiella (Fig. 118) are indistinguishable at the ultrastructural level. Both organisms exhibit a tight mitochondrion-NE association, with EDM-coated convoluted membranes. Starch flanked aggregations of electron dense vesicles are visible in the cytoplasm of both genera (Figs. 117-118). A more extensive examination of tetrasporogenesis in Calliarthron will be necessary to confirm the apparent similarity to Bossiella.

DISCUSSION

A spore represents a totipotent cell capable of undergoing extensive cellular differentiation. According to Guiry (1990), sporangia and spores of all kinds exhibit cellular similarities which reflect a common "form/function" relationship. Regardless of spore type, sporangial development always involves cell enlargement or elongation accompanied by replication and turnover of organelles such as plastids and mitochondria, and a progressive increase in cytoplasmic inclusions. Patterns of Golgi secretion and RER-structural interactions, features common to all developing tetrasporangia, are each addressed separately in this discussion, accompanied by a demonstration of features unique to coralline red algae and to Bossiella in particular. The study concludes with the application of a new aspect of tetrasporangial ultrastructure to an evaluation of the currently prevalent coralline taxonomic scheme.

Golgi- Structure/Function

In all examined accounts of red algal tetrasporogenesis, the nature and timing of Golgi secretion appears to follow a common pattern (Alley and Scott 1977, Chamberlain and Evans 1973, Kugrens and Koslowsky 1981, Kugrens and West 1972, Peel *et al* 1973, Pueschel 1979, Scott and Dixon 1973). In general,

two secretory phases, each with differing Golgi morphology, accompany the process of spore differentiation. The first secretory phase involves the production of mucilage, the polysaccharide coating characteristic of mature spores (Alley and Scott 1977, Pueschel 1990) and unicellular red algae (Scott *et al* 1992). The second phase involves the production of "adhesive vesicles", electron-dense structures which persist in mature, fully-cleaved sporangia. The coralline algae Halitilon (Vesk and Borowitzka 1984) and Bossiella (present study) exhibit this same biphasic secretory pattern.

Mucilage secretion is a dynamic process observed in all differentiating red algal tetraspores. The mucilage-containing secretory vesicles are often described as fibrillar vacuoles/vesicles (Scott and Dixon 1973, Alley and Scott 1977, Pueschel 1979), striated vesicles (Kugrens and West 1972), or non-osmiophilic vesicles (present study). In the non-coralline algae Palmaria (Pueschel 1979) and Ptilota (Scott and Dixon 1973), mucilage deposition follows two pathways. Vesicles may either fuse with the plasmalemma, extruding contents directly into the space delimited by the sporangial wall, or they fuse to form single, large mucilage vesicles, which undergo "mass expulsion". Mucilage deposition in Palmaria is believed to play a direct role in cleavage septa formation (Pueschel 1979). Other functions ascribed to mucilage include prevention of water loss in newly released spores (Pueschel 1990) and actual expulsion of mature spores

(Scott and Dixon 1973, Pueschel 1990). Though the timing of deposition may vary from organism to organism, mucilage secretion always precedes formation of the second type of Golgi-derived vesicle.

Mucilage production first becomes visible in Bossiella during meiosis, and culminates in stage 3 non-vacuolate sporangia, when non-osmiophilic vesicles either associate in clusters in the cytoplasm or are secreted at the plasmalemma. The visible expansion of the region delimited by the sporangial plasmalemma and the TS wall in stage 3 vacuolate Bossiella tetrasporangia is most likely the effect of sustained Golgi secretion begun during meiosis. This apparent mucilage secretion may facilitate the separation of the TS wall from the sporangial plasmalemma. Once this separation has occurred, four distinct layers constitute the sporangial periphery: the sporangial plasmalemma, a mucilage layer, the TS wall, and to the outside, the extracellular TC wall material. Contact points between the sporangial plasmalemma and TS wall are maintained by fibrillar strands of material, capped by electron-dense plugs.

The second secretory phase involves the accumulation of vesicles which are strongly electron-dense in EM preparations. Several authors have referred to these as "adhesive vesicles" (Chamberlain and Evans 1973, Pueschel 1979, Vesk and Borowitzka 1984), though this function has not been confirmed. Pueschel (1979) suggests that these late-appearing vesicles

may play a role in post-discharge spore development. This function was suggested, in part, because of the localization of the vesicles at the sporangial periphery, as noted in mature sporangia of the coralline alga Haliptilon (Vesk and Borowitzka 1984). In Bossiella, however, such localization is never observed. Aggregations of electron-dense vesicles initially which first appear in post-vacuolate stage 3 tetrasporangia are uniformly dispersed in mature, fully-cleaved sporangia.

Sometimes the osmiophilic "adhesive vesicles" have a "scalloped" appearance (Vesk and Borowitzka 1984). In Ptilota, the second secretory vesicle is described as "dark cored" rather than uniformly osmiophilic (Scott and Dixon 1973). Vesk and Borowitzka (1984) interpret the different staining qualities of Golgi-derived vesicles observed in different organisms as important distinguishing features of developing tetrasporangia. The varied chemical composition of the vesicles (Alley and Scott 1977), however, likely reflects ecological factors or varied responses to chemical fixation protocols. In summary, the overall pattern of sporangial Golgi secretion appears similar in all red algal groups examined.

Sporangial Golgi observed in the present study in Bossiella orbigniana and in the coralline alga Haliptilon cuvierii (Vesk and Borowitzka 1984) undergo a comparable morphological transition. In both genera, Golgi are initially

rare with short, straight cisternae, and increase in number during tetrasporocyte elongation to form the mucilage secreting Golgi. The first change in Golgi morphology in Bossiella occurs in stage 3 non-vacuolate sporangia, marking the second secretory phase. The adjacent cisternae at the midregion of these late post-meiotic Golgi are closely appressed and electron-dense. The same morphology was first demonstrated by Scott and Dixon (1973) in Ptilota and has since been shown to be a characteristic of multicellular red algae undergoing sporogenesis (Broadwater and Scott, submitted, Patrone et al 1991). Interestingly, red algal unicells during log phase of growth also possess Golgi with closely appressed cisternae (Scott et al 1992). In Bossiella, Golgi with this appearance are especially prominent at the nuclear periphery in association with mitochondria.

Golgi Associations

The mitochondrion-Golgi association characteristic of red algae (Pueschel 1990) is not always notable in young Bossiella tetrasporocytes, but increases in prominence as sporangia mature. The association is most pronounced during the secretion of osmiophilic vesicles in post-vacuolate stage 3 development. A clear distinction can be made between the Golgi ultrastructure observed in Bossiella stalk cells and that seen in tetrasporocytes/tetrasporangia. A mitochondrion-Golgi association was never seen in the stalk cells. Stalk cell Golgi typically associate in pairs with an ER lamellum

extending between. The stalk cell paired-Golgi pattern does not appear to change over time, in contrast to the distinct transitions in morphology and activity observed in the sporangial Golgi. These observations suggest that different cell types within a single organism may not consistently exhibit a mitochondrion-Golgi association. This observation suggests a reevaluation of the use of this association as a taxonomic indicator.

Endoplasmic Reticulum-Structure/Function

Endoplasmic reticulum, like Golgi, is common in metabolically active cells (Peel et al 1973). In developing tetrasporangia, smooth and rough ER, in contrast with Golgi, exhibit a wider range of organizational and probably also functional variation. RER-starch grain, RER-plasmalemma, and RER-nucleus interactions are three common RER structural associations reported in tetrasporangial development.

RER-Starch Grain Associations

RER is associated with developing starch grains scattered throughout the cytosol of tetrasporangia in the non-coralline alga Palmaria (Pueschel 1979) and in the coralline alga Haliphtilon (Vesk and Borowitzka 1984). Starch is deposited between multiple parallel layers of ER cisternae in tetrasporangia and carposporangia of the coralline alga Lithothrix (Borowitzka 1978). This same unique deposition pattern was observed in an on-going study of the closely related alga Amphiroa (personal observations). Bossiella

tetrasporangia exhibit an additional distinct RER-starch grain association.

The striking localization of forming starch grains with associated RER outside the tonoplast membrane at the periphery of vacuoles in Bossiella, contrasts with all previously reported patterns of starch deposition in the red algae. Unpublished results in the present study indicate a presence of similar starch flanked vacuoles in the coralline alga Corallina vancouveriensis. None of the micrographs in Peel et al (1973) show such structures in Corallina officinalis, although their study, limited to post-meiotic tetrasporangial development, may have documented the period in which the vacuoles had already dispersed. The persistence of a vacuolate condition in developing tetrasporangia has not been reported in studies of non-coralline algae (Kugrens and West 1972, Chamberlain and Evans 1973, Peel et al 1973, Scott and Dixon 1973, Alley and Scott 1977, Kugrens and Koslowsky 1981). Vesik and Borowitzka (1984) noted the presence of small vacuoles in early Halimnion tetrasporocytes, but their micrographs do not reflect as extensive an accumulation as seen in this study for Bossiella. Further observations will be necessary before the RER/vacuole-associated pattern of starch deposition is accepted as a defining feature of coralline algae.

The functional significance of the RER-starch-vacuole association seen in Bossiella and Corallina vancouveriensis is not understood at the present time. Starch polymerization

may result from a direct interaction between RER-derived materials with material derived from the vacuoles. Vacuoles progressively accumulate in Bossiella during pre-meiotic growth and are most extensive during meiosis. Starch grain formation begins in mature stage 1 pre-meiotic sporangia and continues post-meiotically, concurrent with the decrease in size and ultimate resorption of vacuoles. Vacuoles did not stain positively with PAS at any developmental stage, though this does not eliminate the possibility that they contain enzymes or chemical components required for starch polymerization. In plant cells, vacuoles play a role in osmoregulation (turgor) and function as storage sites for proteins, salts, and molecules such as sucrose, as well as waste products (Darnell *et al* 1990, Vitale and Chrispeels 1992). According to Pueschel (1990), unicellular algae which lack firm walls are less able to use small vacuoles to generate turgor. In such organisms, which structurally resemble sporangia/spores, vacuoles are usually presumed to have lysosomal activity (Pueschel 1990). Vacuolation may also promote cell elongation during post-discharge spore development (Dixon 1973, Pueschel 1990, Pueschel and Cole 1985). In some cases, vacuolation during spore germination is so extensive that the entire cell becomes almost completely filled with vacuoles (Pueschel 1990).

Vacuoles may play a role in the orientation and placement of cleavage furrows. In Fosliella, of the few vacuoles

present in the cytoplasm of the young sporangium, the most prominent ones are located at the predicted sites of cleavage initiation. The location of starch-flanked vacuoles at the sporangial periphery in Bossiella may likewise represent one of the first steps in the delineation of cleavage sites. Although the role of these structures remains speculative at present, extensive vacuolation during cell elongation is clearly an important component of tetrasporogenesis in Bossiella.

RER-Plasmalemma Associations

Cleavage of tetrasporangia involves RER interactions with the sporangial plasmalemma. In Bossiella, the formation of a continuous peripheral RER system beneath the sporangial plasmalemma precedes cleavage completion and final modifications of the sporangial periphery. Multi-layered peripheral RER becomes especially prominent at the cleavage furrows in late stage 3 non-vacuolate Bossiella sporangia. Extensive peripheral RER at maturing cleavage sites was also noted by Vesik and Borowitzka (1984) in Haliptilon. The peripheral RER system in both Haliptilon and Bossiella is ultimately replaced during stage 4 by a peripheral tubule system which has been demonstrated to be a common feature of mature sporangia (Avanzini et al 1982, Avanzini and Honsell 1984). Vesik and Borowitzka (1984) speculate that the peripheral tubule system, together with associated RER cisternae, increases sporangial surface area, thus potentially

facilitating exchange between the sporangial interior with the external environment.

RER-Nucleus Associations

Perinuclear RER (PER), appearing at prophase, peaking by metaphase, and dispersing by late anaphase-telophase, is a common feature of dividing nuclei in multinucleate organisms within the Rhodophyta (Pueschel 1990, Scott and Broadwater 1990). Layered RER surrounds the premeiotic tetrasporangial nuclei of Ceramium (Chamberlain and Evans 1973), Palmaria (Pueschel 1979) and Ptilota (Scott and Dixon 1973). In Dasya, RER initially surrounds nuclei in the Prophase I tetrasporocyte and disperses prior to subsequent karyokinesis (Broadwater et al 1986a). PER is once again established and becomes most extensive during Metaphase I and II in Dasya (Broadwater et al 1986b). In the Corallinales, elaborations of the PER system, present both before and after cell division, potentially represent a phylogenetically significant distinguishing feature at the generic and supra-generic levels of classification.

The first study to note the organization of PER and EDM around nuclei in coralline tetrasporangia was Peel et al (1973). These authors describe a PER network, with an associated electron dense material (EDM), tentatively identified as RNA in nature, in Corallina officinalis. This initial examination addressed developmental rather than

phylogenetic questions. In order to gain a legitimate picture of the developmental process, as Peel *et al* (1973) intended, it is crucial to document EDM formation from appearance to dispersal. Instead, the examination centered on post-meiotic tetrasporangia. Even within the post-meiotic framework, other tetrasporangial nuclei undergo a series of developmental transitions. Peel *et al* (1973), however, document a single post-meiotic PER-EDM pattern for Corallina. In addition, they overlook distinctions in nuclear organization, which likely represent developmental changes in the process of EDM accumulation and dispersal. Two light micrographs included in the study reveal a slightly different PER-EDM pattern than that depicted in the electron micrographs. Specifically, the EM photographs show PER radiating from the nucleus, with EDM in diffuse localization at the nuclear surface, coating the PER cisternae. The light micrographs show a tighter association of EDM at the NE, with PER cisternae arranged in a distinct "eyelash" configuration (Diagram 1). The authors did not discuss these apparently distinct patterns of perinuclear organization. Without the perspective of the overall process of tetrasporogenesis, the authors' interpretations and conclusions are incomplete. Moreover, although Peel *et al* (1973) noted differences in tetrasporangial nuclear ultrastructure between coralline genera, phylogenetic inferences were not attempted.

Vesk and Borowitzka (1984) were more thorough in their

documentation of perinuclear development in the coralline alga Haliphtilon cuvierii. Interkinesis marks the first appearance of EDM in Haliphtilon. Initial accumulation, seen at nuclear envelope invaginations, is delimited by concentric layers of PER. Personal observations on Haliphtilon indicate that the NE invaginations can persist post-meiotically. Post-meiotic Haliphtilon tetrasporangia, with established cleavage furrows, exhibit two nuclear patterns (Vesk and Borowitzka 1984). The first consists of a tight association of EDM at the NE, with radiating PER. This corresponds with the Corallina pattern shown in the light micrographs of Peel et al (1973) and in the present study. Later in sporangial development, the EDM appears more diffused than the previously more compact organization. Vesk and Borowitzka (1984) demonstrated that the PER in the fully cleaved Haliphtilon sporangium is reduced and the EDM is dispersed.

Reports are inconsistent regarding the ultrastructure of developing tetrasporangial nuclei in Jania. Duckett et al (1978) describe cytoplasmic "pockets" of EDM at NE invaginations in Jania rubens, but note that precisely oriented PER, as observed in Corallina, is apparently absent. Vesk and Borowitzka (1984) similarly express doubt regarding the presence of a Corallina-type perinuclear organization in Jania. In the present study, however, Jania was observed to have both developmental patterns described for Corallina and Haliphtilon tetrasporangial nuclei. The first corresponds with

the tight PER-EDM association seen in Corallina (Peel et al 1973, present study), and in Haliptilon (Vesk and Borowitzka 1984). Later in the developmental process, a looser PER-EDM association is observed, with ER cisternae radiating from nuclei, as noted previously in both Corallina and Haliptilon. It is likely therefore, that Jania exhibits a developmental sequence similar to that seen in Haliptilon, commencing with EDM-filled invaginations of the NE, and progressing from a tight PER-EDM association, to a more diffuse association, prior to EDM dispersal. Although NE-invaginations have not yet been documented in Corallina, such a pattern is expected. Overall this pattern will be referred to as a rough ER-EDM association: RER-EDM.

In order to eliminate or reduce the problem of misinterpretation due to incomplete analysis, the present in-depth study on Bossiella orbigniana provides comprehensive documentation of initial EDM appearance, accumulation and ultimate dispersal. Cytochemical tests tentatively confirm that there is an RNA component to the EDM. Consistent results were not achieved with RNase treatments due to pH and staining problems. The best results were obtained with acid hydrolysis. Treatment of tissue in 1 N HCl hydrolyzes single stranded RNA and dissociates the paired strands of the DNA double helix. The ability of RNA to bind stain is thus removed, while the remaining single stranded nucleic acid (DNA) stains as RNA would prior to the treatment (Chayen et al

1973). Compared with controls, the affinity of the methyl green-pyronin Y and azure B stains was selectively reduced in the perinuclear zone following HCl treatment. The non-specific nature of the hydrolysis treatment, however, precludes a definitive establishment of the nature of the enigmatic EDM.

The nuclear organization observed in Bossiella orbigniana (present study) clearly differs from the RER-EDM pattern. EDM begins to accumulate in Bossiella tetrasporocytes prior to the onset of meiosis. The appearance of the convoluted smooth surfaced membrane system (SM) surrounding the pre-meiotic nuclei suggests a smooth ER origin. EDM coats the membranes, while mitochondria abut the membrane-EDM region. This pattern will be referred to as the smooth membrane-mitochondrial-EDM organization: SMM-EDM. The mitochondria-nuclear envelope association is interesting in light of recent evidence which suggests that mitochondria may direct aspects of embryonic development in Drosophila (Kobayashy et al 1993). Localization of an extramitochondrial ribosomal RNA is thought to orient the pole cell formation in developing Drosophila embryos. Molecular biology techniques beyond the scope of this project might be applied to ascertain whether mitochondria-derived RNA is present in the EDM of Bossiella.

Observations on two Bossiella sporangia undergoing the second meiotic division support the proposed, four stage developmental sequence. The EDM and associated membranes are

most extensive during meiosis II, the most highly vacuolate phase observed in Bossiella. Peel *et al* (1973) cite two studies which indicate that ER membranes may be induced to stack in response to osmotic changes. Nir *et al* (1969) postulated that a stacking of RER membranes could be observed in maize seeds germinated under water stress. Similarly, Heath and Greenwood (1971) indicated that vacuole development in Saprolegnia lead to cytoplasmic dehydration and subsequent ER stacking. Whether a similar mechanism is occurring in Bossiella is a matter of speculation at this point.

During mitotic prometaphase in Bossiella, six or more PER cisternae can be identified. Additionally, smooth surfaced tubular membranes build up at the polar regions (Broadwater *et al* 1993). However, the mitotic membranes and RER do not ultrastructurally resemble the elaboration of the EDM-membrane system seen during meiotic division. Interestingly, the supposedly mitotic bisporangia of Bossiella possess the same nuclear pattern as tetrasporangia. The pattern is thus either not restricted to meiotic cells but is characteristic of sporangia, or the bisporangia may not be mitotic. The former suggestion is interesting in light of the observation that in Dasya that the elaboration of smooth endoplasmic reticulum (SER) seen at the division poles during meiosis is absent during mitosis (Broadwater *et al* 1986b).

In his light microscope summary of tetrasporogenesis, Johansen (1981) states that post-meiotic nuclei are aligned

along the longitudinal axis of the zonate sporangium. This description requires refinement in order to accurately reflect post-meiotic placement of nuclei in Bossiella.

Movement of post-meiotic Bossiella nuclei toward each other and to the sporangial center is pronounced and can be seen in both vacuolate and non-vacuolate pre-cytokinesis sporangia. Such nuclear movement appears to be a common feature in red algae. Broadwater *et al* (1986b) document the phenomenon in Dasya. Although direct nuclear fusion was not reported in this genus, Scott and Thomas (1975) show that in other red algae fusion of nuclei can occur. In Bossiella, the two distal nuclei and the two proximal nuclei form interacting pairs. The location of the nuclei within the sporangium suggests that the distal-most and proximal-most nuclei migrate inwards, towards the two central nuclei. Once pairs are established, the nuclei continue to move towards the sporangial midregion. All four nuclei, however, were never observed in proximity at the midregion of the sporangium, and it is not known whether this position is ever achieved. In Dasya, all four nuclei approached the center of the tetrahedral sporangium and were commonly observed in close proximity (Broadwater *et al* 1986b). Because paired nuclei are observed at early and late pre-cytokinesis stages in Bossiella, it is possible that back and forth movements are continual, rather than reflecting a single approach prior to cleavage completion.

The orientation of RER in association with tetrasporangial nuclei described in Bossiella and other coralline red algae is clearly a dynamic process. Current research suggests that structural interactions of the ER may involve an association with the motor molecules kinesin, dynein, and myosin (Terasaki 1990). ER structural interactions in the central regions of cells are widely noted, and may function in the directing of bulk cytoplasmic movements and, importantly, in the positioning of nuclei (Terasaki 1990).

Phylogenetic Survey of Tetrasporangial Nuclei

In addition to refining known details of tetrasporogenesis in coralline red algae, a major goal of this study was to identify tetrasporangial features that might facilitate taxonomic analyses of the Rhodophyta. A cursory survey of several geniculate and non-geniculate coralline genera reveals that pre- and post-meiotic nuclear ultrastructure might represent one such feature.

The most prevalent coralline classification scheme in current use (Johansen 1969, 1976, 1981, Woelkerling 1988) emphasizes the presence or absence of genicula as a primary taxonomic feature. A second, less widely accepted scheme, put forth by Cabioch (1971a,b, 1972) emphasizes the similar organization of reproductive conceptacles, rather than the apparently "simpler" organization of the non-geniculate vegetative thallus. Cabioch places geniculate and non-

geniculate genera with similar conceptacle organization in the same subfamilies and tribes (Chamberlain 1978).

Segregation of coralline algae on the basis of tetrasporangial nuclear ultrastructure, correlated with cellular connection features and conceptacle-type results in the grouping of geniculate and non-geniculate genera (Table 3). Thus, preliminary results of the present study support the Cabioch's classification scheme (1971a,b, 1972).

Although Johansen agreed with Cabioch that tetrasporangial conceptacles in the geniculate genera Amphiroa and Lithothrix are "basically identical" in structure and development to those in the non-geniculate genera Tenarea and Lithophyllum, he criticized her "lumping" of geniculate and non-geniculate genera as "unwarranted" (Johansen 1972). Yet a surprising amount of evidence suggests that Johansen's scheme (Table 1) may be incorrect. Analyses of spore germination patterns support the deemphasis of genicula as primary classification features (Chihara 1973, 1974a,b). Chihara unites geniculate and non-geniculate genera in two groups, Amphiroa/Lithophyllum and Corallina/Lithothamnium, based on spore segmentation patterns (Chihara 1974). Chamberlain (1978, 1983) considers the Johansen scheme (1969, 1976, 1981) to be an inaccurate reflection of evolutionary relationships. Johansen rejects Cabioch's scheme which suggests that the geniculate evolved from the non-geniculate morphology more than once, in spite of his agreement with this

evolutionary concept (Chamberlain 1978). Johansen's separation of genera on the basis of presence or absence of genicula may be as "unnatural" as the placement of genera within the Porphyridiales on the basis of unicellular/colonial mode of organization (Garbary and Gabrielson 1990, Broadwater et al 1993 in press). Cabioch's scheme, in contrast, represents both a taxonomic and an evolutionary grouping (Chamberlain 1978).

A modification of Cabioch's classification scheme (Cabioch 1971a,b, 1972) segregates the Corallinales into four subfamilies (Chamberlain 1978; Table 4). The Sporolithoideae contains a single genus, Sporolithon, and represents the most primitive extant group of coralline red algae. The Sporolithoideae lack exclusively zonate tetrasporangia and possess both secondary pit connections and lateral cell fusions. The Lithothamnoideae consists of organisms characterized by multiporate tetrasporangial conceptacles and lateral cell fusions. The last two subfamilies, the Corallinoideae and Lithophylloideae, both with uniporate conceptacles, are segregated on the basis of lateral cell fusions and secondary pit connections, respectively.

Corallina, Jania, Halitilon, Bossiella, and Calliarthron, the geniculate genera examined in this study, are united with the non-geniculate genus Chiharaea in one tribe within the Corallinoideae (Table 4). Similarly, the non-geniculate genus Fosliella is grouped in a tribe with the

geniculate genus Metagoniolithon. Metamastophora is placed in a separate tribe within the Corallinoideae. All of these genera possess lateral cell fusions.

Amphiroa and Lithothrix are placed in Cabioch's fourth subfamily, the Lithophylloideae (Table 4). Both lack PER-EDM elaboration and possess secondary pit connections. Titanoderma, a non-geniculate genus also grouped with the Lithophylloideae, similarly lacks PER-EDM.

PER elaborations were only seen in the Corallinoideae (*sensu* Cabioch 1972). Patterns observed fall into the two categories: RER-EDM (Corallina-type) and SMM-EDM (Bossiella-type). It will be necessary to examine Fosliella in greater detail to determine whether a third, intermediate PER pattern emerges. It would be particularly interesting to see whether a Fosliella-like PER pattern is observed in Metagoniolithon (Table 4).

All of the geniculate genera exhibiting a common PER organization share similar conceptacular types. For example, conceptacles in Jania, Corallina, and Haliptilon all form at the axial position on intergenicula. Each of these organisms has the RER-EDM nuclear pattern. Bossiella and Calliarthron, organisms which share the SMM-EDM arrangement, both possess marginal conceptacles (Johanson 1969, 1972). Axial and marginal conceptacles are associated with primary growth of the intergeniculum. Axial conceptacle primordia form at the apex of terminal intergenicula, while marginal primordia

develop at the margins of flat, subterminal intergenicula (Johansen 1969, 1972). Lateral conceptacles are characteristic of Amphiroa and Lithothrix, organisms which lack PER-EDM associations. Lateral primordia form in either primary or secondary tissue, in the cortex of compressed intergenicula (Johansen 1969, 1972).

This survey is limited in scope and will require expansion in order to confirm the relationships suggested here. The number of surveyed non-geniculate genera should be increased. Also, it would be informative to thoroughly compare at least two species within a single genus. A cursory comparison of Corallina officinalis (Peel *et al* 1973) and Corallina vancouveriensis (personal observations) suggests that there may be little interspecific variation. With expanded analyses, it is likely that the ultrastructural patterns of tetrasporangial nuclei in the Corallinales will be added to the list of sporangial features useful in coralline classification.

APPENDIX
Biological Stain Protocols

Azure B

(modified from Chayen, Bitensky, and Butcher 1973
and Jensen 1962)

Solutions:

Citrate Buffer.....4.7 vols of .1 M Citric acid and
15.4 vols of .1 M Na₃Citrate.
Adjust to pH 4.00 with 1 N HCl

Azure B.....2mg/mL azure B in citrate buffer

Procedure:

Immerse for 6 min in azure B stain solution followed by 3 dips
in citrate buffer. Rinse in running tap water.

Results:

Azure B stains RNA blue and DNA pink. DNA in glutaraldehyde
fixed material is very difficult to discern in this
preparation. Nucleoli and perinuclear zone in Bossiella are
prominently blue.

Methyl Green-Pyronin Y

(modified from Taft's method for nucleic acids in Luna 1968)

Solutions:

2% Pyronin Y.....2 g pyronin Y in distilled water

2% Methyl green.....Add 2 g methyl green to 100 mL hot
distilled water. When cool,
extract in separatory funnel with
50 mL aliquots of chloroform until
violet color is removed.

0.1 M Acetic acid

0.1 M Sodium acetate

Staining solution.....Combine 2 mL 2% methyl green, 3 mL 2% pyronin Y , 1 mL 100% ETOH, 26.4 mL 0.1 M sodium acetate and 17.6 mL 0.1 M acetic acid. Adjust to pH 6 with 1 N HCl.

Procedure:

Dip slide once in distilled water. Stain in methyl green/pyronin Y solution for 8 to 12 min. Rinse in 2 changes of distilled water using 2 dips each. Dehydrate in 95% ETOH for 30 s and dry.

Result:

Perinuclear region in Bossiella and Corallina tetrasporangia stains strongly pink, as do nucleoli. DNA should appear green but is only faintly visible. High degree of non-specific staining within the range of pH 4-8 at staining intervals from 5 min to 25 min.

PAS

Solutions:

1 % Periodic Acid
Schiff's Reagent (Fischer)

Procedure:

Soak slide in 1 % periodic acid solution for 5 min. Rinse in distilled water in coplin jar for 5-10 min. Stain in Schiff's reagent for 1-3 min. Rinse in running tap water. Counterstaining with 1% toluidine blue requires 5-10 min for optimal contrast.

Result:

Red or purple red indicates a positive PAS reaction

Hydrochloric Acid Method for RNA Hydrolysis
(modified from Chayen, Bitensky, and Butcher 1973)

Procedure:

Incubate slide in 1 N HCl at 60 C for 5-8 min. Incubate control slide in distilled water at the same temperature. Rinse under running tap water for 3 min and dry. Stain as desired.

RNase Methods for RNA Localization
(Modified from Coleman 1978)

Solution 1:

15 mM NaCl.....Dissolve .0877 g NaCl in
100 mLs distilled water

10 mM TrisCl.....Dissolve .158 g TrisCl
in 100 mLs distilled
water

Combine both solutions and adjust pH to 7.5. Add 10 mg Bovine pancreatic RNase A-5x crystallized (Sigma R 4875) to 1 mL distilled water for 10 mg/mL solution. Boil at 100 C for 15 min to remove DNase.

Procedure:

Flood experimental tissue section with RNase solution and incubate at 35 C for 2 h. Control section is incubated in buffer without RNase. Rinse for 5 min in running tap water. Dry and stain as desired.

Solution 2:

Add 5×10^{-4} g RNase A to 1 mL 2mM Sodium Acetate, pH 5.5. Heat at 100 C for 15 min to remove DNase.

Procedure:

Flood experimental tissue section with RNase solution. Incubate at 35 C for 2 h. Rinse for 60 min in 2 mM sodium acetate buffer followed by tap water rinse for 5 min. Dry and stain as desired. Incubate control in sodium acetate buffer alone.

BIBLIOGRAPHY

- Adey, W.H. and H.W. Johansen. 1972. Morphology and taxonomy of Corallinaceae with special reference to Clathromorphum, Mesophyllum, and Neopolyporolithon gen. nov. (Rhodophyceae, Cryptonemiales). *Phycologia* 11: 159-180.
- Alley, C.D. and J.L. Scott. 1977. Unusual dictyosome morphology and vesicle formation in tetrasporangia of the marine red alga Polysiphonia denudata. *J. Ultrastruct. Res.* 58:289-298.
- Avanzini, A., Honsell, G. and S. Gardonio. 1982. Some aspects of germination and cell wall formation in tetraspores of Nitophyllum punctatum (Rhodophyta). *Caryologia* 35: 352-353.
- Avanzini, A., and G. Honsell. 1984. Membrane tubules in the tetraspores of a red alga. *Protoplasma* 119: 156-158.
- Borowitzka, M.A. 1978. Plastid development and floridean starch grain formation during carposporogenesis in the coralline red alga Lithothrix aspergillum Gray. *Protoplasma* 95:217-228.
- Broadwater, S., Scott, J., and B. Pobiner. 1986 a. Ultrastructure of meiosis in Dasya baillouviana (Rhodophyta). I. Prophase I. *J. Phycol.* 22: 490-500.
- Broadwater, S., Scott, J., and B. Pobiner. 1986 b. Ultrastructure of meiosis in Dasya baillouviana (Rhodophyta). II. Prometaphase I-telophase II and post-division nuclear behavior. *J. Phycol.* 22: 501-512.
- Broadwater, S., Scott, J., Field, D., Saunders, B. and J. Thomas. 1993. An electron microscopic study of cell division in the coralline red alga Bossiella orbigniana. *Can. J. Bot.* 71: 434-446.
- Broadwater, S., and J. Scott. 1993. Ultrastructure of unicellular red algae. In press.
- Cabioch, J. 1971a. Essai d'une nouvelle classification des Corallinacees actuelles. *C.R. hebd. Seanc. Acad. Sci. Paris D*, 272: 1616-1619.
- Cabioch, J. 1971b. Etude sur les Corallinacees, I. Caracteres generaux de la cytologie. *Cah. Biol. mar.* 12: 121-186.

- Cabioch, J. 1972. Etude sur les Corallinacees, 2. La morphogenese: consequences systematiques et phylogenetiques. Cah. Biol. mar. 13: 137-288.
- Chamberlain, Y.M. 1978. Investigation of taxonomic relationships amongst epiphytic, crustose Corallinaceae. In Irvine, D.E.G. and Price, J.H. (eds), Modern Approaches to the Taxonomy of Red and Brown Algae. Academic Press, New York, 223-246.
- Chamberlain, Y.M. 1983. Studies in the Corallinaceae with special reference to Fosliella and Pneophyllum in the British Isles. Bull. Br. Mus. Nat. Hist. (Bot.) 11: 291-463.
- Chamberlain, A.H.L. and L.V. Evans. 1973. Aspects of spore production in the red alga Ceramium. Protoplasma 76:139-159.
- Chayen, J., Bitensky, L., and R.G. Butcher. 1973. Practical Histochemistry. New York, John Wiley and Sons.
- Chihara, M. 1973. The significance of reproductive and spore germination characteristics in the systematics of the Corallinaceae: articulated coralline algae. Jap. J. Bot. 20: 369-379.
- Chihara, M. 1974a. The significance of reproductive and spore germination characteristics to the systematics of the Corallinaceae: non-articulated coralline algae. J. Phycol. 10: 266-274.
- Chihara, M. 1974b. Reproductive cycles and spore germination of the Corallinaceae and their possible relevance in the systematics of five species of Fosliella. J. Jap. Bot. 49: 89-95.
- Coleman, A.W. 1978. Visualization of chloroplast DNA with two fluorochromes. Expt. Cell Res. 114: 95-100.
- Darnell, J., Lodish, H., and D. Baltimore. 1990. Molecular Cell Biology. W.H. Freeman and Co.: New York.
- Duckett, J.G., and M.C. Peel. 1978. The role of transmission electron microscopy in elucidating the taxonomy and phylogeny of the Rhodophyta. In Irvine, D.E.G. and Price, J.H. (eds), Modern Approaches to the Taxonomy of Red and Brown Algae. Academic Press, New York, 157-204.
- Gabrielson, P.W. and D.J. Garbary. 1986. Systematics of red algae (Rhodophyta). CRC Press Crit. Rev. Plant Sci. 3:329-366.

- Gabrielson, P.W. and D.J. Garbary. 1987. A cladistic analysis of Rhodophyta: florideophycidean orders. *Br. Phycol. J.* 22: 125-138.
- Gabrielson, P.W., Garbary, D.J., and R.F. Scagel. 1985. The nature of the ancestral red alga: inferences from a cladistic analysis. *Biosystems* 18: 335-346.
- Gabrielson, P.W., Garbary, D.J., Sommerfeld, M.R., Townsend, R.A. and P.L. Tyler. 1991. Phylum Rhodophyta. In L. Margulis (ed), *Handbook of Proctista*, pp. 102-118.
- Garbary, D.J., and P.W. Gabrielson. 1990. Taxonomy and evolution. In *Biology of the Red Algae*. Eds. K.M. Cole and R.G. Sheath. Cambridge University Press. pp. 477-498.
- Goff, L.J. and A.W. Coleman. 1984. Elucidation of fertilization and development in a red alga by quantitative DNA microspectrofluorometry. *Dev. Bio.* 102: 173-194.
- Goff, L.J. and A.W. Coleman. 1990. DNA: microspectrofluorometric studies. In *Biology of the Red Algae*. Eds. K.M. Cole and R. G. Sheath. Cambridge University Press, pp. 43-71.
- Guiry, M.D. 1978. The importance of sporangia in the classification of the Florideophyceae. In *Modern Approaches to the Taxonomy of Red and Brown Algae*. Systematics Association Special Vol. 10, eds. D.E.G. Irvine and J.H. Price, pp. 111-144. London: Academic Press.
- Guiry, M.D. 1990. Sporangia and spores. In *Biology of the Red Algae*. Eds. K.M. Cole and R.G. Sheath. Cambridge University Press, pp. 347-376.
- Guiry, M.D. and L.M. Irvine. 1989. Sporangial form and function in the Nemalialiophycidae (Rhodophyta). In *Phykotalk Vol. I.*, ed. H.D. Kumar, pp. 155-184. Meerut: Rastogi Publ. (India).
- Heath, I.B., and A.D. Greenwood. 1971. Ultrastructural observations on the kinetosomes and Golgi bodies during the asexual life cycle of *Saprolegnia*. *Z. Zellforsch.* 112: 371-389.
- Jensen, W.A. 1962. *Botanical Histochemistry: Principles and Practice*. W.H. Freeman and Co.

- Johansen, H.W. 1969. Morphology and systematics of coralline algae with special reference to Calliarthron. University of California Publications in Botany Volume 49. University of California Press.
- Johansen, H.W. 1971. Bossiella, a genus of articulated corallines (Rhodophyceae, Cryptonemiales) in the eastern Pacific. *Phycologia* 10: 381-396.
- Johansen, H.W. 1972. Conceptacles in the Corallinaceae. In Proceedings of the 7th International Seaweed Symposium. pp. 114-207. New York: John Wiley and Sons.
- Johansen, H.W. 1976. Current status of generic concepts in coralline algae (Rhodophyta). *Phycologia* 15(2): 221-244.
- Johansen, H.W. 1981. Coralline Algae: a First Synthesis. Boca Raton: CRC Press.
- Kobayashi, S., Amikura, R. and M. Okada. 1993. Presence of mitochondrial large ribosomal RNA outside mitochondria in germ plasm of Drosophila melanogaster. *Science* 260: 1521-1523.
- Kugrens, P. and D.J. Koslowsky. 1981. Electron microscopic Studies on a unique cytokinetic structure in tetrasporocytes of the red alga Harveyella sp. (Cryptonemiales, Choreocalaceae). *Protoplasma* 108:197-209.
- Kugrens, P. and J.A. West. 1972. Ultrastructure of tetrasporogenesis in the parasitic red alga Levringiella gardneri (Setchell) Kylin. *J. Phycol.* 8:370-383.
- Luna, L. G. 1968. Manual of Histologic Staining Methods of the Armed Forces Institute of Pathology. McGraw Hill.
- Nir, I., Klein, S., and A. Poljakoff-Mayber. 1969. Effects of moisture stress on submicroscopic structure of maize roots. *Aust. J. biol. Sci.* 22: 17-33.
- Patrone, L., Broadwater, S., and J. Scott. 1991. Ultrastructure of vegetative and dividing cells of the unicellular red algae Rhodella violacea and Rhodella maculata. *J. Phycol.* 27: 742-753.
- Peel, M.C., Lucas, I.A.N., Duckett, J.G. and A.D. Greenwood. 1973. Studies of sporogenesis in the Rhodophyta. I. An association of the nuclei with endoplasmic reticulum in post-meiotic tetraspore mother cells of Corallina officinalis L. *Z. Zellforsch. Mikrosk. Anat.* 147:59-74.

- Pueschel, C.M. 1979. Ultrastructure of tetrasporogenesis in Palmaria palmata (Rhodophyta). J. Phycol. 15:409-424.
- Pueschel, C.M. 1990. Cell structure. In Biology of the Red Algae. Eds. K.M. Cole and R.G. Sheath. Cambridge University Press, pp. 7-41. .
- Scott, J.L. and P.S. Dixon. 1973. Ultrastructure of tetrasporogenesis in the marine red alga Ptilota hypnoides. J. Phycol. 9: 29-46.
- Scott, J.L., and S.T. Broadwater. 1990. Cell division. In Biology of the Red Algae. Eds. K.M. Cole and R.G. Sheath. Cambridge University Press, pp. 123-145.
- Scott, J.L., Broadwater, S.T., Saunders, B.D., Thomas, J.P., and P.W. Gabrielson. 1992. Ultrastructure of vegetative organization and cell division in the unicellular red alga Dixoniella grisea gen.nov. (Rhodophyta) and a consideration of the genus Rhodella. J. Phycol. 28: 649-660.
- Scott, J.L. and J.P. Thomas. 1975. Electron microscope observations of telophase II in the Florideophyceae. J. Phycol. 11: 474-476.
- Searles, R.B. 1968. Morphological studies of red algae of the order Gigartinales. Univ. Calif. Pub. Bot. 43: 1-86.
- Silva, P.C. and H.W. Johansen. 1986. A reappraisal of the order Corallinales (Rhodophyceae). Br. Phycol. J. 21: 245-254.
- Terasaki, M. 1990. Recent progress on structural interactions of the endoplasmic reticulum. Cell Motil. and Cytoskel. 15: 71-75.
- Vesk, M. and M.A. Borowitzka. 1984. Ultrastructure of tetrasporogenesis in the coralline alga Halimtilon cuvieri (Rhodophyta). J. Phycol. 20:501-515.
- Vitale, A. and M.J. Chrispeels. 1992. Sorting of proteins to the vacuoles of plant cells. Bioess. 14: 151-160.
- Woelkerling, W. J. 1988. The Coralline Red Algae. British Museum (Natural History). Oxford University Press.

Table 1
Summary of Coralline Taxonomic Schemes

Johansen (1981)

<u>NON-GENICULATE</u>	<u>GENICULATE</u>
Subfamily Melobesoideae	Subfamily Corallinoideae
Tribe Lithothamnieae	Tribe Corallineae
Tribe Phymatolitheae	Tribe Janiae
Subfamily Mastophoroideae	Subfamily Amphiroideae
	Tribe Amphiroae
Subfamily Lithophylloideae	Tribe Lithotricheae
	Subfamily Metagoniolithoideae

Cabioch (1972)

Subfamily Sporolithoideae
Tribe Sporolithaeae
Subfamily Lithothamnoideae
Tribe Lithothamnieae
Subfamily Corallinoideae
Tribe Mastophoreae
Tribe Neogoniolitheae
Tribe Corallineae
Subfamily Lithophylloideae
Tribe Amphiroeae
Tribe Lithophylleae
Tribe Dermatolitheae

Table 2
Tetrasporogenesis in Bossiella orbigniana

Stage 1	Stage 2	Stage 3	Stage 4
Pre-meiosis	Meiosis	Post-meiosis	Post-meiosis
		-initiation of and arrest of cleavage	-cleavage completion
1. preEDM/pre starch 2. postEDM/post starch		1. vacuolate 2. non-vacuolate -EDM-dispersal	

Table 3
Summary of Tetrasporangial Nuclei Survey

Subfamily	Genus	Genicula	2° pit connections	cell fusions	EDM Corallina type	Bossiella type	Conceptacle Type*
Amphiroideae	<u>Amphiroa</u>	+	+	-	-	-	L
	<u>Lithothrix</u>	+	+	-	-	-	L
Lithophylloideae	<u>Titanoderma</u>		+				
Mastophoroideae	<u>Metamastophora</u>			+	+		
	<u>Fosliella</u>			+	?		-
Corallinoideae	<u>Jania</u>	+		+	+		A
	<u>Corallina</u>	+		+	+	-	A
	<u>Halptilon</u>	+		+	+	-	A
	<u>Bossiella</u>	+	-	+	-	+	M
	<u>Calliarthron</u>	+	-	+	-	+	M,L

* A = axial
M = marginal
L = lateral
Conceptacle type designations
apply only to geniculate genera

Table 4
Coralline Classification *sensu* Cabioch

		[Kvaleyia]	[Melobesia]	[Phymatolithon] [Lithothamnium] [Mesophyllum] [Polyporolithon]	
Lithothamnioideae	-multiporate, cell fusions	[----->			
		LITHOTHAMNIEAE			
		[Choreonema]	[Fosliella]	[Porolithon] [Neogoniolithon]	[Metagoniolithon]
		[----->			
		MASTOPHOREAE			
			[Yamadaeae]	[Chiharaeae]	[Jania] [Haliptilon] [Bossiella] [Corallina] [Calliarthron]
Corallinoideae	-uniporate, cell fusions	[----->			
		CORALLINEAE			
			[Lithoporella]	[Mastophora]	[Metamastophora]
		[----->			
		NEOGONIOLITHEAE			
		[Ezo]	[Pseudolithophyllum]	[Lithophyllum]	
		[----->			
		DERMATOLITHEAE			
					[Amphiroa]
Lithophylloideae	-uniporate, secondary pit connections	[----->			
		AMPHIROEAE			
		[Tenarea]	[Titanoderma]		[Lithothrix]
		[----->			
		LITHOPHYLLEAE			
					[Sporolithon]
		[----->			
		SPOROLITHEAE			
Sporolithoideae	-isolated sporangia, cell fusions and secondary pit connections				

(Modified from Chamberlain 1978)

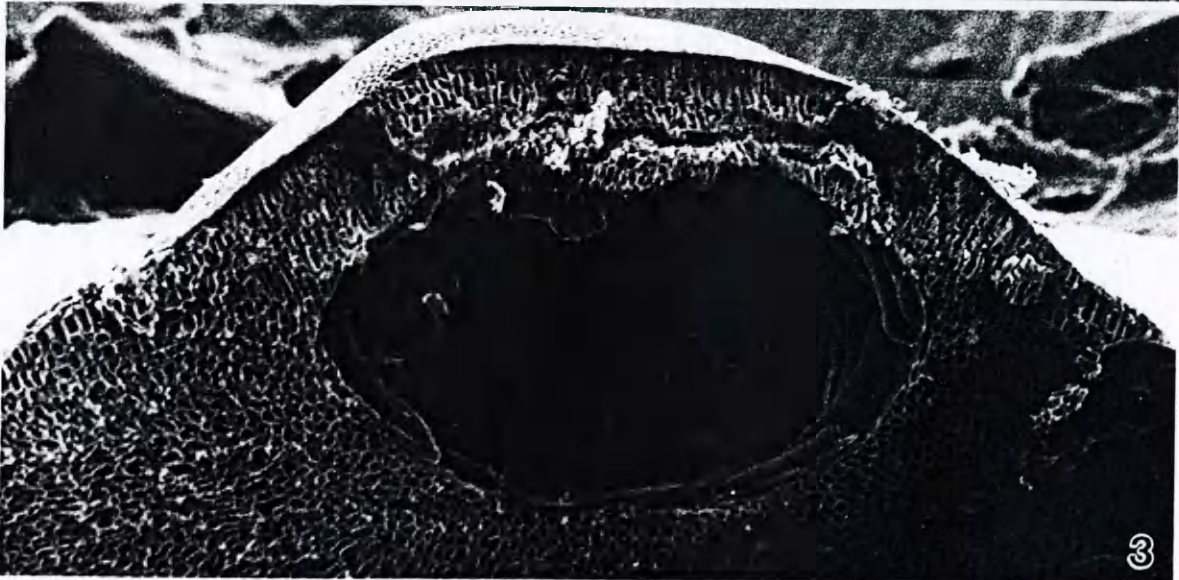
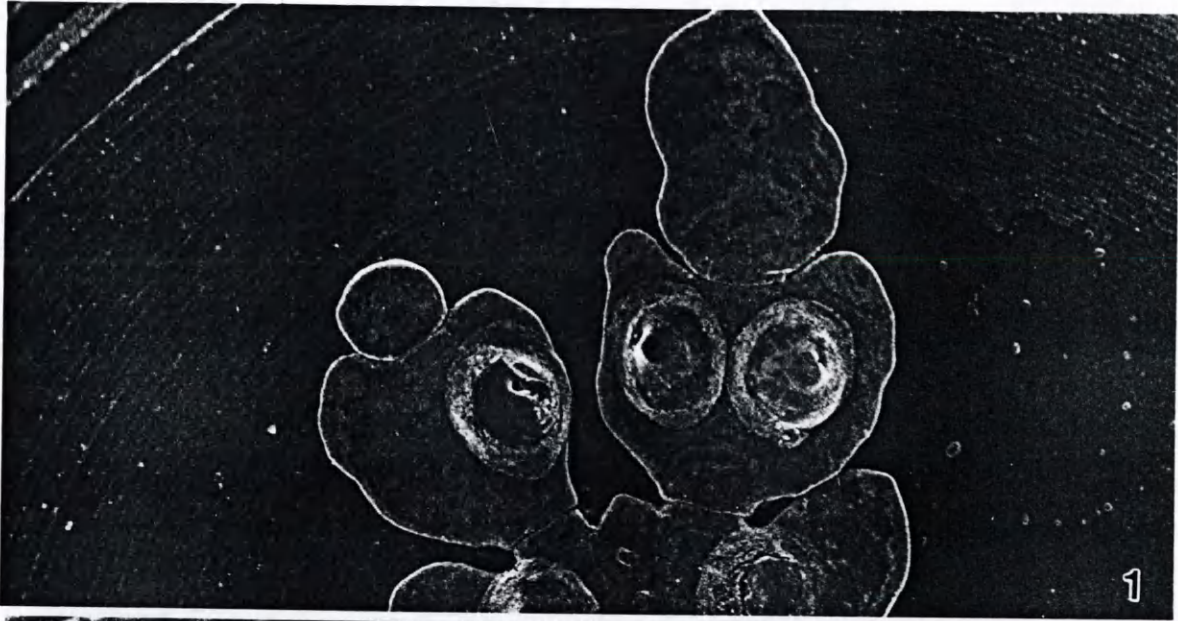
Genera surveyed in this study are shown in italics.

Photographic Plates

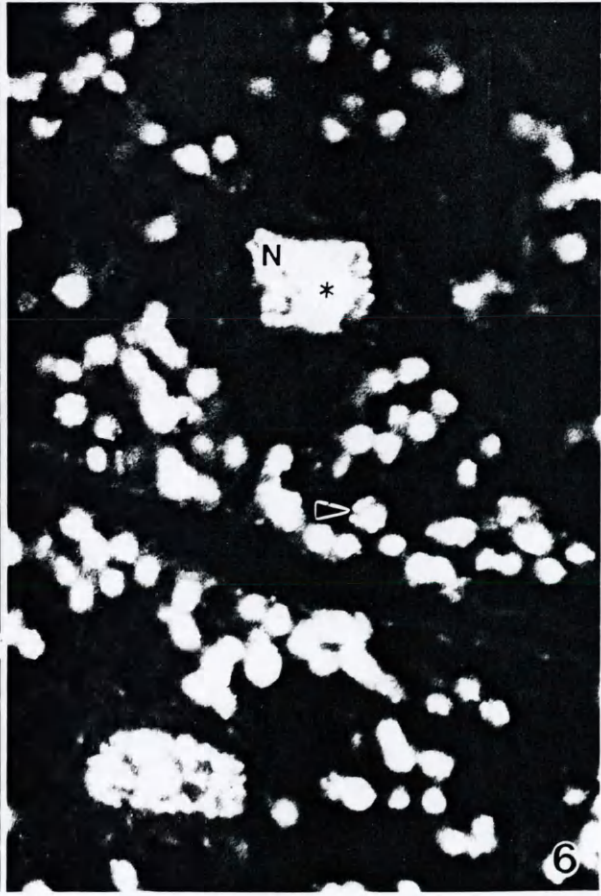
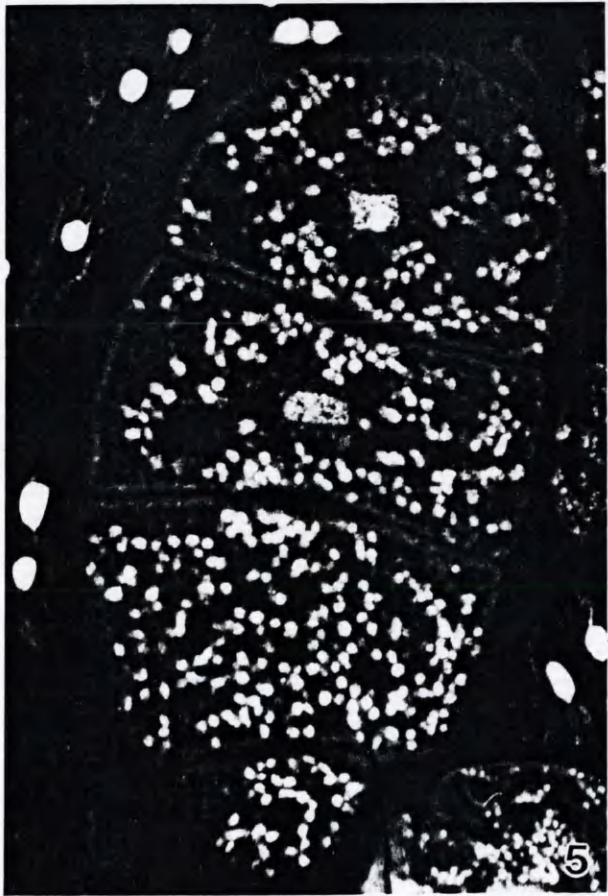
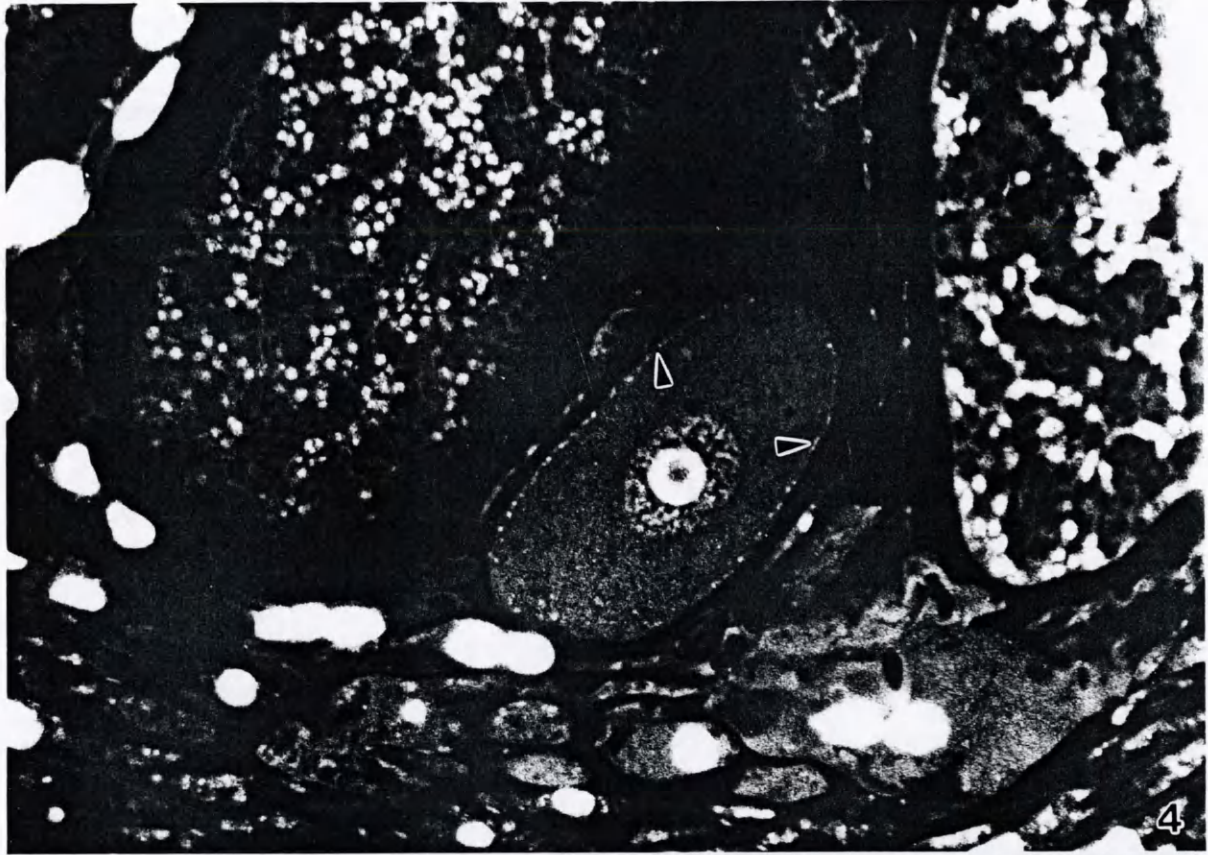
KEY TO ABBREVIATIONS

b	border
BS	bisporangium
BSW	bisporangial wall
C	chloroplast
EDM	electron-dense material
edv	electron-dense vesicle
fz	fibrillar zone
G	Golgi
m	mucilage
M	mitochondrion
N	nucleus
NE	nuclear envelope
PER	perinuclear endoplasmic reticulum
PC	pit connection
RER	rough endoplasmic reticulum
s	starch
SER	smooth endoplasmic reticulum
SM	smooth membrane
TC	tetrasporocyte (pre-meiotic)
TCW	tetrasporocyte wall
TMC	tetrasporangial mother cell
TS	tetrasporangium (post-meiotic)
TSW	tetrasporangial wall
v	mucilage vesicle
V	vacuole

- Figure 1. Scanning electron micrograph of subterminal, conceptacle-bearing intergenicula. x 19.
- Figure 2. Scanning electron micrograph of longitudinal section through intergeniculum bearing two tetrasporangial conceptacles. Note presence of bisporangium in conceptacle at the left (asterisk). x 130.
- Figure 3. Scanning electron micrograph of longitudinal section through intergeniculum bearing one tetrasporangial conceptacle. x 160.



- Figure 4. Longitudinal section through TC. Note peripheral ring of DAPI stained chloroplast DNA (arrowheads), prominent staining of nucleolus and presence of nucleolar "vacuole". Fluorescence microscopy. x 1,100.
- Figure 5. Longitudinal section through fully cleaved, stage 4 tetrasporangium. Fluorescence microscopy. x 600.
- Figure 6. Detail of tetrasporangium shown in Fig. 5. Note DAPI staining of mature chloroplasts (arrowhead) and small nucleoli (asterisk) in nuclei (N) with irregular NE. Fluorescence microscopy. x 1,500.



- Figure 7. DAPI stained tetrasporangial conceptacle. Compare staining of young TC (asterisk) with staining in surrounding mature TS (arrowhead). Fluorescence microscopy. x 130.
- Figure 8. Toluidine blue stained tetrasporangial conceptacle. Note presence of bisporangium (arrowhead). Light microscopy. x 130.
- Figure 9. DAPI stained stage 3 TS. Note stain affinity for nucleoli and perinuclear region (arrowheads). Fluorescence microscopy. x 500.
- Figure 10. Toluidine blue stain of stage 3 TS shown in Fig. 9. Note staining of perinuclear region (arrowhead). Light microscopy. x 500.

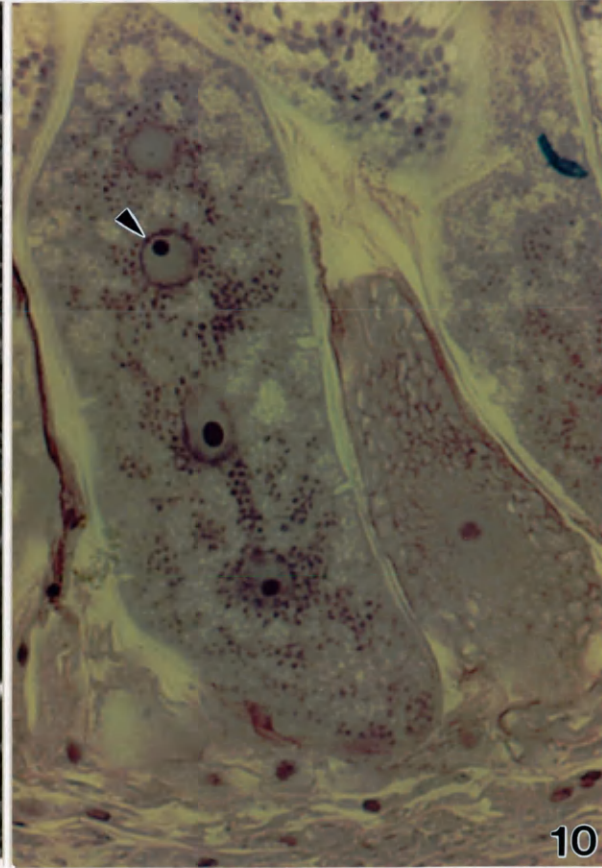
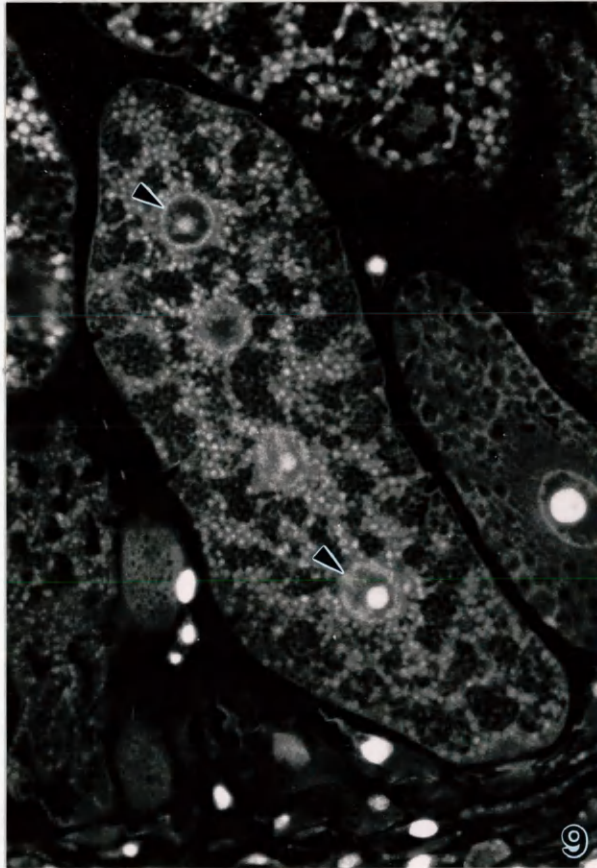
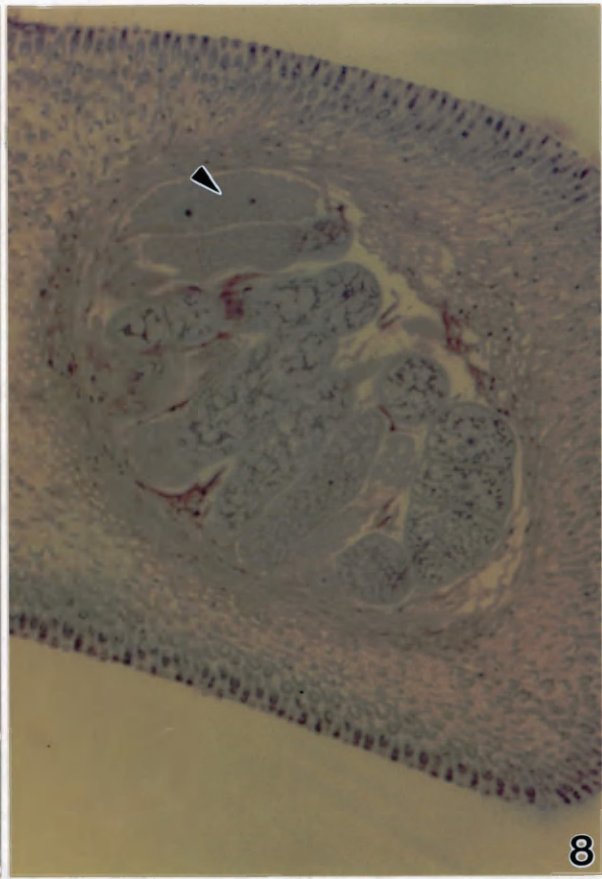
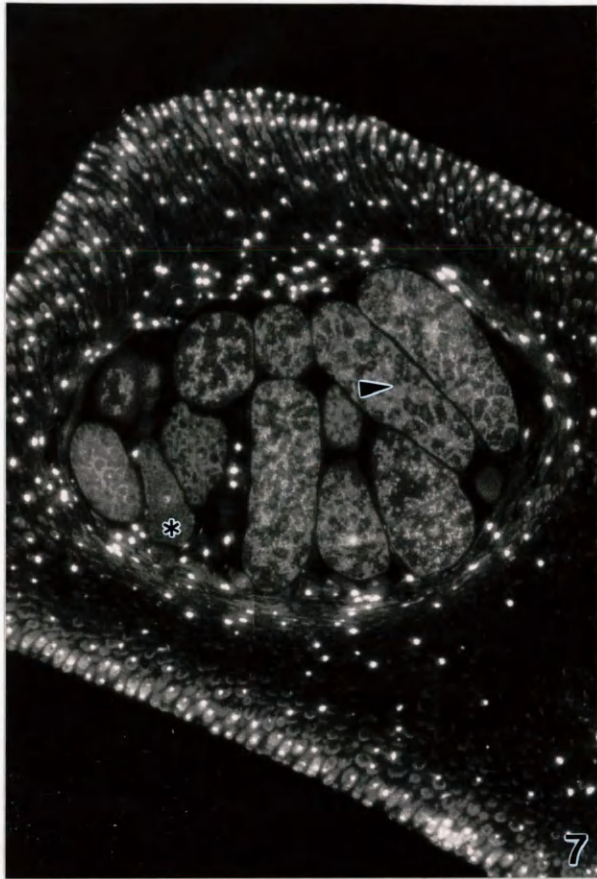
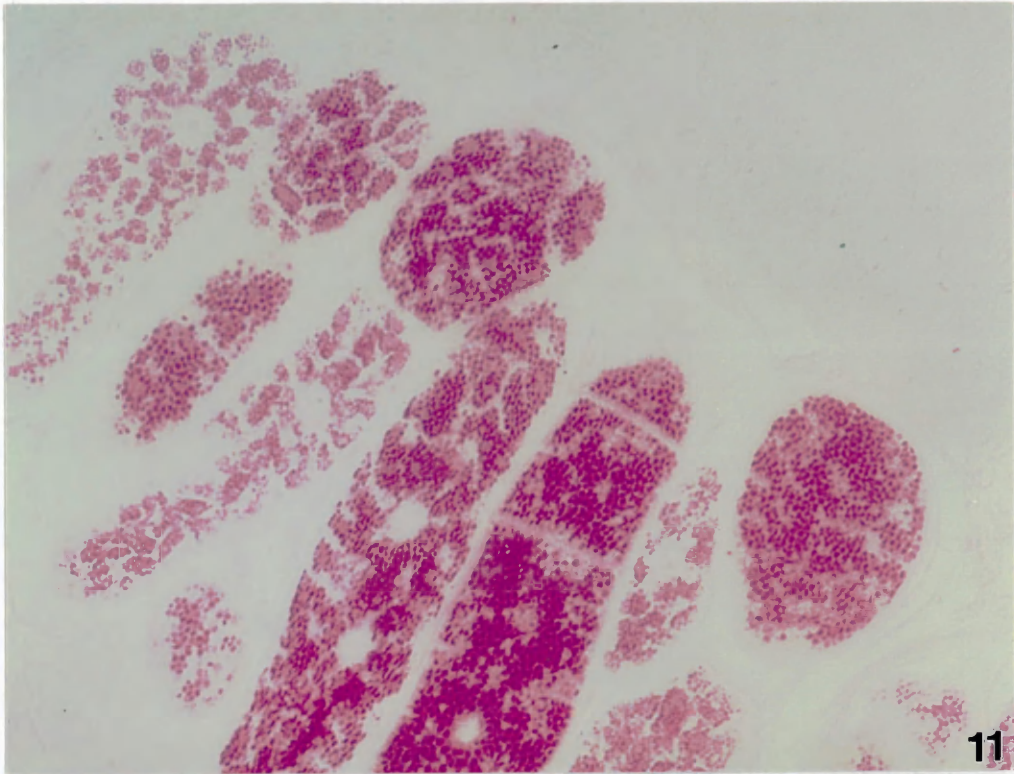


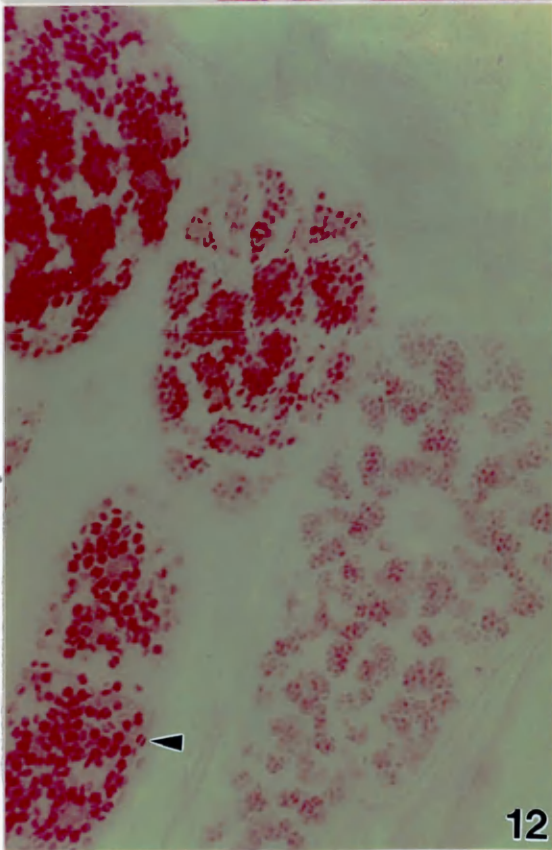
Figure 11. PAS stained TS conceptacle. Light microscopy.
x 200.

Figure 12. Three PAS stained tetrasporangia showing
progressive starch accumulation (right to left).
Note clustered starch deposition pattern and paired
starch grain organization (arrowhead). Light
microscopy. x 500.

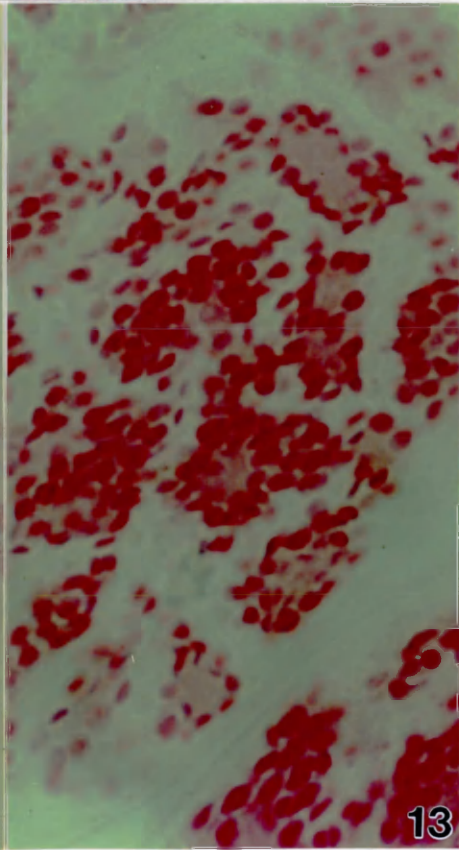
Figure 13. Detail of PAS stained stage 3 tetrasporangium.
Note presence of PAS positive material within the
starch ring. Light microscopy. x 1,300.



11



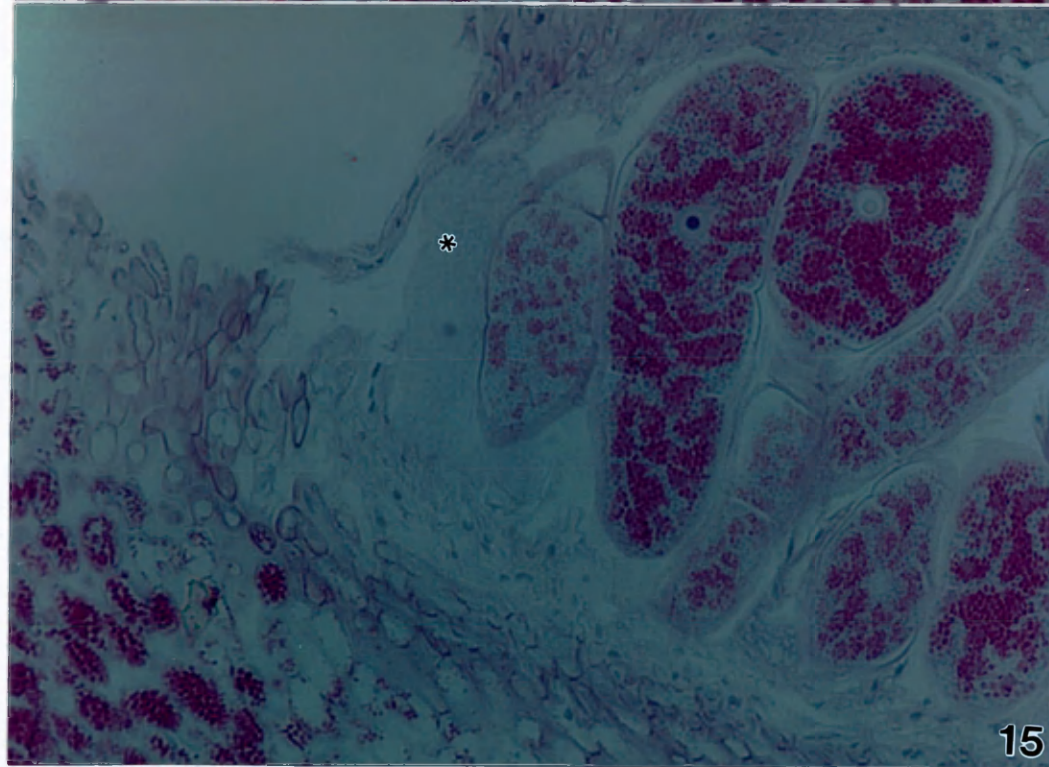
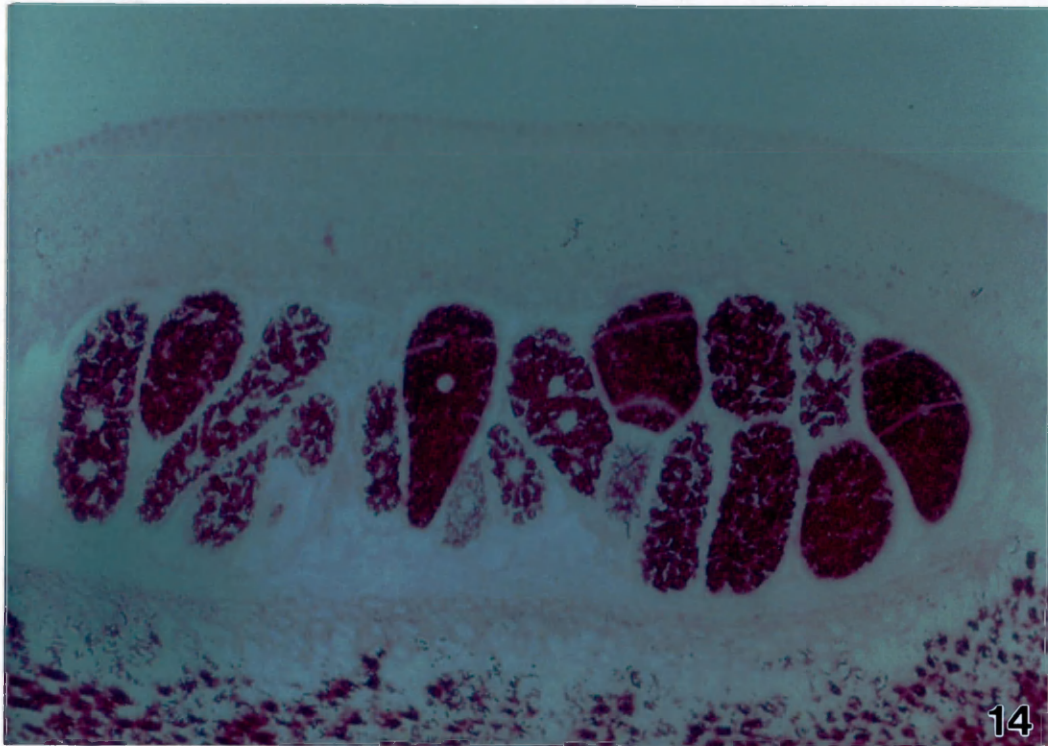
12



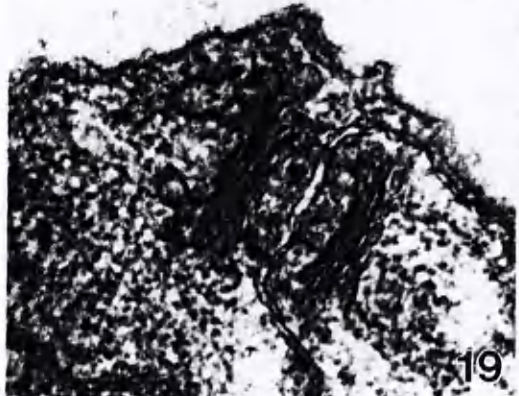
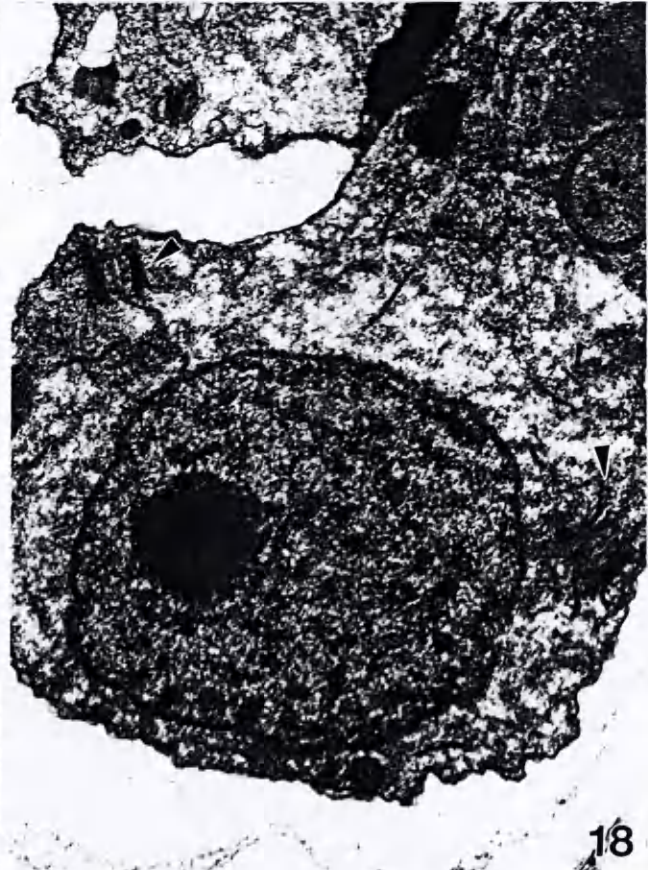
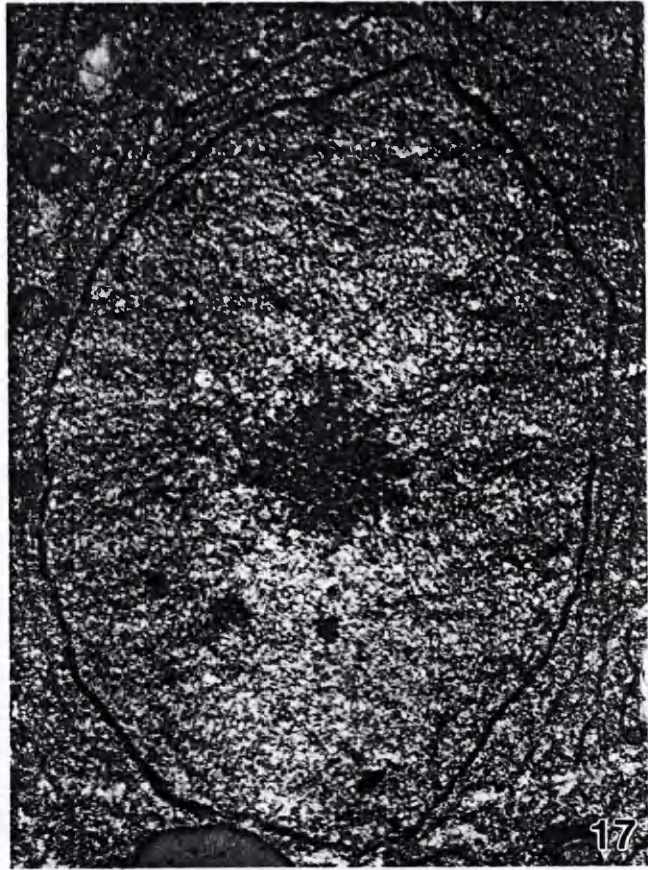
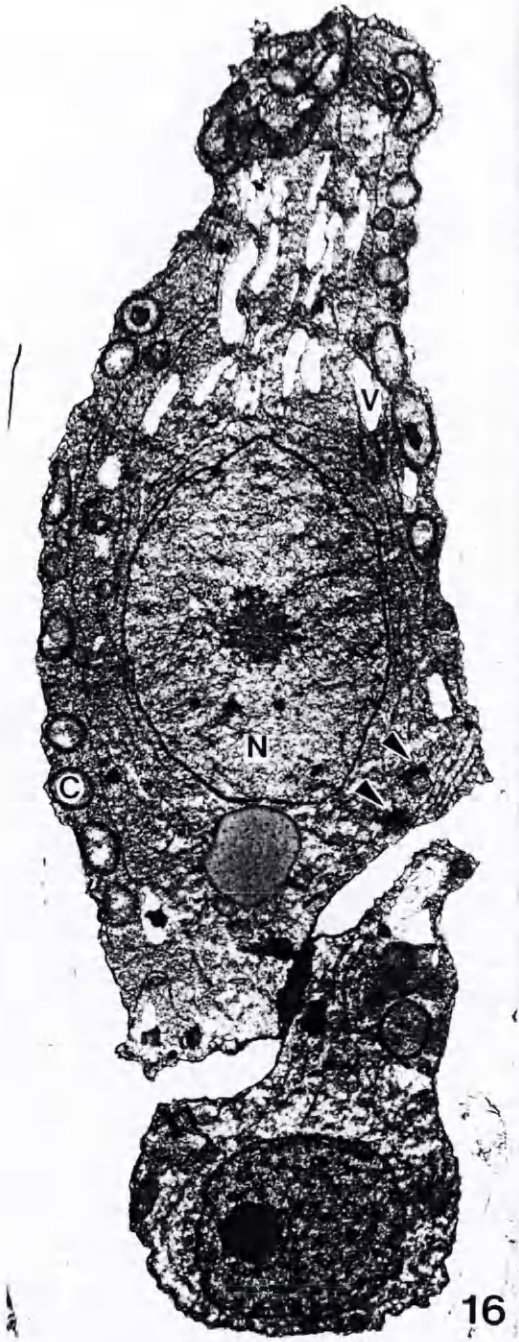
13

Figure 14. PAS stained TS conceptacle. Note absence of stain in nuclear region. Light microscopy. x 100.

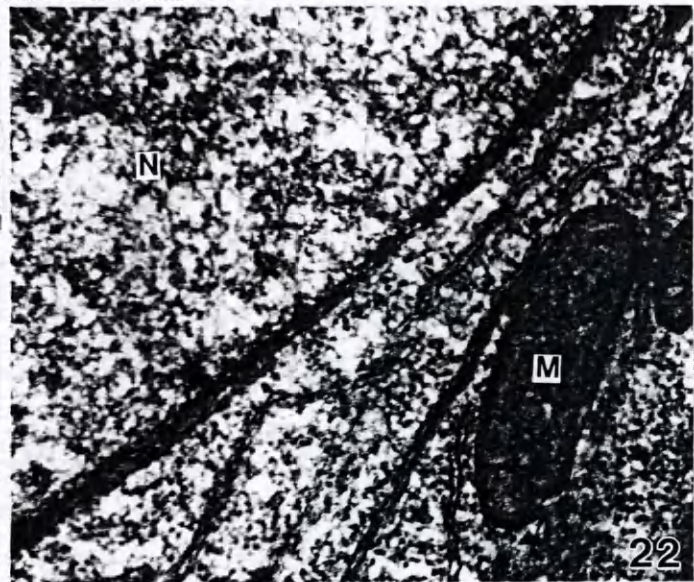
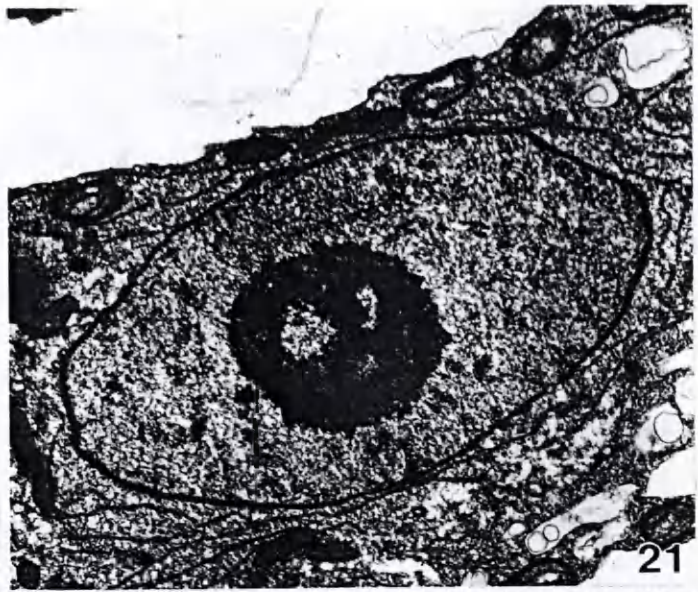
Figure 15. PAS/Toluidine blue stained sporangia. Note absence of cytoplasmic inclusions in stage 1 tetrasporocyte (asterisk). Light microscopy. x 1,000.



- Figure 16. Early stage 1 TC with PC to subtending TMC. Note beginning accumulation of vacuoles (V) in TC, the basal location of the TC nucleus (N) and the peripheral location of young chloroplasts (C). The TC nucleus is larger than the TMC nucleus. The mitochondrion-Golgi association seen in the TC (arrowheads) is absent in the TMC. x 7800.
- Figure 17. TC nucleus with PER. EDM and associated membranes have not yet formed. x 18,600.
- Figure 18. TMC with 2 sets of paired Golgi (arrowheads). x 18,600.
- Figure 19. TMC Golgi shown in Fig. 18. Note ER tract running between paired Golgi stacks. x 56,200.



- Figure 20. Stage 1 TC. Mitochondria (M) have increased in number and chloroplasts (C) have maintained a peripheral position during elongation. x 6100.
- Figure 21. Elongate pre-meiotic TC nucleus. Note diffused organization of nucleolus. x 12,200.
- Figure 22. Detail of NE on TC nucleus shown in Fig. 21. Note PER with adjacent mitochondrion (M). x 52,000.
- Figure 23. Large electron-dense lipid globule seen during stage 1 development. x 49,600.



- Figure 24. Late stage 1 TC. Note numerous vacuoles (V) small forming starch grains (arrowhead) at vacuole periphery, and TCW outside TC plasmalemma. x 2,000.
- Figure 25. Tangential section of late stage 1 TC nucleus. Smooth surfaced membranes (SM) coated with EDM seen for the first time surrounding the nucleus. Mitochondria surround the SM region. x 7100.
- Figure 26. Small Golgi with flat straight cisternae located in nuclear region shown in Fig. 25. Small mucilage vesicles (v) seen for the first time. x 69,500.
- Figure 27. Longitudinal section through midregion of late stage 1 TC nucleus. SM at NE is absent at nuclear poles (asterisks). Note nucleolar "vacuole". x 5700.
- Figure 28. SM at NE on nucleus (N) shown in Fig. 27. Mitochondria (M) abut the SM system and EDM coats SM cisternae. x 7800.

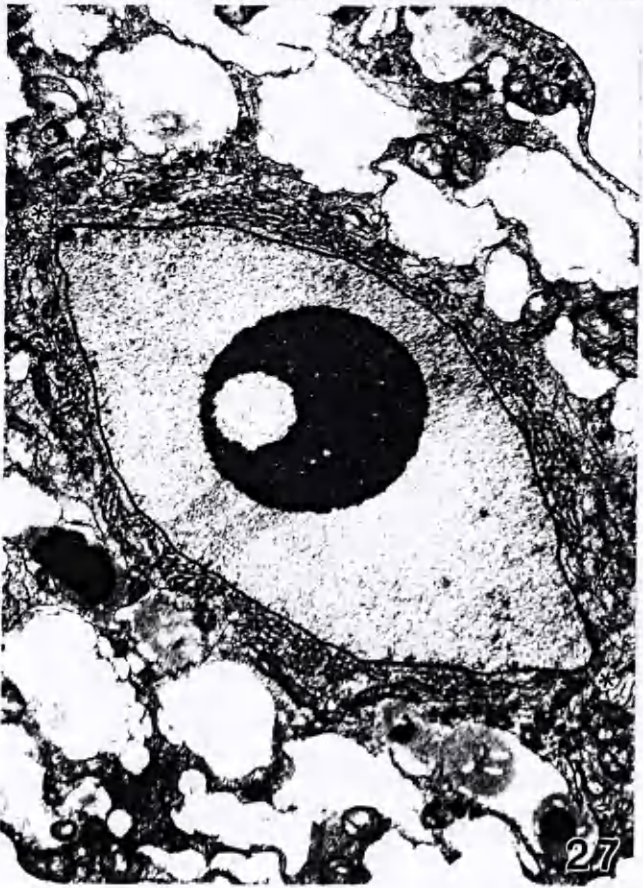
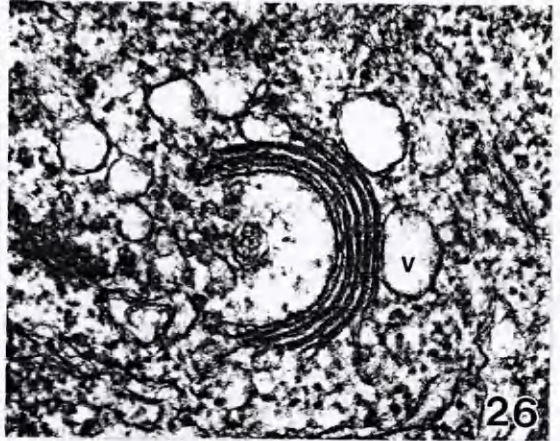
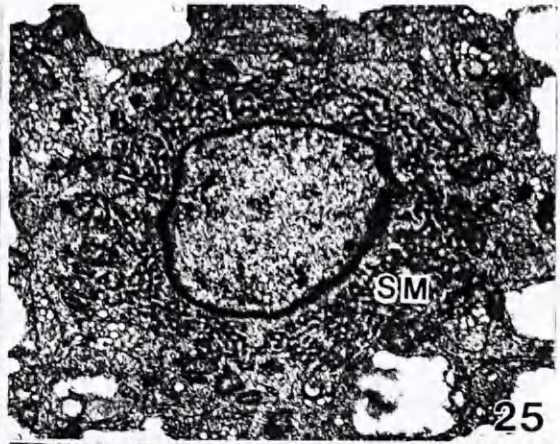
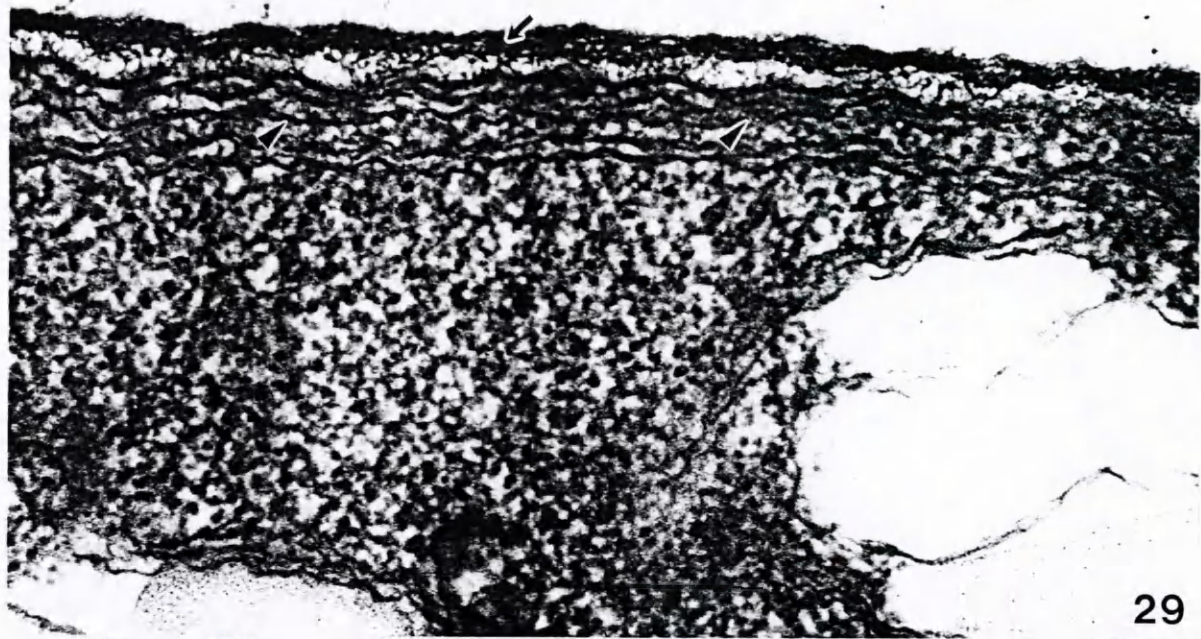


Figure 29. Periphery of late stage 1 TC. Peripheral RER is present (arrowheads). Dark fibrous layer (arrow) to the outside of the plasmalemma indicates beginning tetrasporangial wall (TSW) formation. x 89,000.

Figure 30. Late stage 1 TC vacuole (V) containing membranous material. RER (arrowhead) delimits starch (s) at vacuole periphery. x 33,400.



29



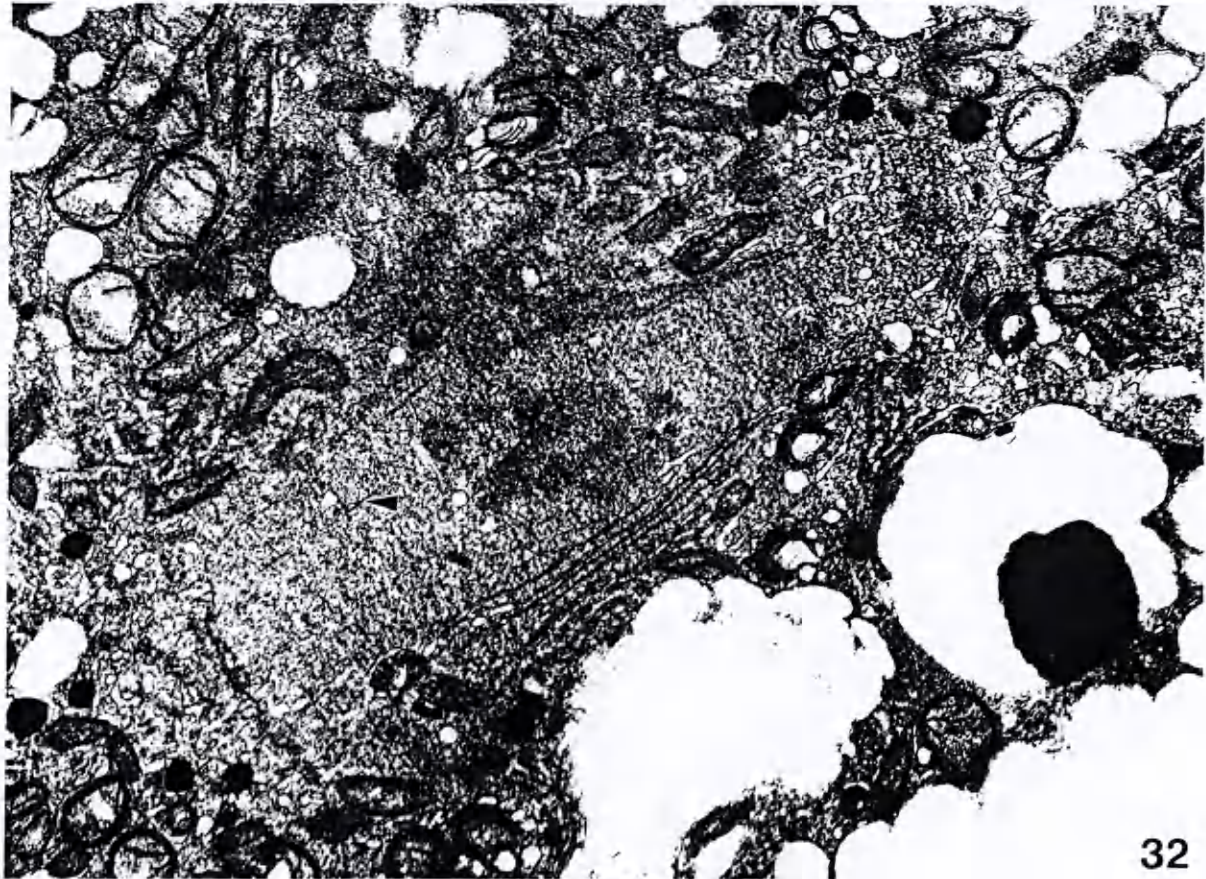
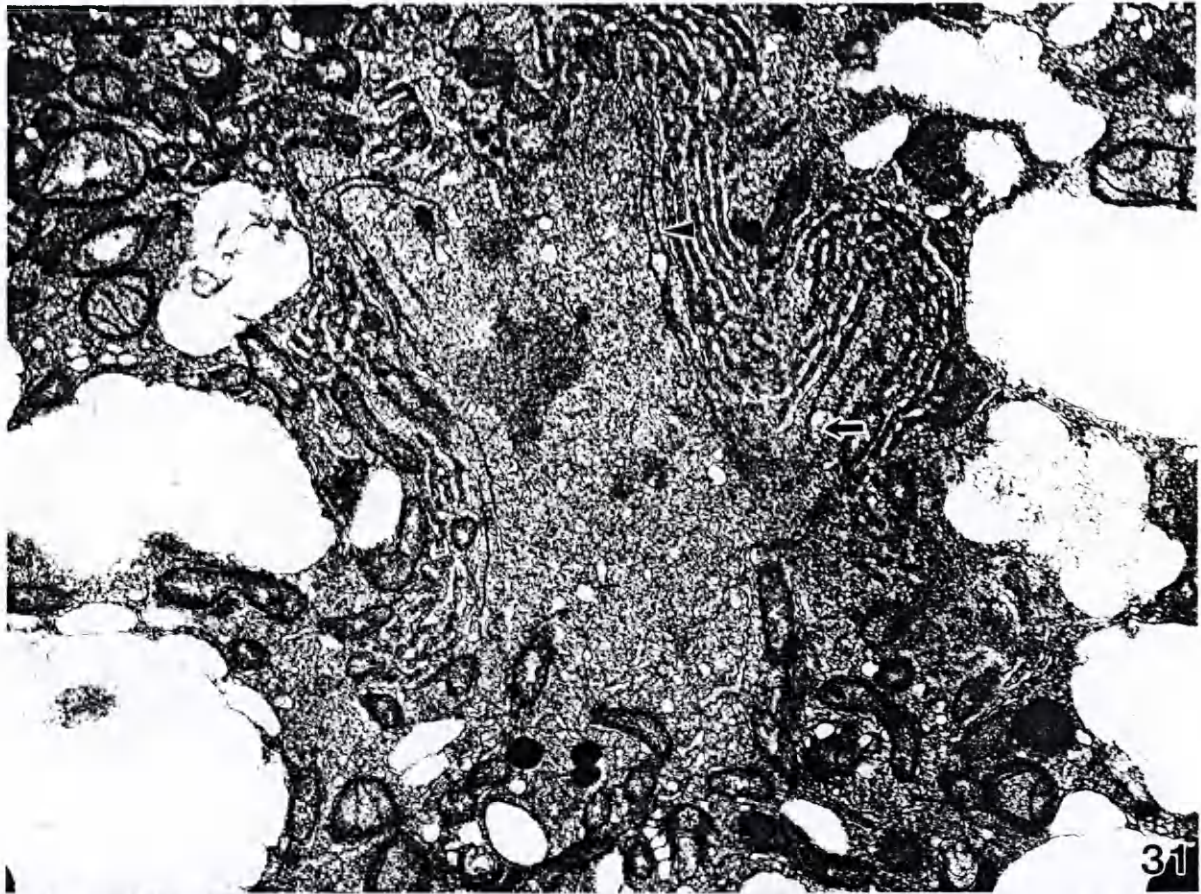
v

s

30

Figure 31. Stage 2 distal meiotic nucleus. Single layer of PER seen outside NE (arrowhead). EDM coated SM are oriented parallel to NE and non-EDM coated SM occupy the division poles. Note irregular contour of nucleus and sloughing of nucleoplasm (arrow). Mucilage secreting Golgi are common in the nuclear vicinity (asterisk). Starch-flanked vacuoles persist from Stage 1. x 11,500.

Figure 32. Stage 2 proximal meiotic nucleus. Smooth membranes at poles are prominent in this plane of sectioning. Microtubules (arrowhead) and smooth membranes are seen within the nucleus. x 11,500.



- Figure 33. Starch-flanked V at plasmalemma in stage 2 meiotic sporangium. Contact region lacks starch. TCW material visible to outside of dark TSW layer. x 15,100.
- Figure 34. Starch-flanked V located at the plasmalemma opposite the vacuole shown in Fig. 33. x 47,000.
- Figure 35. Starch-free region of contact on vacuole shown in Fig. 33. Note fine fibrils associated with plasmalemma. x 15,000.
- Figure 36. Detail of starch-free contact region on vacuole shown in Fig. 34. Note tonoplast membranes (arrowhead) in vacuole. 111,300.

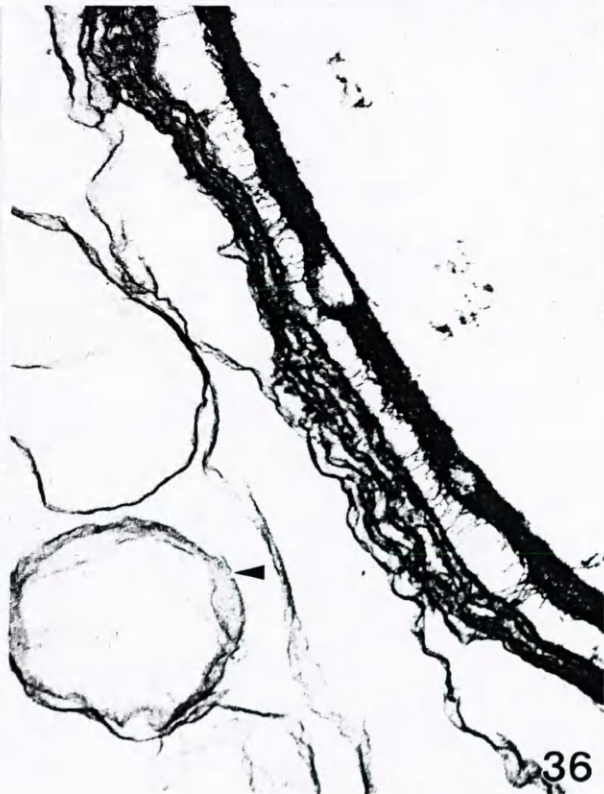
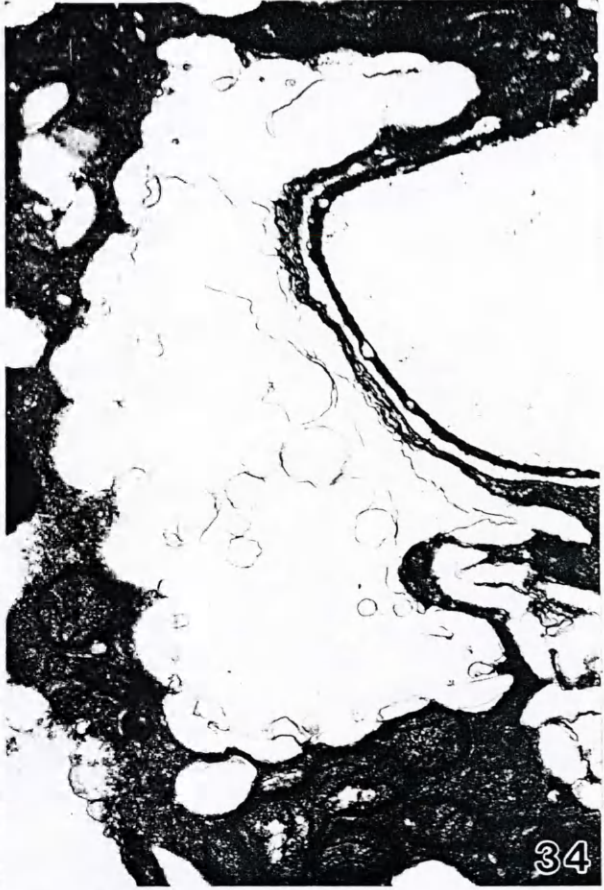
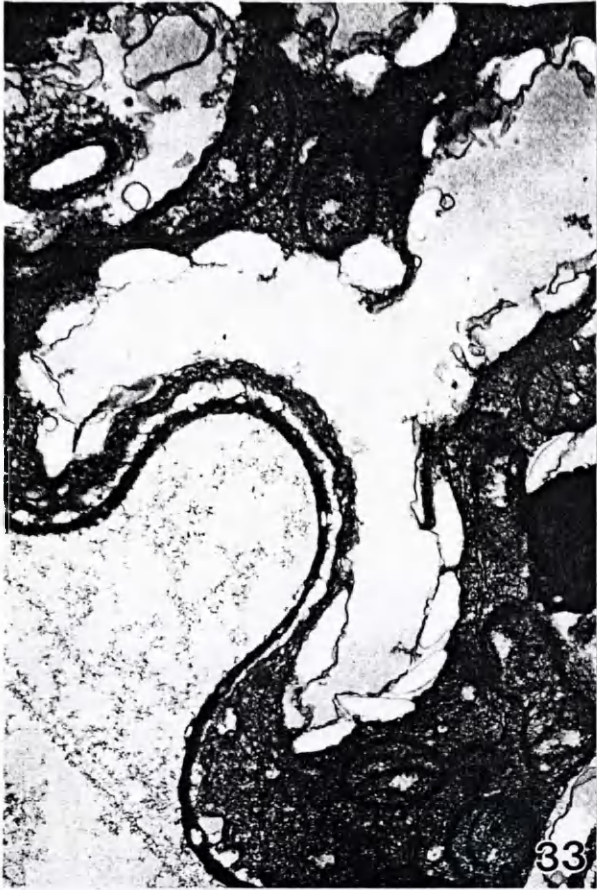
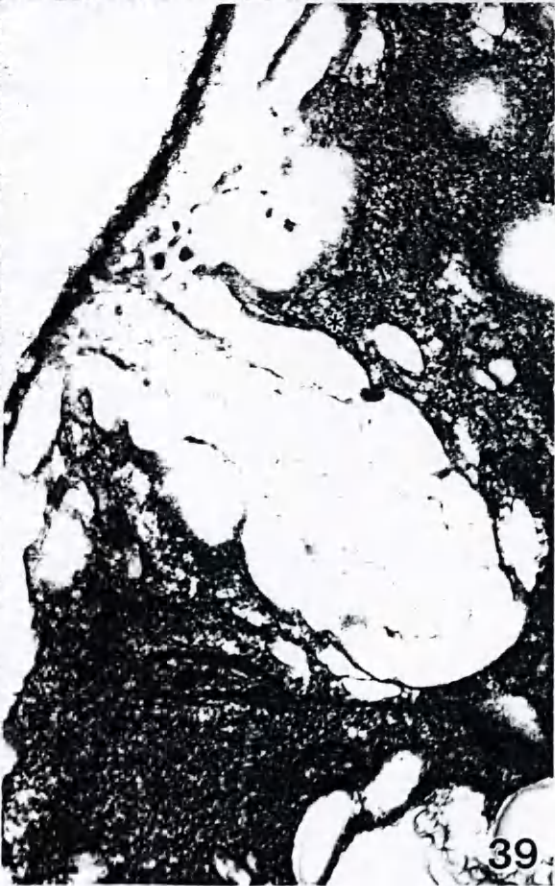
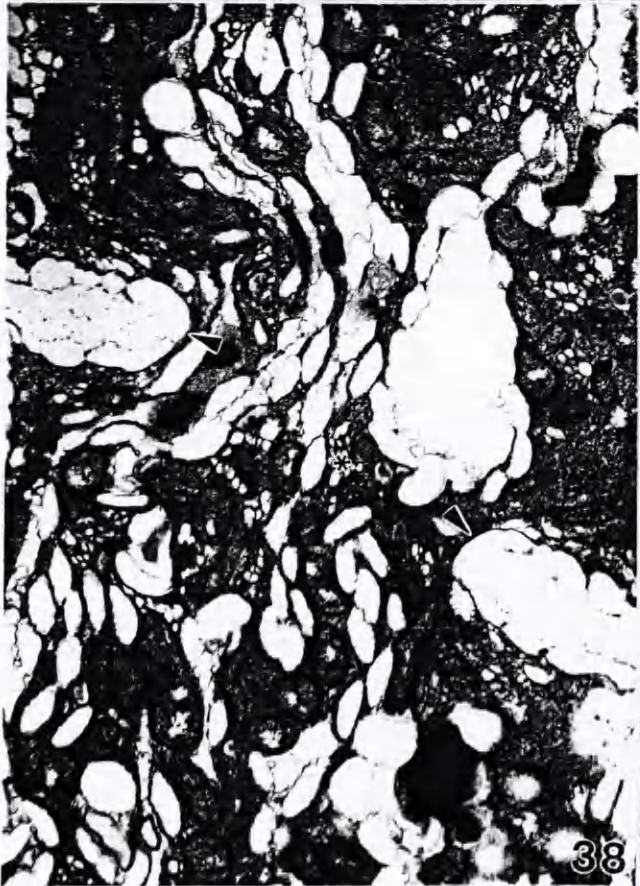
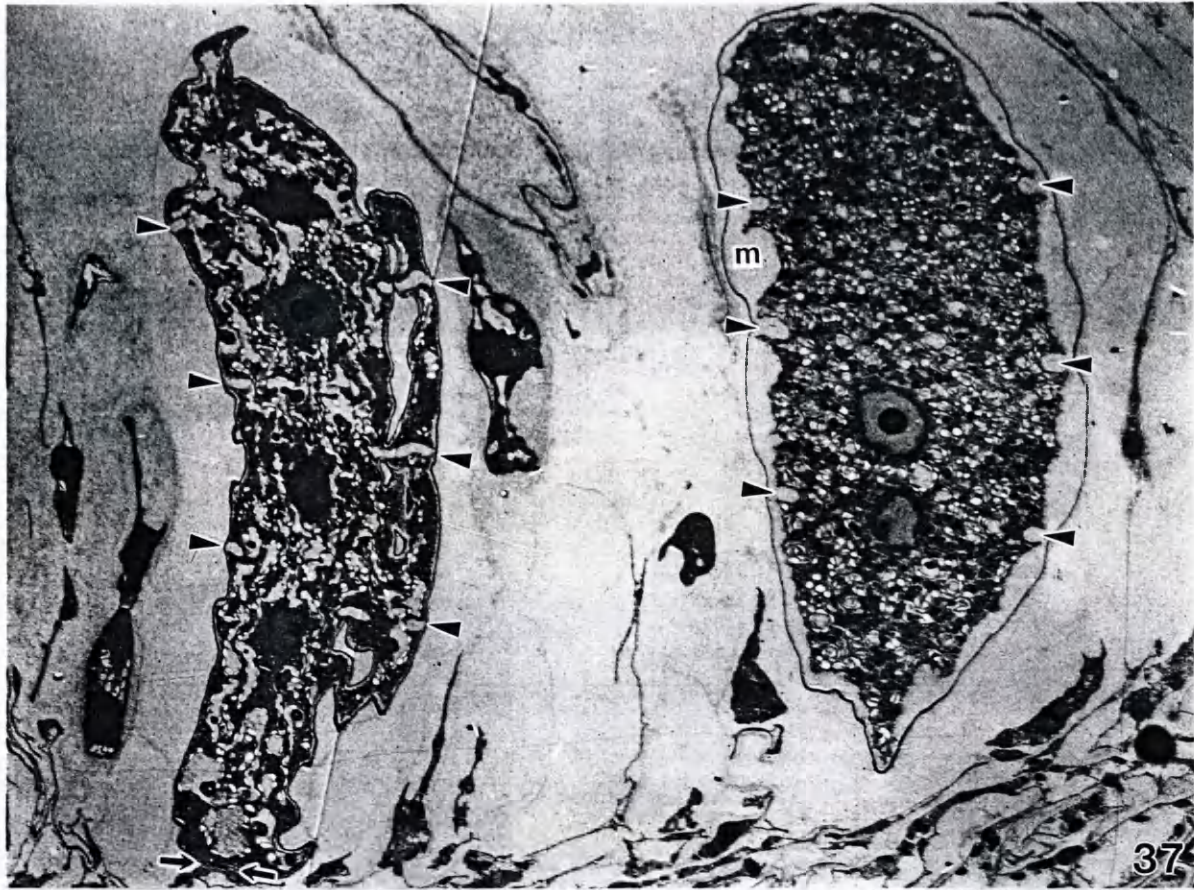


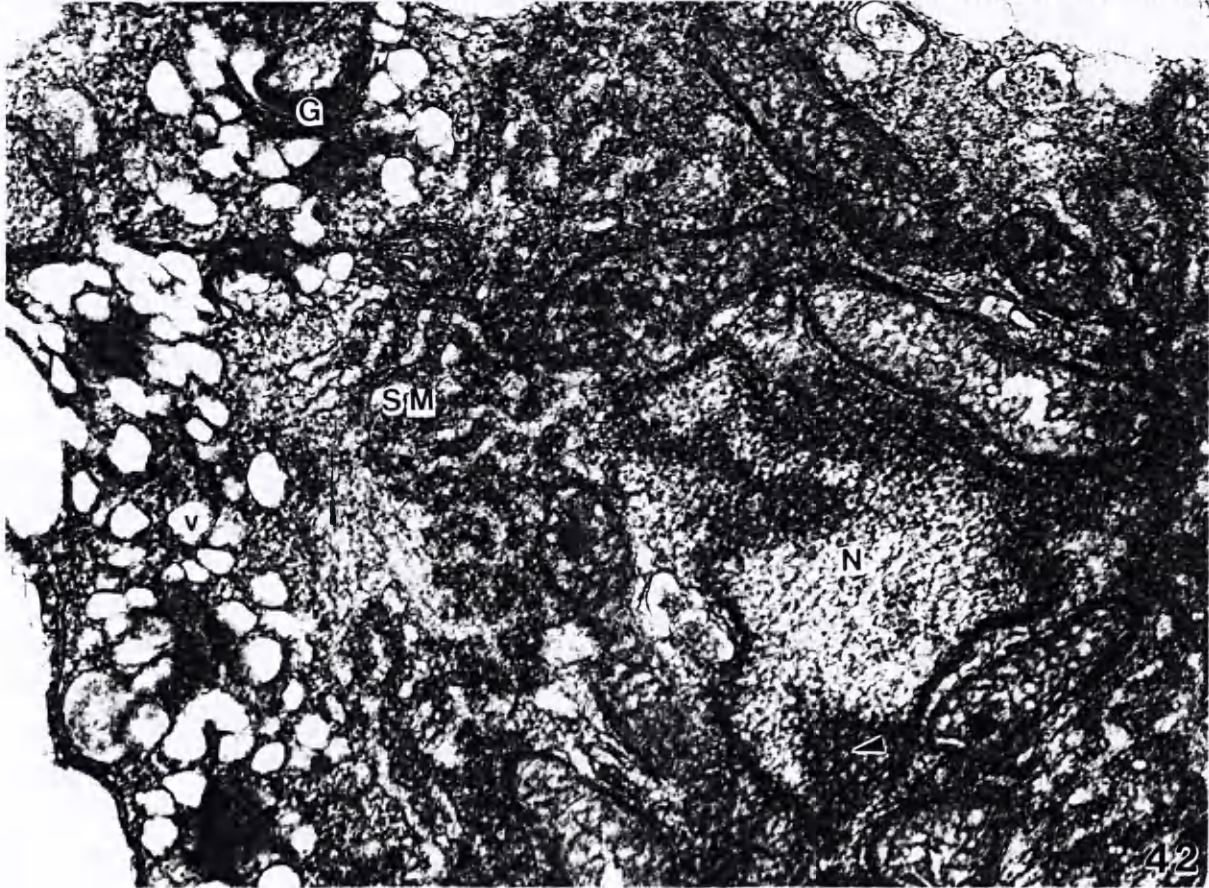
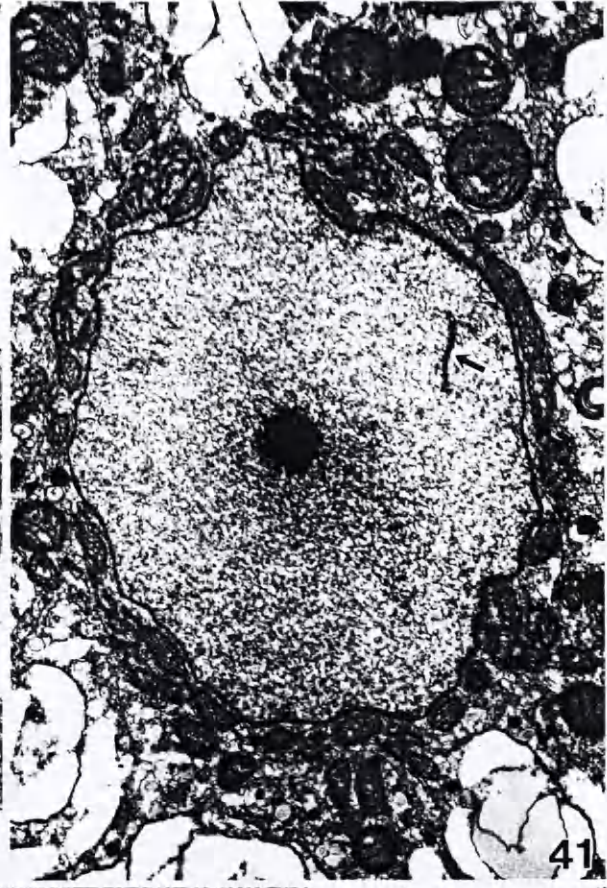
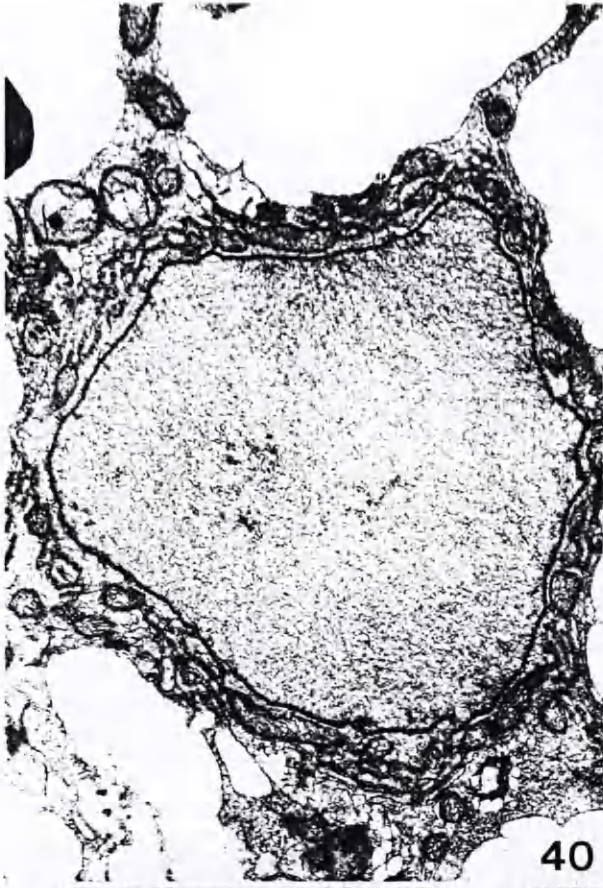
Figure 37. Stage 3 vacuolate TS. Sporangium at left shows highly vacuolate condition seen during meiosis. Small, singular starch grains are seen at periphery of each vacuole. Thin mucilage layer separates TS wall from TS plasmalemma. TMC pit connection (arrow) still visible. Sporangium at right shows reduction in vacuole size with greater than one layer of concentric starch grains at vacuole periphery. Thick mucilage layer (m) separates TS wall from TS plasmalemma. Cleavage furrows are visible in both sporangia, with an earlier developmental stage seen in sporangium at left (arrowheads). x 880.

Figure 38. Early cleavage furrows on stage 3 vacuolate TS at left in Fig. 37. Vacuoles (arrowheads) located on opposite sides of TS mark sites of cleavage initiation. Note presence of mucilage vesicles (asterisk) throughout TS cytoplasm. x 21,000.

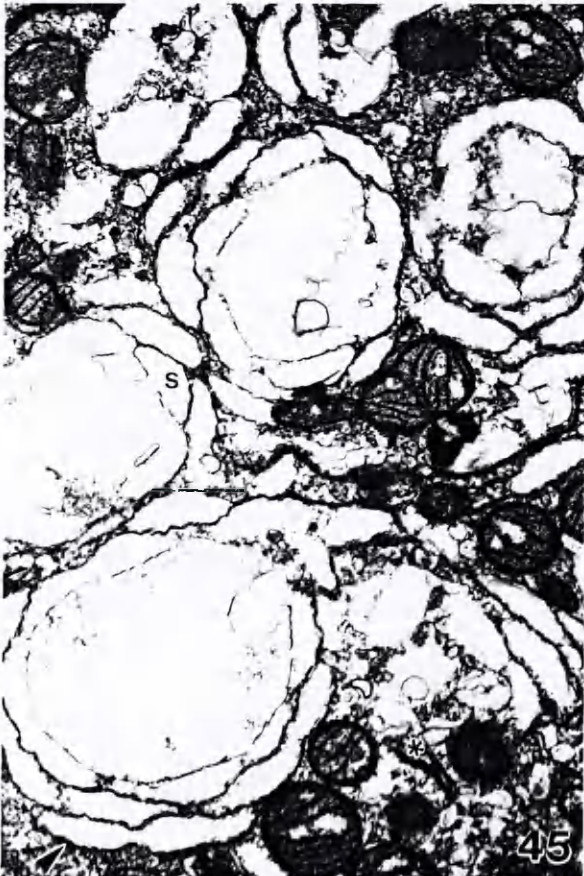
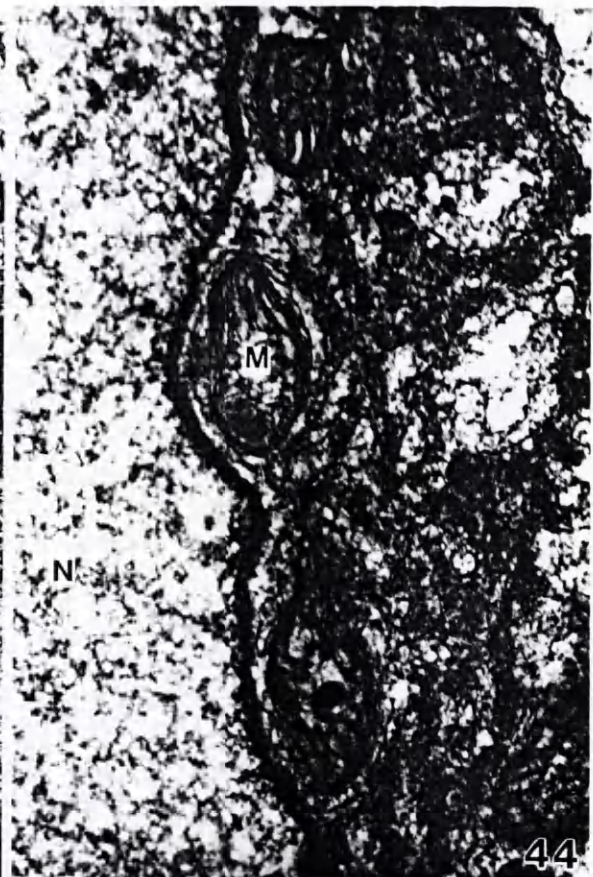
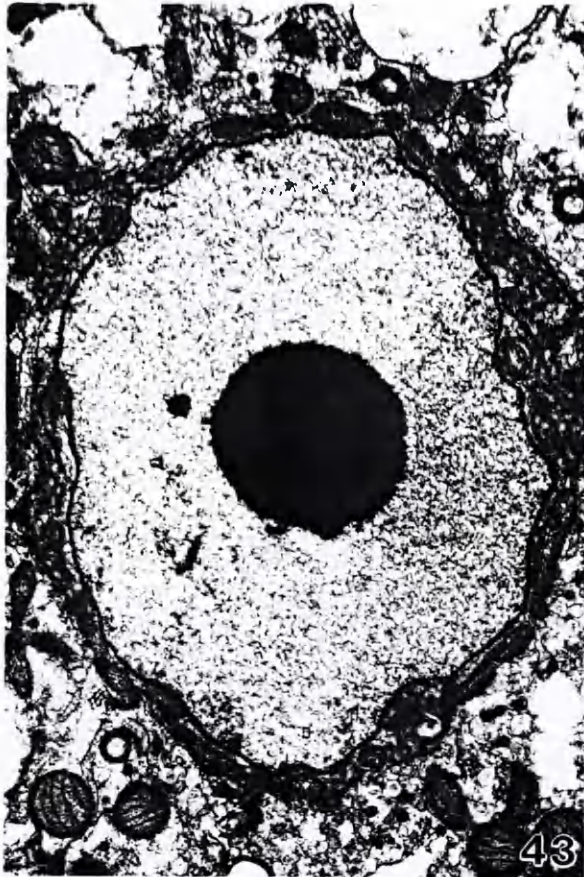
Figure 39. Detail of cleavage furrow at right in Fig. 38. Note dark material extending to TS wall. ER-starch grain association no longer visible at vacuole periphery (asterisk). x 56,000.



- Figure 40. Nucleus from TS at left in Fig. 37. Close association of mitochondria seen for first time at NE. SM-EDM reduced from meiosis. x 38,000.
- Figure 41. Nucleus from TS at left in Fig. 37. Note close association of mitochondria with NE and annulate lamellae inside nucleus (arrow). x 38,000.
- Figure 42. Glancing section of nucleus (N) from TS at left in Fig. 37 showing nuclear pores (arrowhead), mitochondria (M), and smooth membranes (SM) coated with electron-dense material (EDM). Golgi (G) and mucilage vesicles (v) are abundant in nuclear vicinity. x 92,600.



- Figure 43. Nucleus from TS at right in Fig. 37. x 21,000.
- Figure 44. Mitochondria (M) at NE on nucleus (N) shown in Fig. 43. Note irregular nuclear outline and EDM coated SM region. x 22,300.
- Figure 45. Vacuoles in mature stage 3 vacuolate TS. Note concentric organization of lenticular starch grains (s) at vacuole periphery. Each starch grain is surrounded by a single ER cisternum (arrowhead). Elongate, flattened membranes are present in the cytoplasm (asterisk). x 12,900.
- Figure 46. Chloroplast replication seen in stage 3 vacuolate TS. x 40,300.



- Figure 47. Periphery of stage 3 vacuolate TS. Clusters of mucilage vesicles (arrowheads) seen in cytoplasm. Note mucilage accumulation (m) and separation of TSW from TS plasmalemma (arrow). x 7,800.
- Figure 48. Cluster of mucilage vesicles. Note darkened material surrounding central vesicle (v) in cluster. x 56,200.
- Figure 49. Periphery of stage 3 vacuolate TS. Note swollen Golgi cisternae (asterisk), mucilage vesicle (v) secretion and elongate flattened membranes (arrowhead). x 56,000.

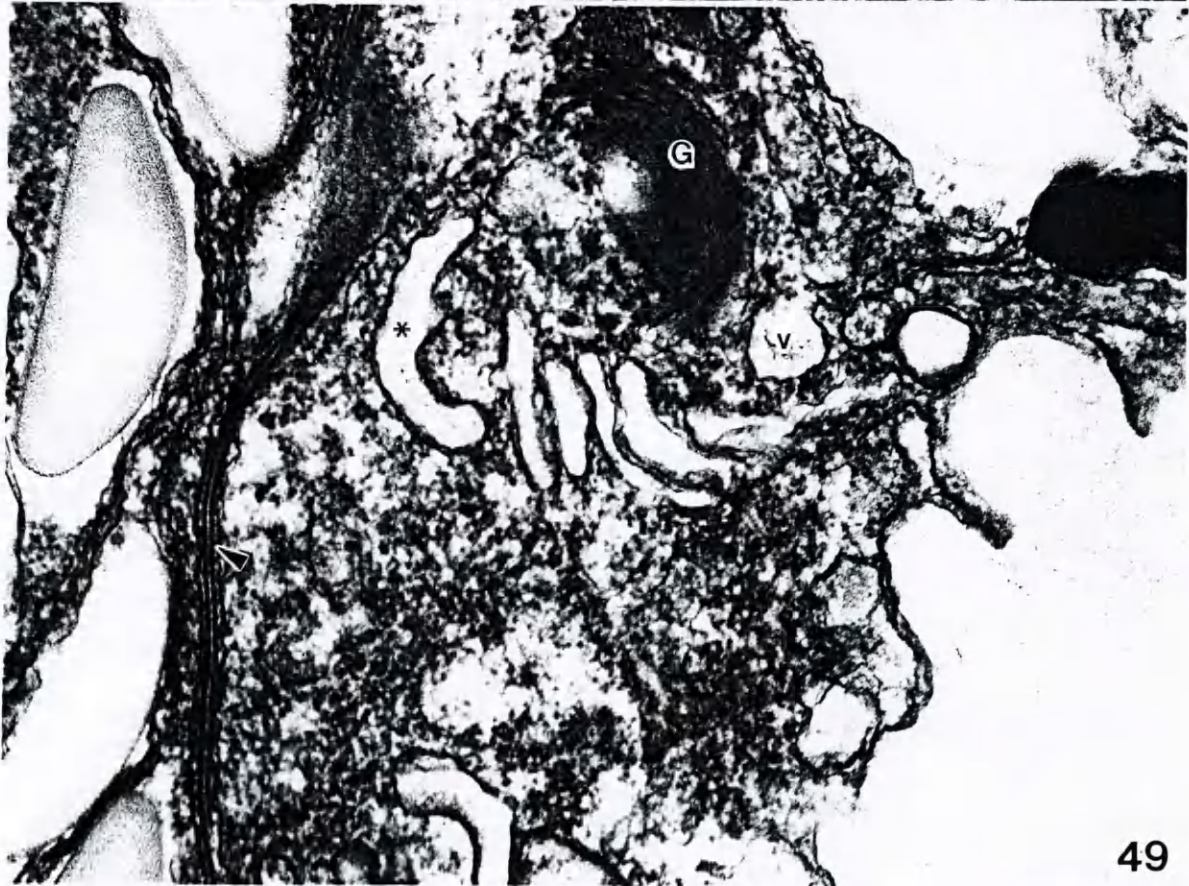


Figure 50. Stage 3 post-vacuolate TS. Note starch-flanked edv aggregations (asterisk) and paired starch grain pattern. x 1400.

Figure 51. Detail of edv aggregations. x 6400.

Figure 52. edv-secreting Golgi at sporangial periphery. Note mitochondrion-Golgi association and peripheral RER at plasmalemma (arrowhead). x 42,500.

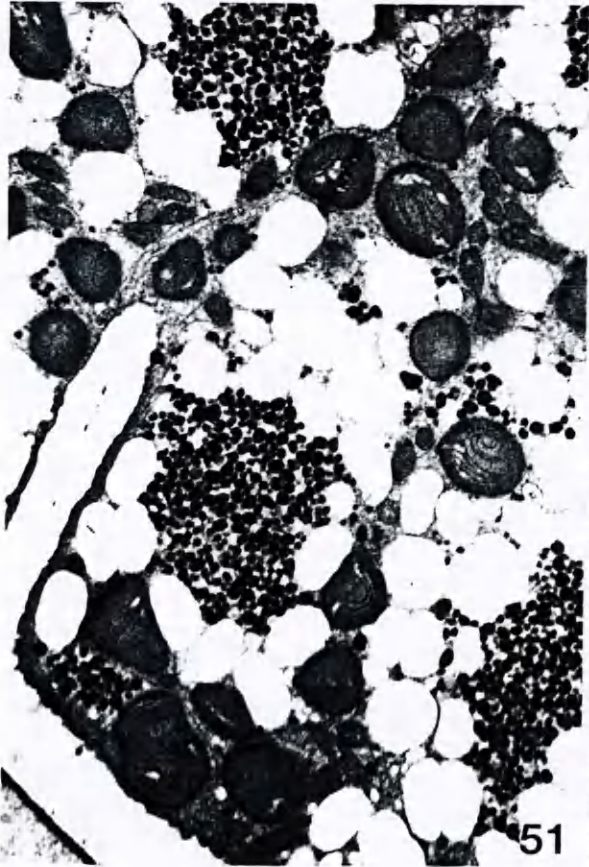
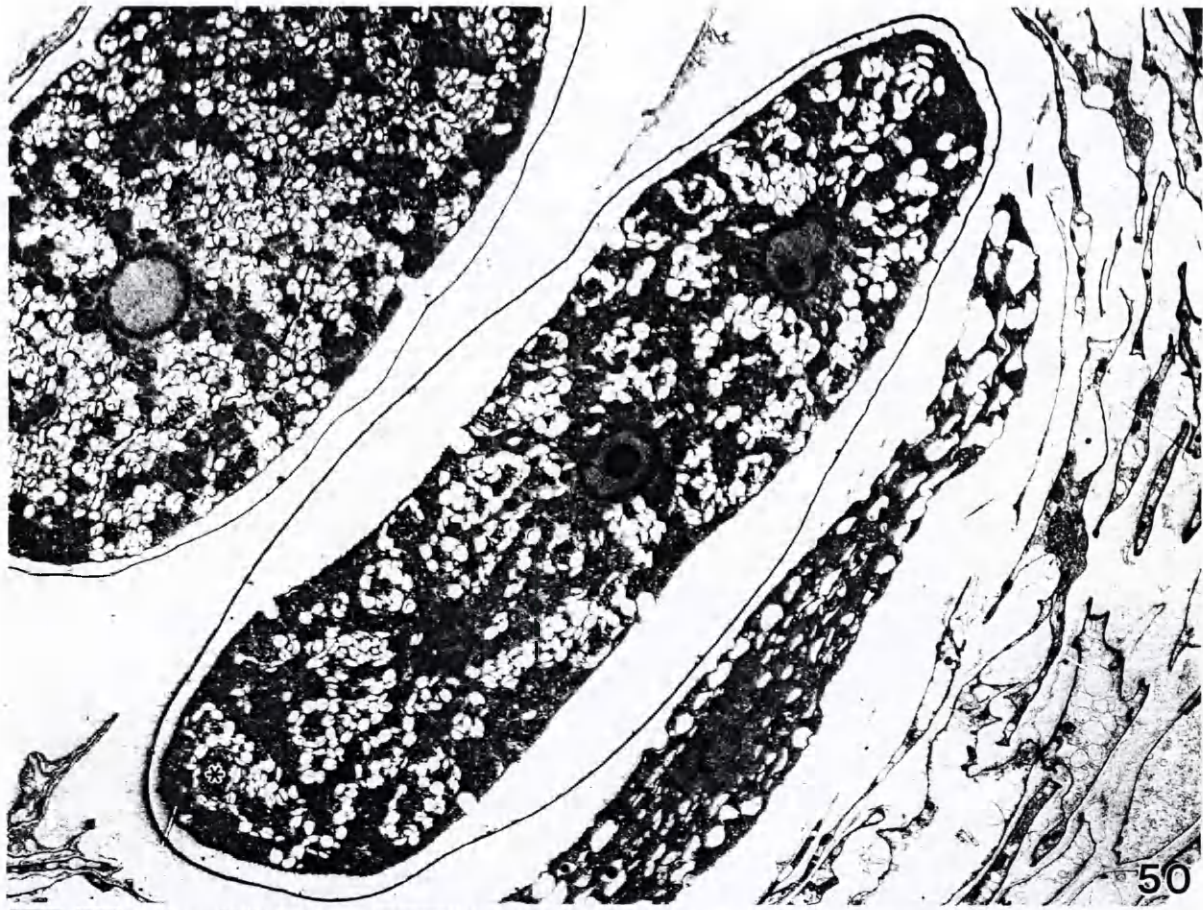


Figure 53. Stage 3 post-vacuolate TS nucleus. Note Golgi (arrowheads) at nuclear periphery and ER tracts radiating from the nucleus (arrows). x 7800.

Figure 54. Periphery of nucleus shown in Fig. 53. Note mitochondrion-Golgi association and appressed cisternae at Golgi midregion. x 53,700.

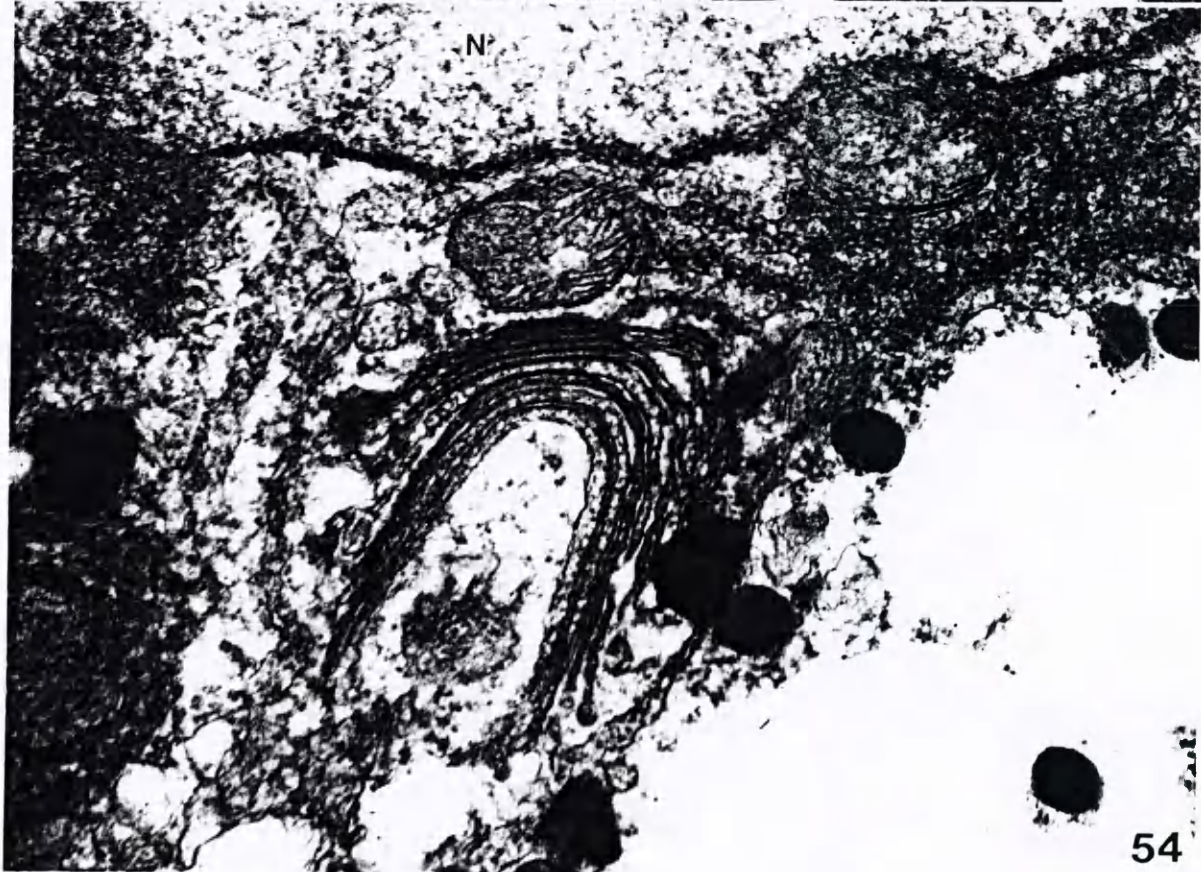
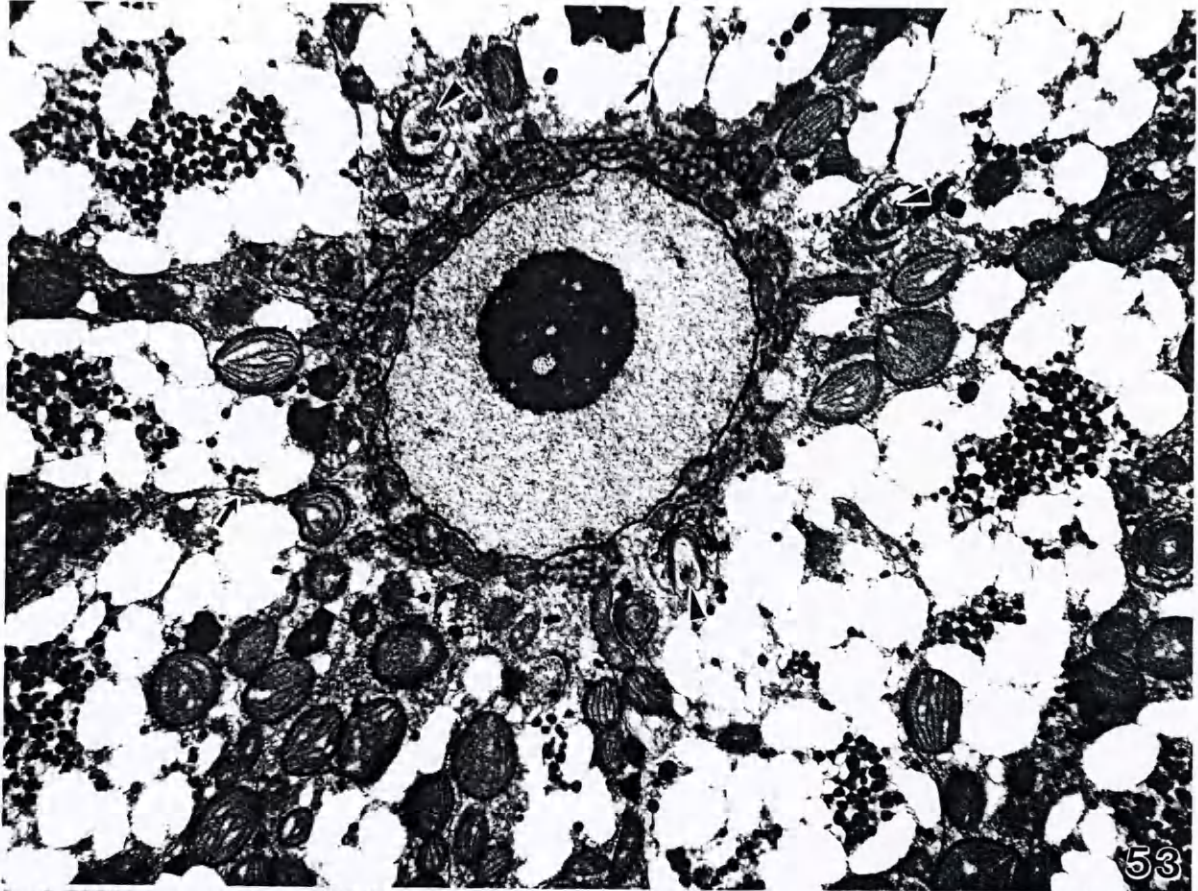
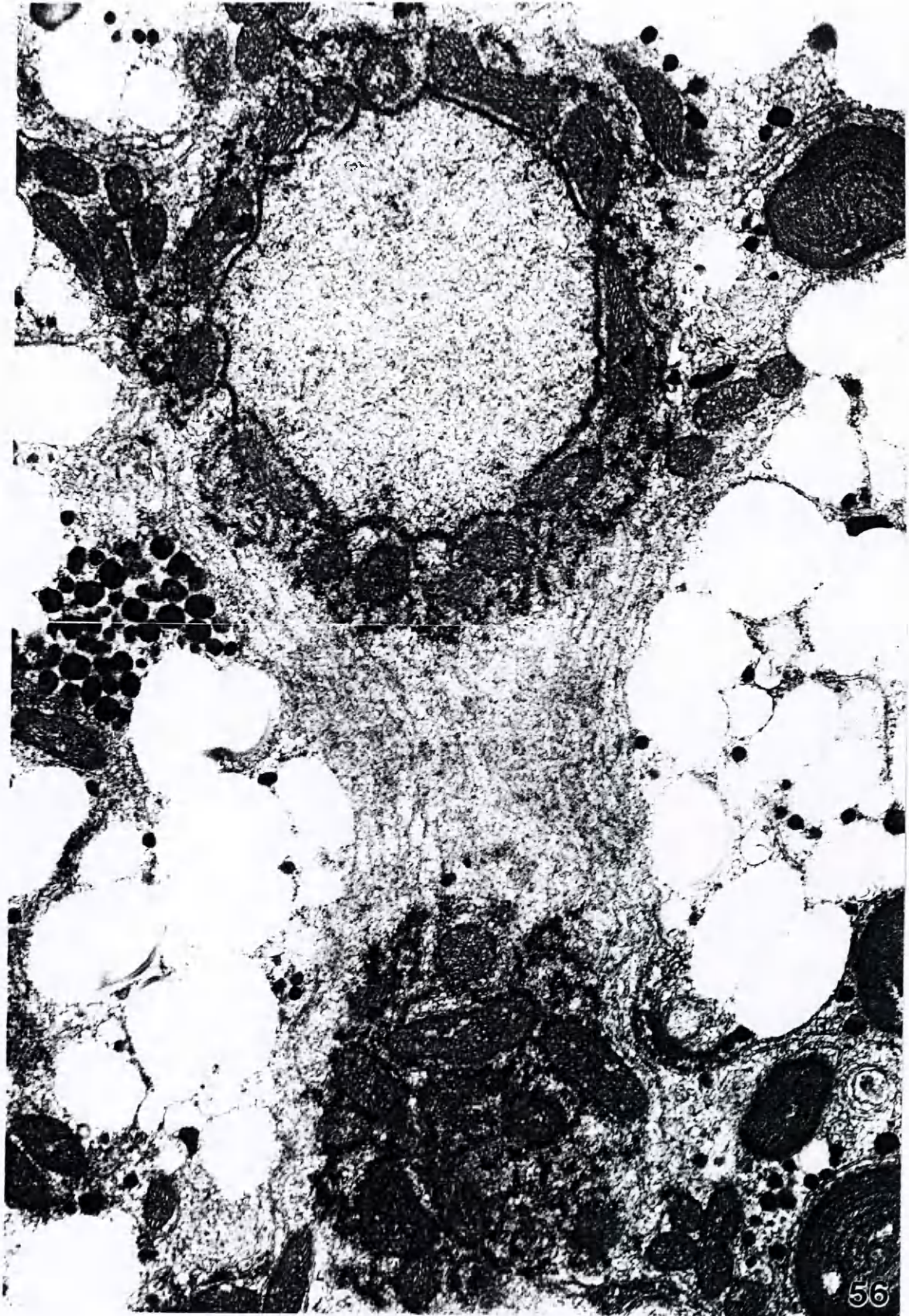


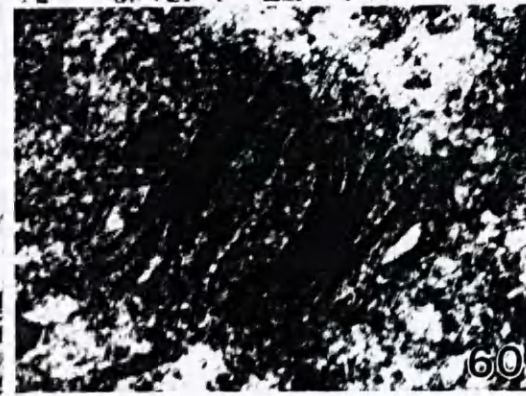
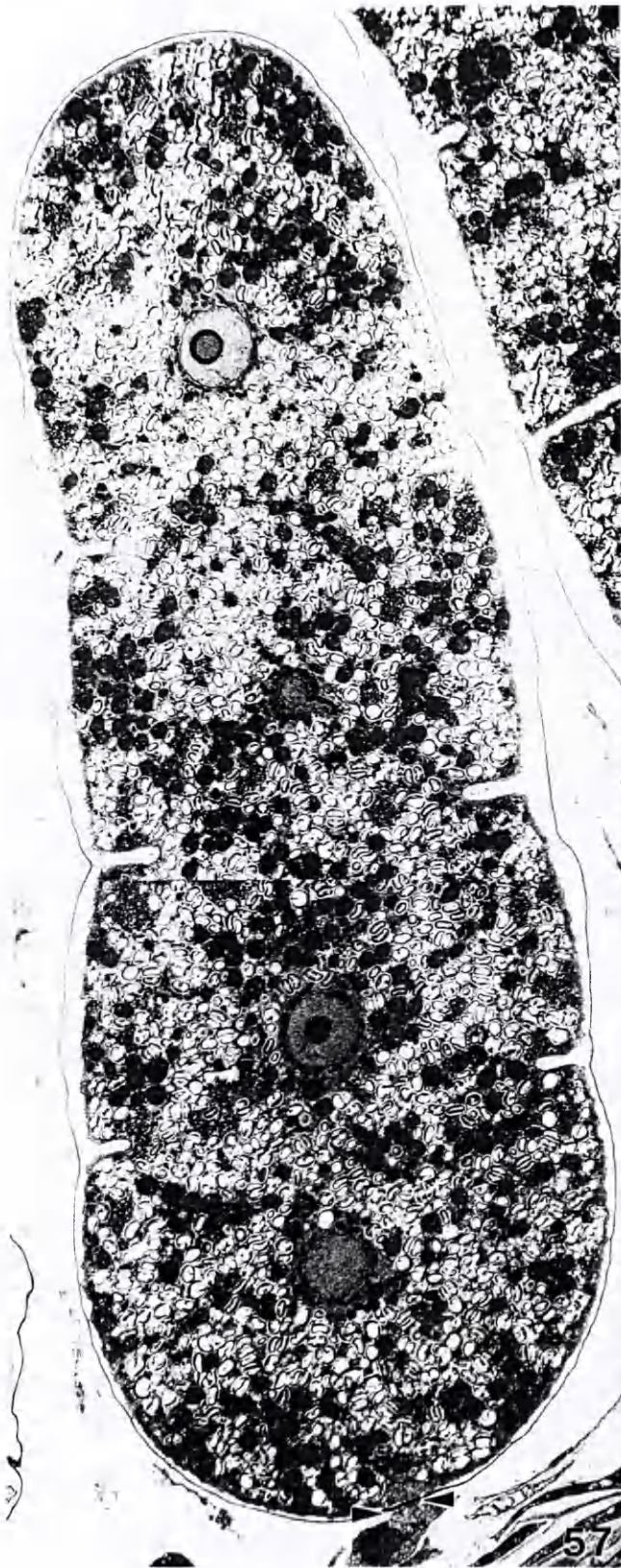
Figure 55. Stage 3 post-vacuolate TS showing post-meiotic nuclear movements. Distal nuclei and proximal nuclei form interacting pairs. Note intermingling of EDM-coated SM in proximal pair (arrowheads). edv aggregations and paired starch grain association visible in the cytoplasm. Cleavage furrows are established and a thin line of material is seen extending through center of furrow to TSW. x 2500.



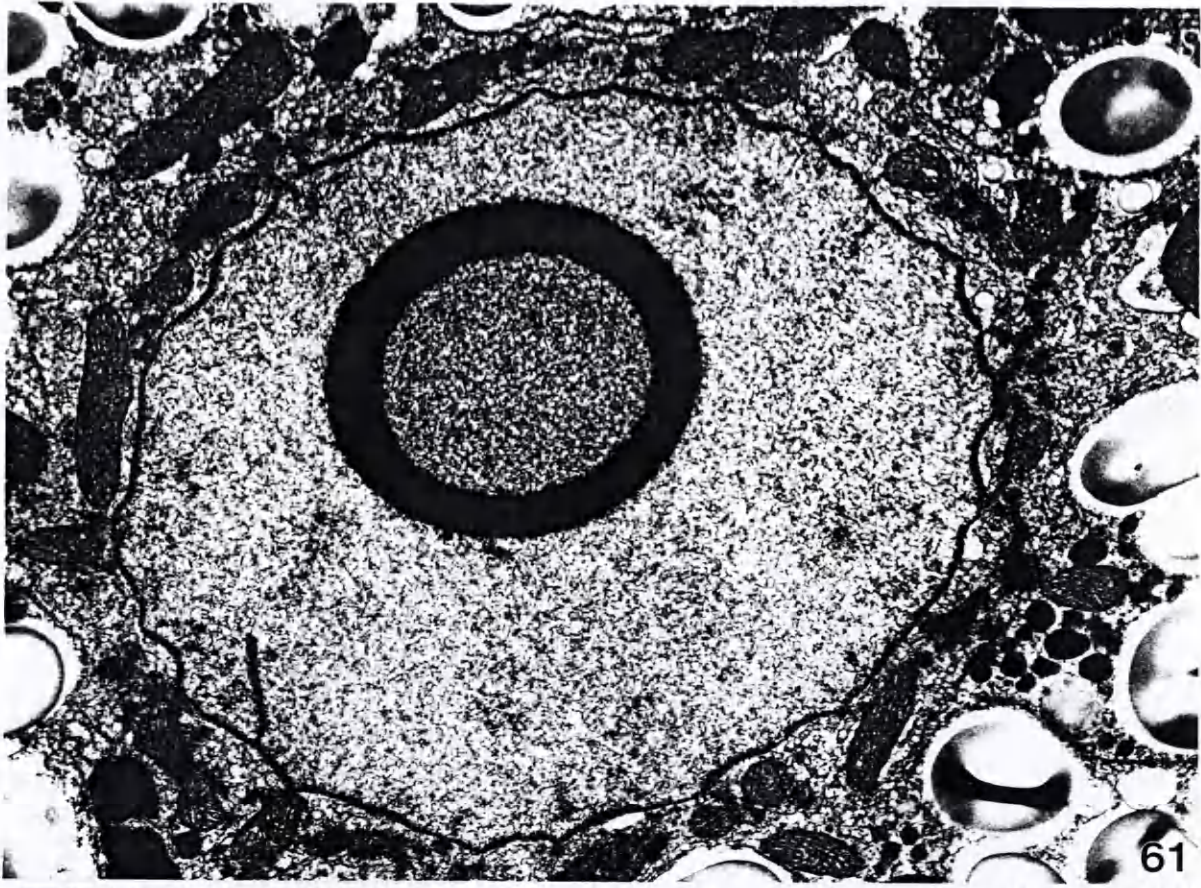
Figure 56. Different section of distal nuclei pair shown in Fig. 55. Nuclei are skewed with respect to each other. Mitochondrion-NE association is visible especially in glancing section. Thick, multi-layered tracts of RER surround and extend between the nuclei in the pair. x 8100.



- Figure 57. Late stage 3 post-vacuolate TS. Pit connection to subtending TMC still visible (arrowheads). x 2,400.
- Figure 58. TMC. Nucleus appears same as in early stage 1 (Fig. 16). Paired Golgi lacking mitochondrion association visible as in stage 1. x 19,800.
- Figure 59. Detail of pit connection (PC) between TS and TMC. Continuity between cytoplasm of TS and TMC no longer apparent (Compare with Fig. 16). PC shows signs of degradation. x 35,800.
- Figure 60. TMC paired-Golgi. Note ER tract extending between Golgi pairs. x 69,500.



- Figure 61. Nucleus from TS shown in Fig. 57. Note annulate lamellae and nucleolar "vacuole". Mitochondrion-NE association is not as close as earlier in stage 3, and a reduction of the PN EDM-coated SM system is apparent. x 15,500.
- Figure 62. Detail of nuclear periphery and single-layered annulate lamellae shown in Fig. 61. SM no longer well formed. EDM is present but reduced. x 41,000.
- Figure 63. Detail of nuclear periphery on different late stage 3 nucleus. Multiple RER tracts (arrowhead) visible in nuclear vicinity. x 40,300.



61



62



63

- Figure 64. Glancing section of late stage 3 post-vacuolate TS nucleus. Mitochondrion-nucleus association still visible and EDM-coated SM system present but reduced. x 10,800.
- Figure 65. Plugged connection to TSW in late stage 3 post-vacuolate TS shown in Fig. 57. Note TCW material to the outside of TSW. x 62,800.
- Figure 66. Cleavage furrow on late stage 3 post-vacuolate TS. Note multiple ER layers surrounding furrow and thin line of electron-dense material connected to TSW. x 8,700.
- Figure 67. Detail of cleavage furrow shown in Fig. 66. Note initial stages of punctate border formation (arrowhead). x 42,500.
- Figure 68. Cytoplasmic inclusions in late stage 3 post-vacuolate TS. Mature chloroplasts (C), paired starch grains, small-rounded starch grains (s), and edv (asterisk) dispersed from aggregations shown. x 6,800.

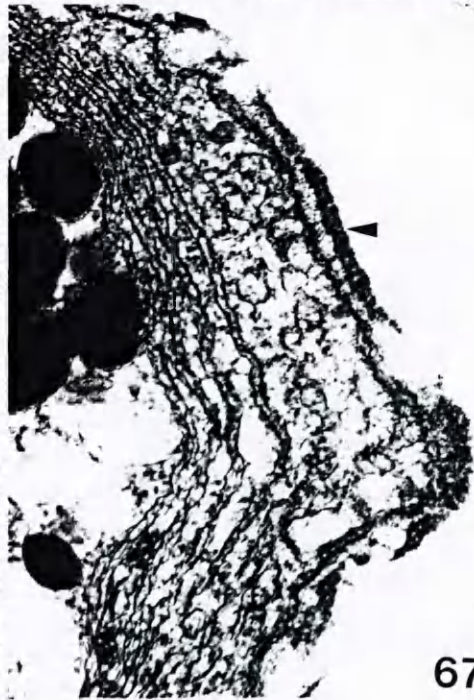
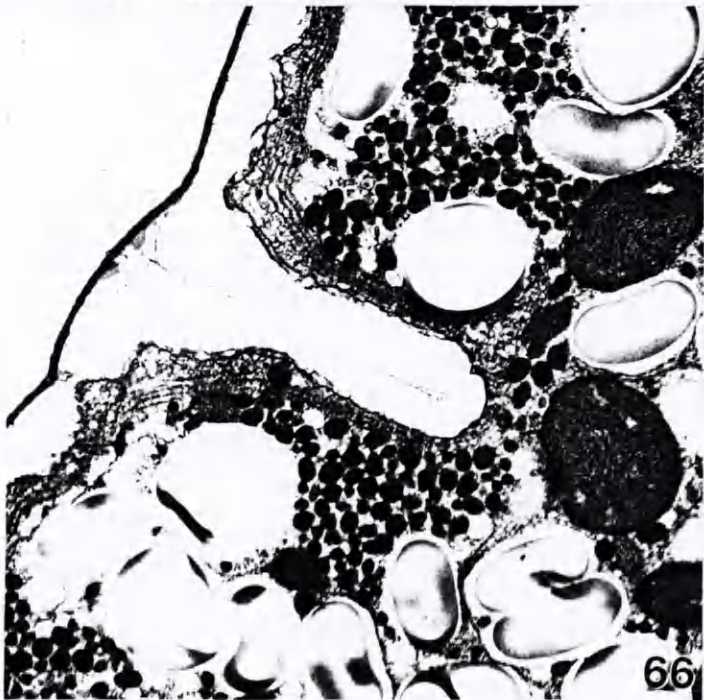
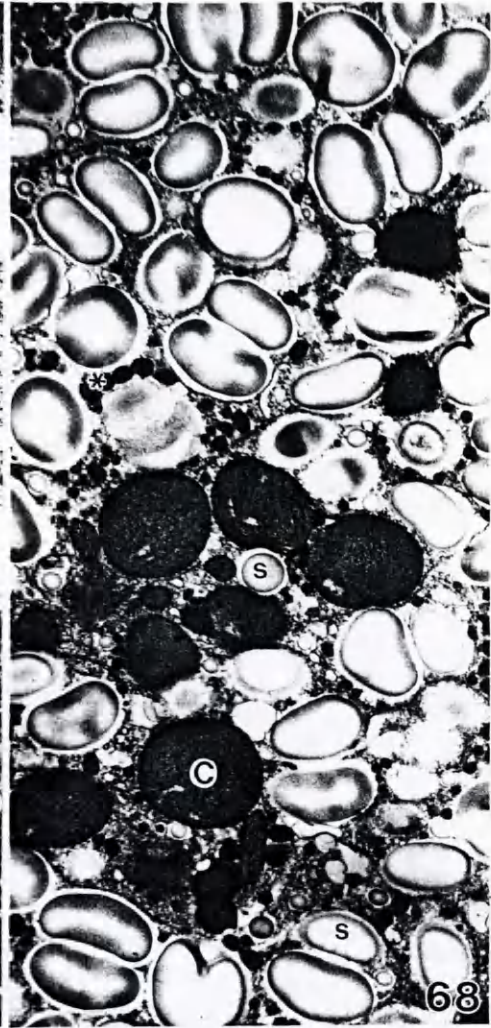
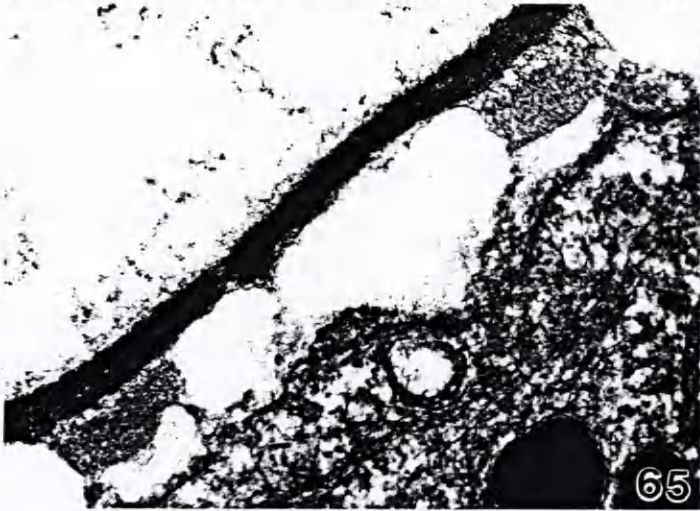
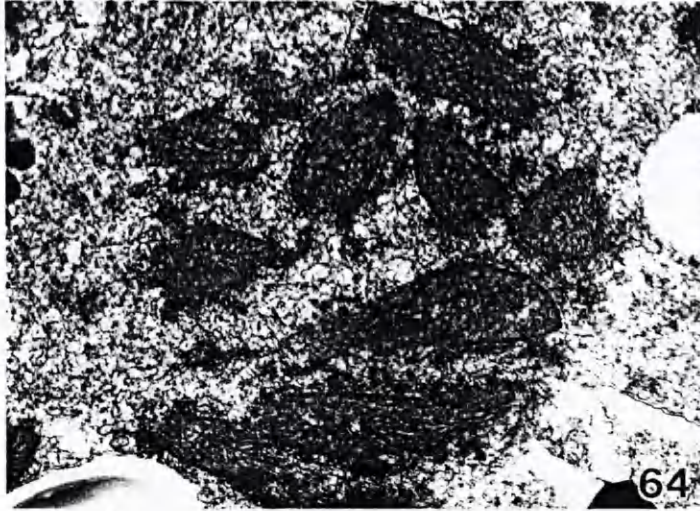
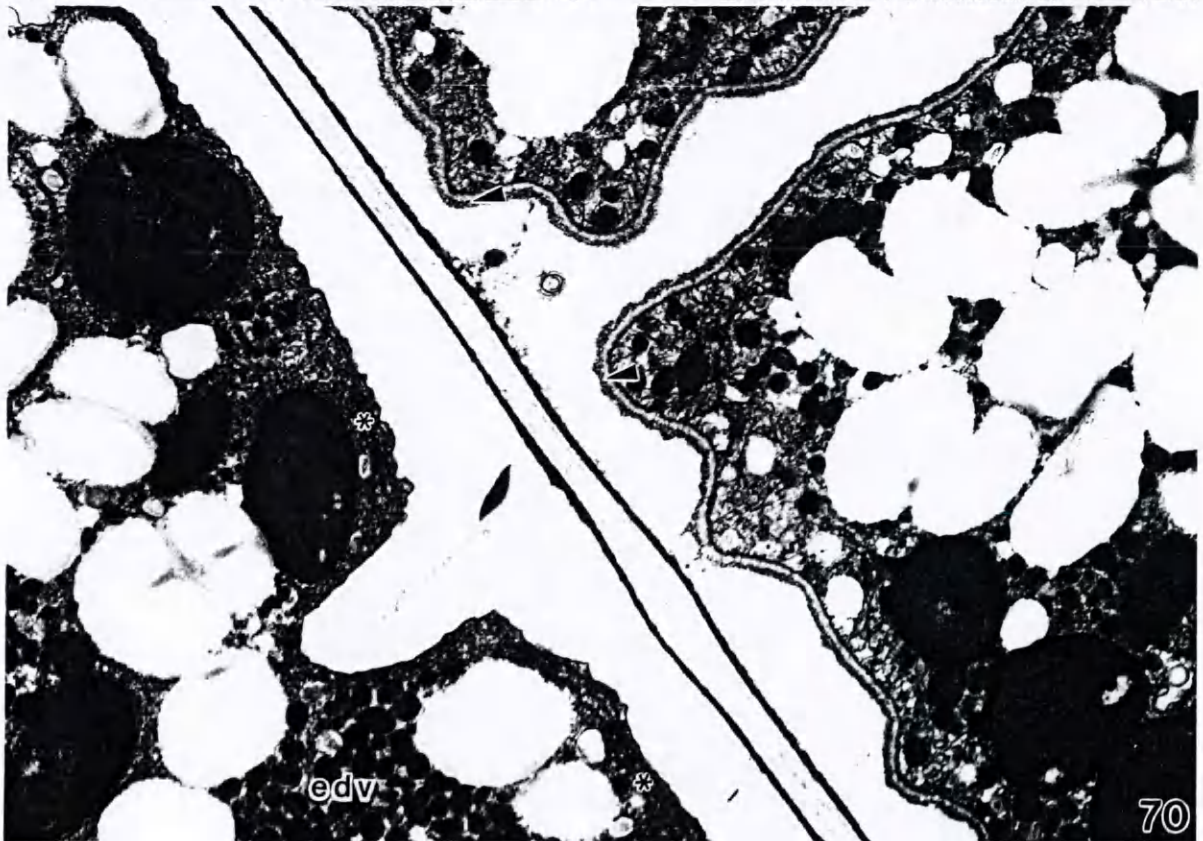
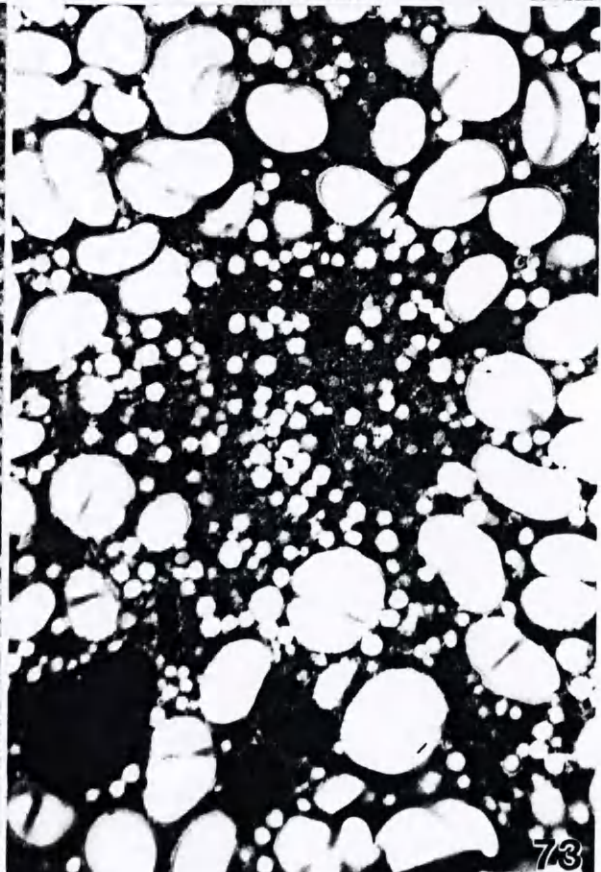
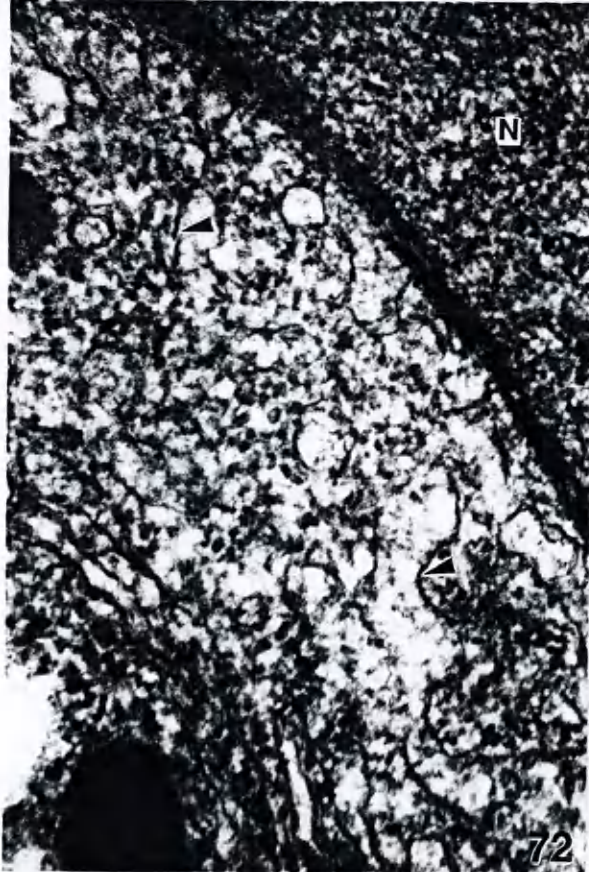
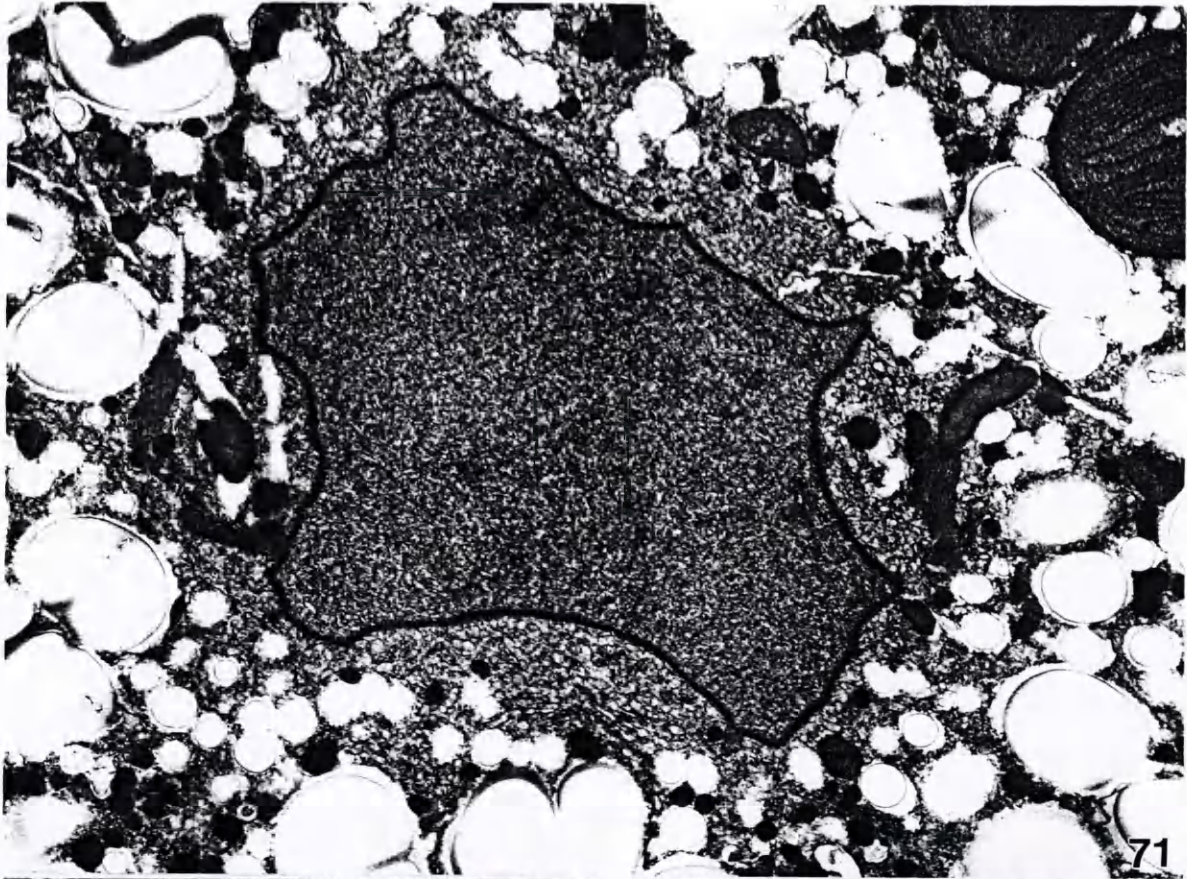


Figure 69. Fully-cleaved stage 4 TS. x 1,200.

Figure 70. Comparison of periphery on stage 4 TS and stage 3 post-vacuolate TS. Note punctate sporangial border (arrowheads) and dispersed edv in stage 4 TS and peripheral RER (asterisks) and aggregated edv in stage 3 TS. x 9,600.



- Figure 71. Nucleus on stage 4 TS. Note irregular outline of NE. x 16,500.
- Figure 72. Periphery on nucleus (N) shown in Fig. 71. EDM is no longer visible. Smooth membranes (arrowheads) and SER-like vesicles shown. x 72,800.
- Figure 73. Glancing section of nuclear region shows presence of small starch grains and electron-dense vesicles. x 7,400.



- Figure 74. Stage 4 TS periphery. Punctate border with peripheral tubule system shown. x 35,800.
- Figure 75. Detail of TS periphery shown in Fig. 74. Three layers comprise the periphery: plasmalemma (arrowhead) with associated tubules, a fibrillar zone (fz), and a punctate border (b). x 79,500.
- Figure 76. Periphery of cleavage mid-region between two TS. Post-cleavage connection with plug of electron dense material (asterisk) shown. x 47,000.
- Figure 77. Detail of plugged connection shown in Fig. 76. Note peripheral tubules (arrowheads). x 69,500.



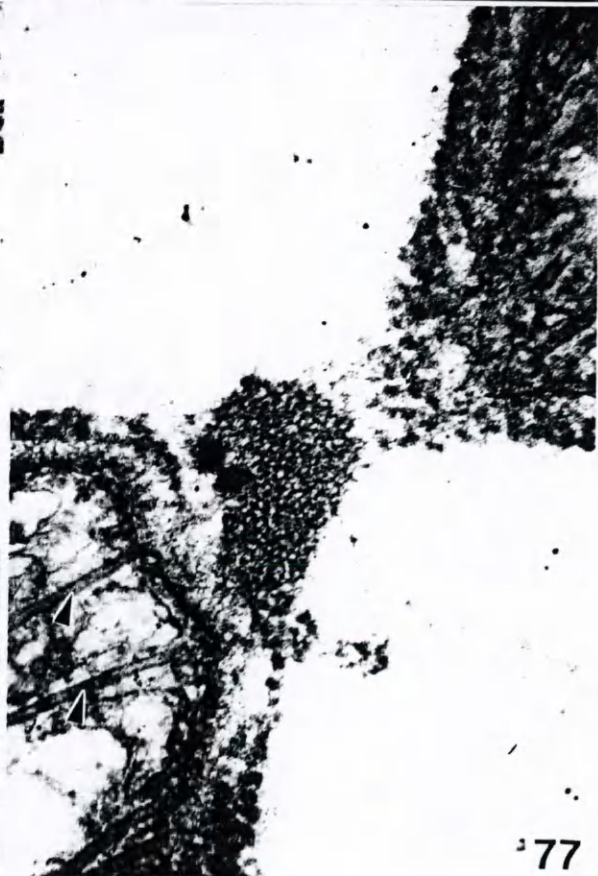
74



75

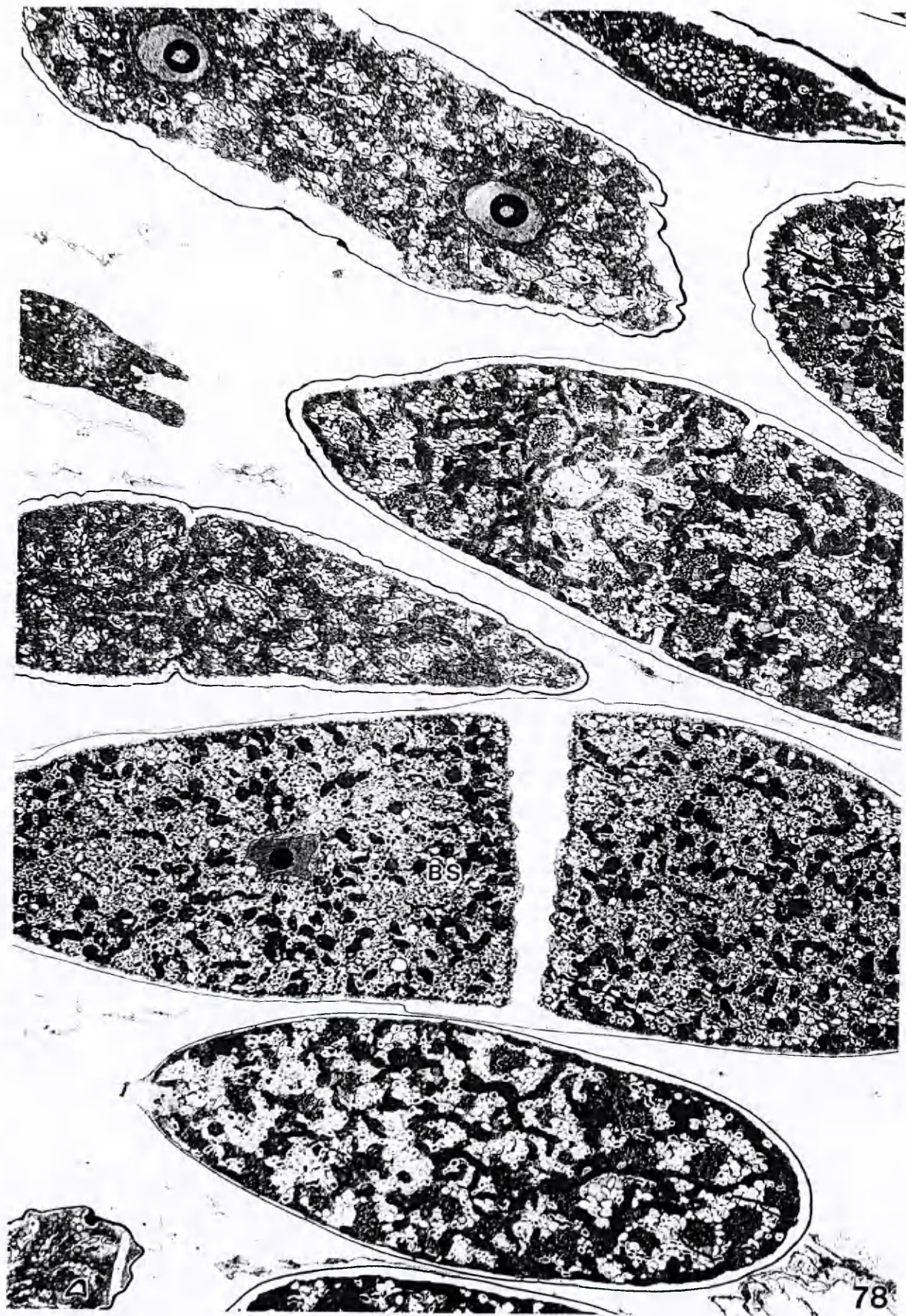


76

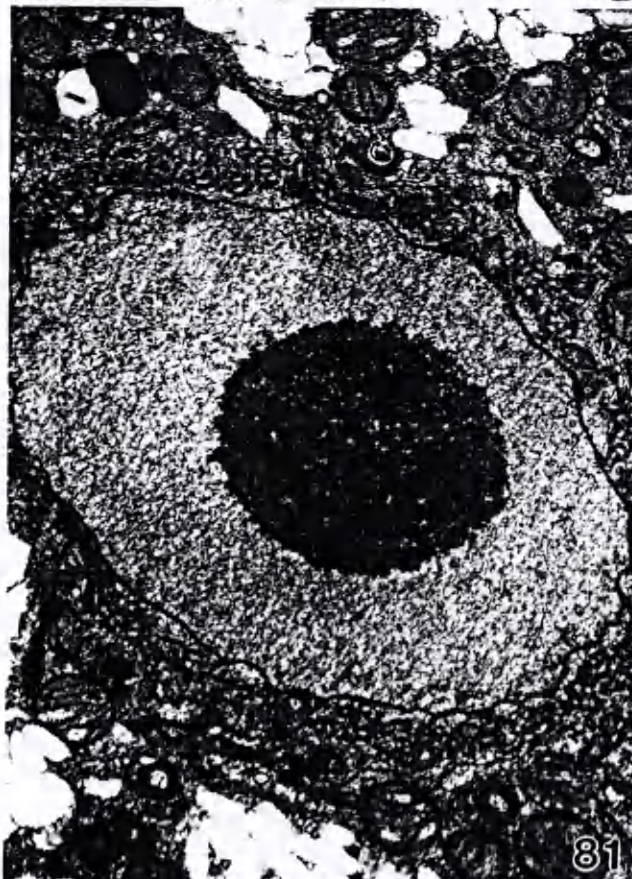
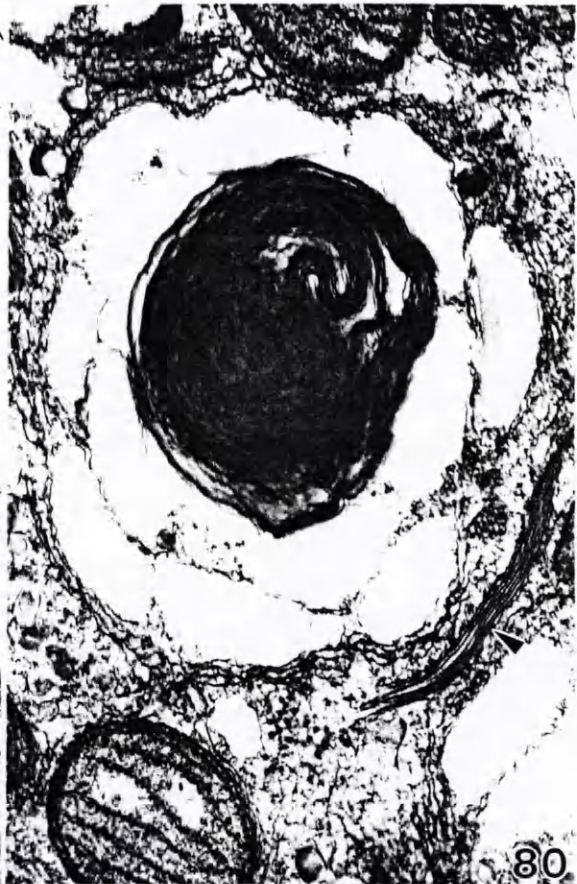


77

Figure 78. Bisporangial conceptacle. Volume of mature stage 4 bisporangium (BS) equivalent to total volume of stage 4 TS. Stage 3 BS in vacuolate and post-vacuolate conditions shown. x 1200.



- Figure 79. Stage 3 vacuolate BS. Note placement of cleavage furrows (arrowheads) and presence of starch-flanked vacuoles. x 970.
- Figure 80. Starch-flanked vacuole from BS shown in Fig. 79. RER surrounds starch grains. Elongate flattened membranes present resemble attenuated Golgi (arrowhead). x 56,200.
- Figure 81. Nucleus from stage 3 BS in Fig. 79. EDM-coated SM and mitochondria surround nuclear periphery. x 7300.
- Figure 82. Periphery of nucleus shown in Fig. 81. Note mitochondrion-Golgi association and RER (arrowhead) surrounding EDM-SM region. x 35,800.



- Figure 83. Stage 3 post-vacuolate BS. Note starch-flanked aggregations of edv (asterisk). x 1,200.
- Figure 84. Nucleus on BS shown in Fig. 83. Note annulate lamellae, mitochondrion-NE association, and EDM-coated smooth membranes at nuclear periphery. x 11,500.
- Figure 85. Mitochondrion-Golgi association at nuclear periphery. Note appressed cisternae at Golgi mid-region and secretion of edv (asterisk). x 84,800.
- Figure 86. BS periphery showing connection between plasmalemma and BS wall (arrowheads). Note edv aggregations and Golgi. x 15,100.
- Figure 87. Detail of plugged-connection at BSW shown in Fig. 86. Note peripheral RER. x 84,800.

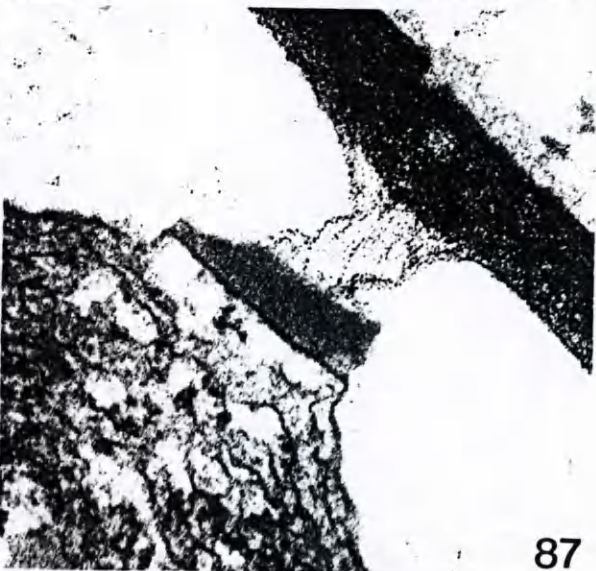
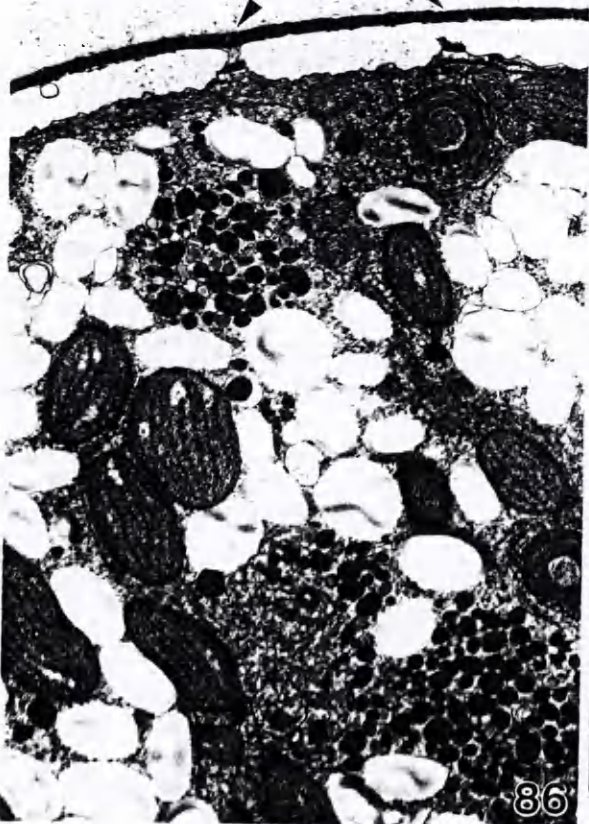
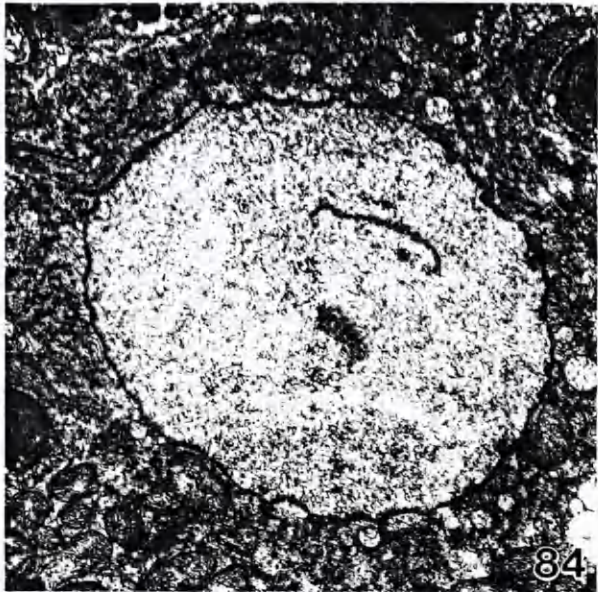
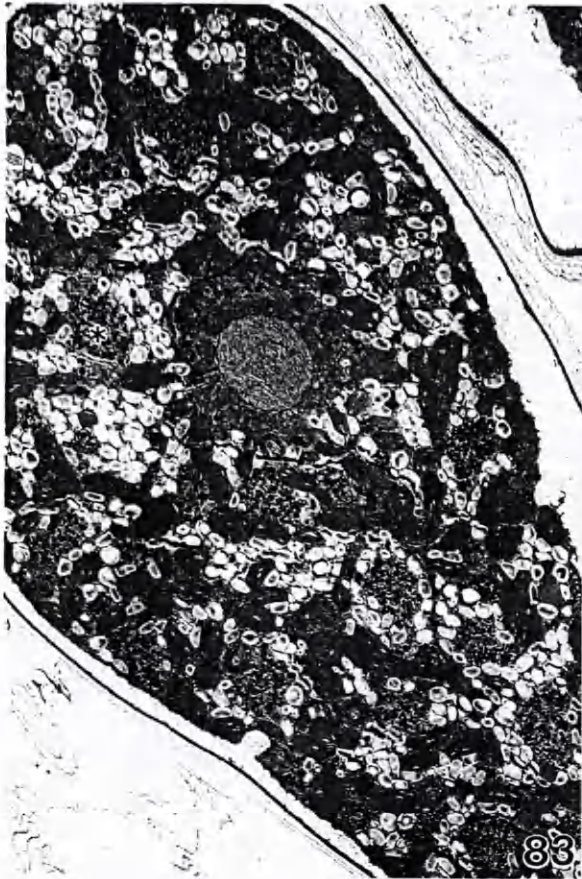


Figure 88. Stage 4 BS nucleus. x 10,500.

Figure 89. Periphery of nucleus shown in Fig. 88. Note presence of SER-like membranes, small starch grains, and edv. x 76,100.

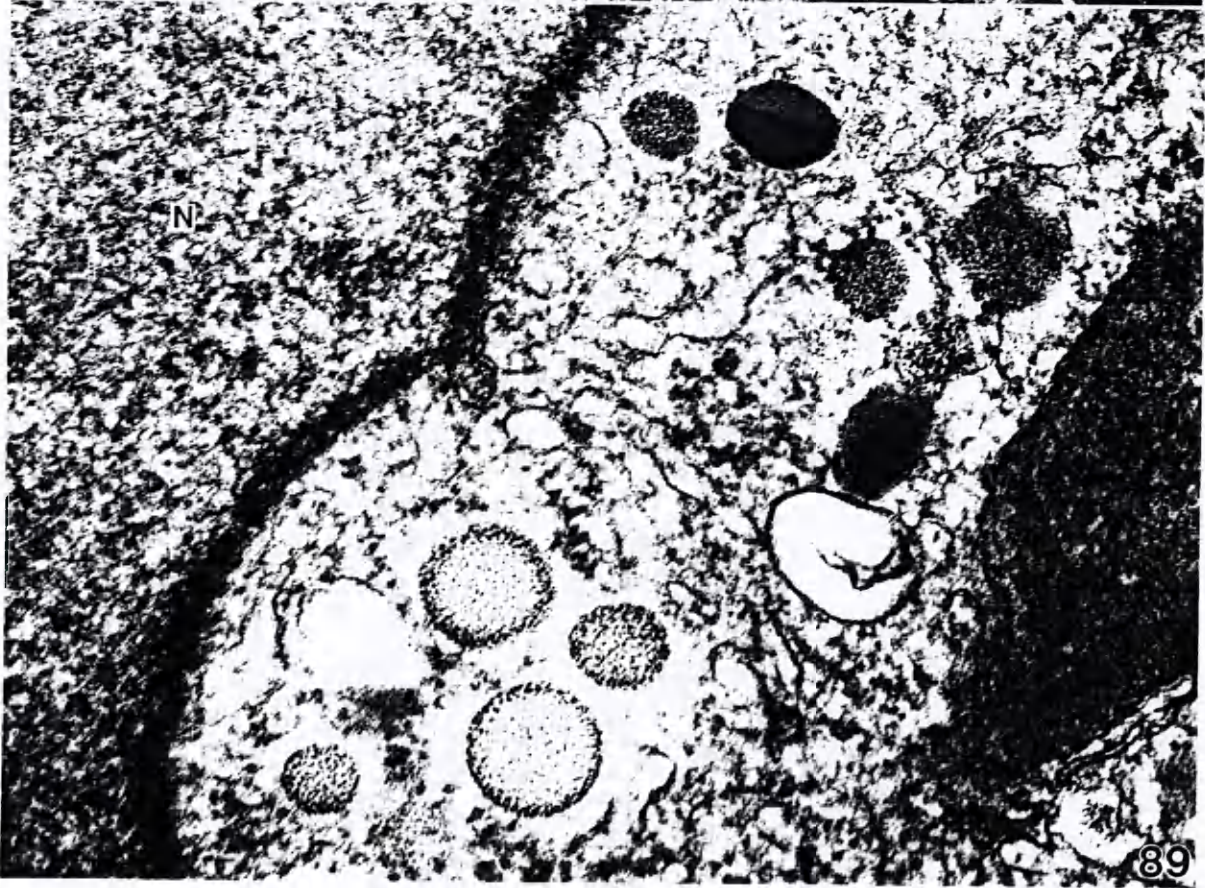
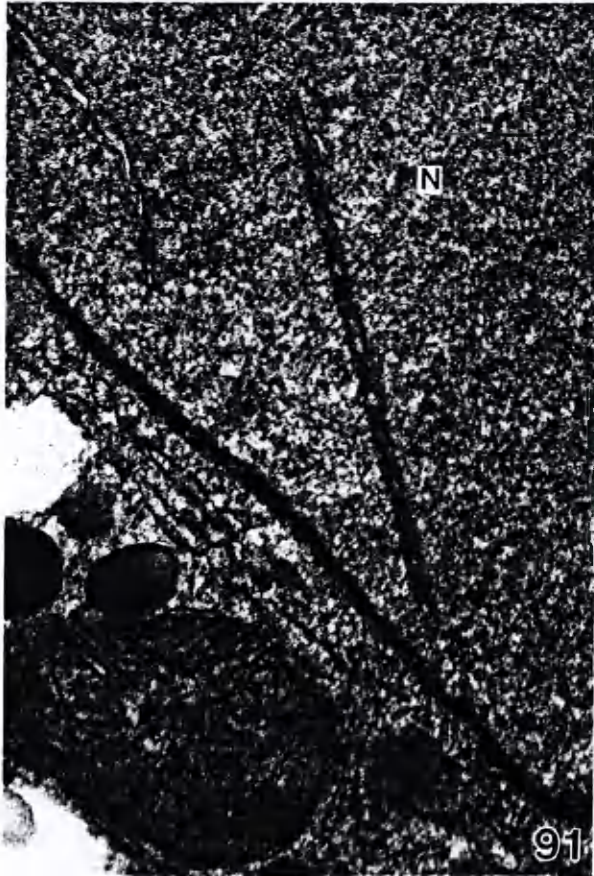
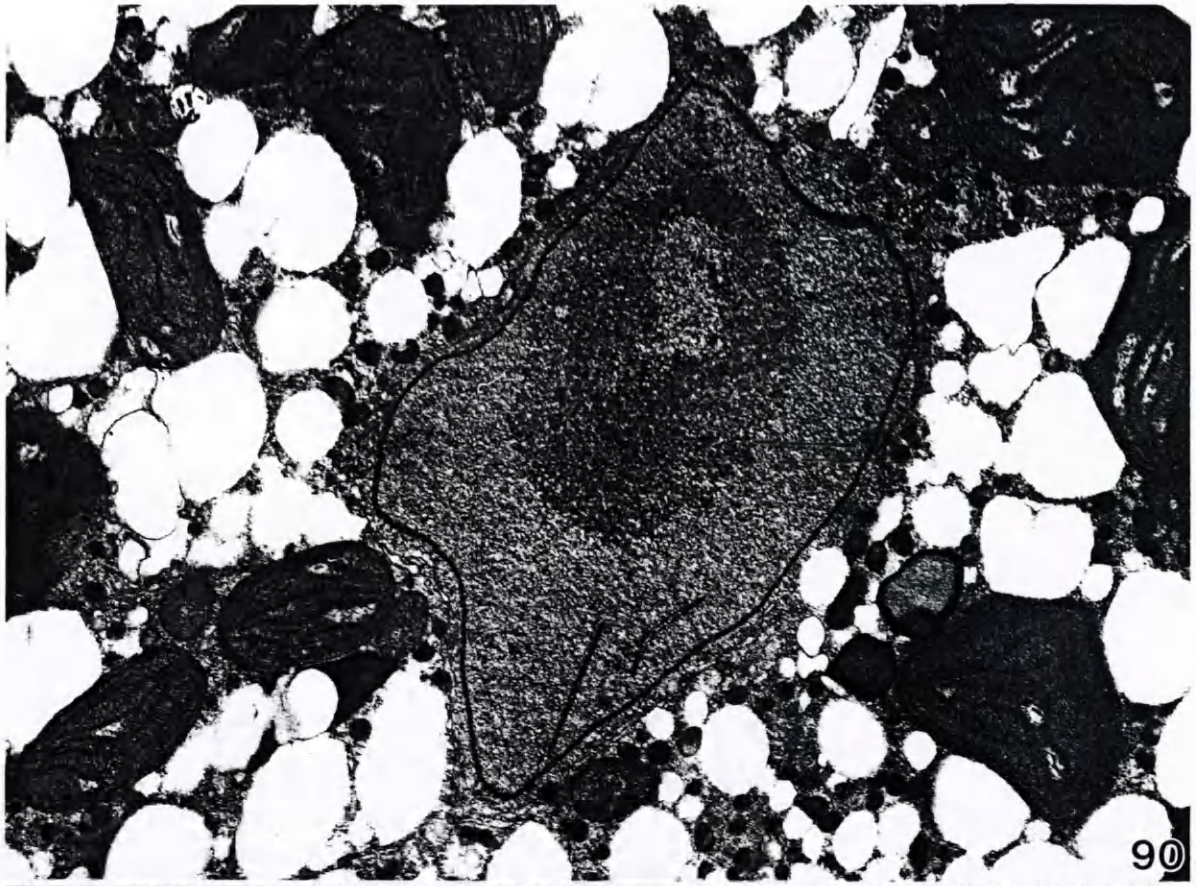


Figure 90. Amphiroa TS nucleus. x 19,000.

Figure 91. Periphery of nucleus shown in Fig. 90. Note SER-like membranes and absence of EDM. x 59,300.

Figure 92. Starch deposition in Amphiroa. x 59,300.



- Figure 93. Lithothrix TS nucleus. Note RER-starch grain association at NE and flocculent nucleolar ring. x 10,500.
- Figure 94. Periphery of nucleus shown in Fig. 93. x 47,000.
- Figure 95. Starch deposition in Lithothrix. Note similarity with deposition pattern seen in Amphiroa (Fig. 92). x 47,000.

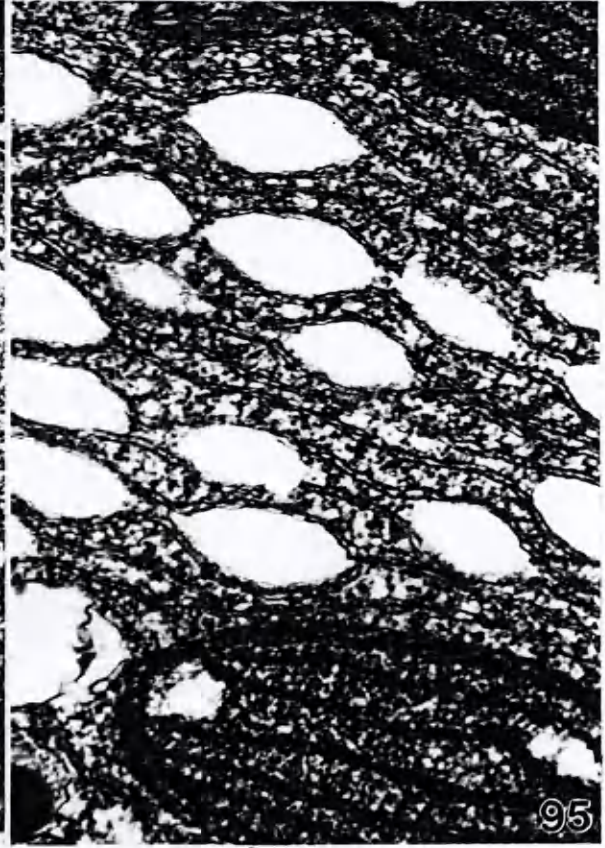
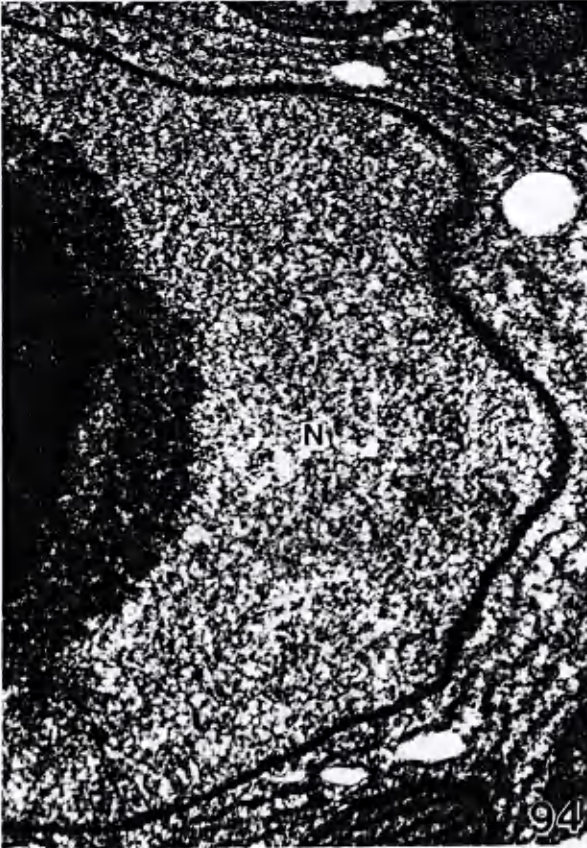
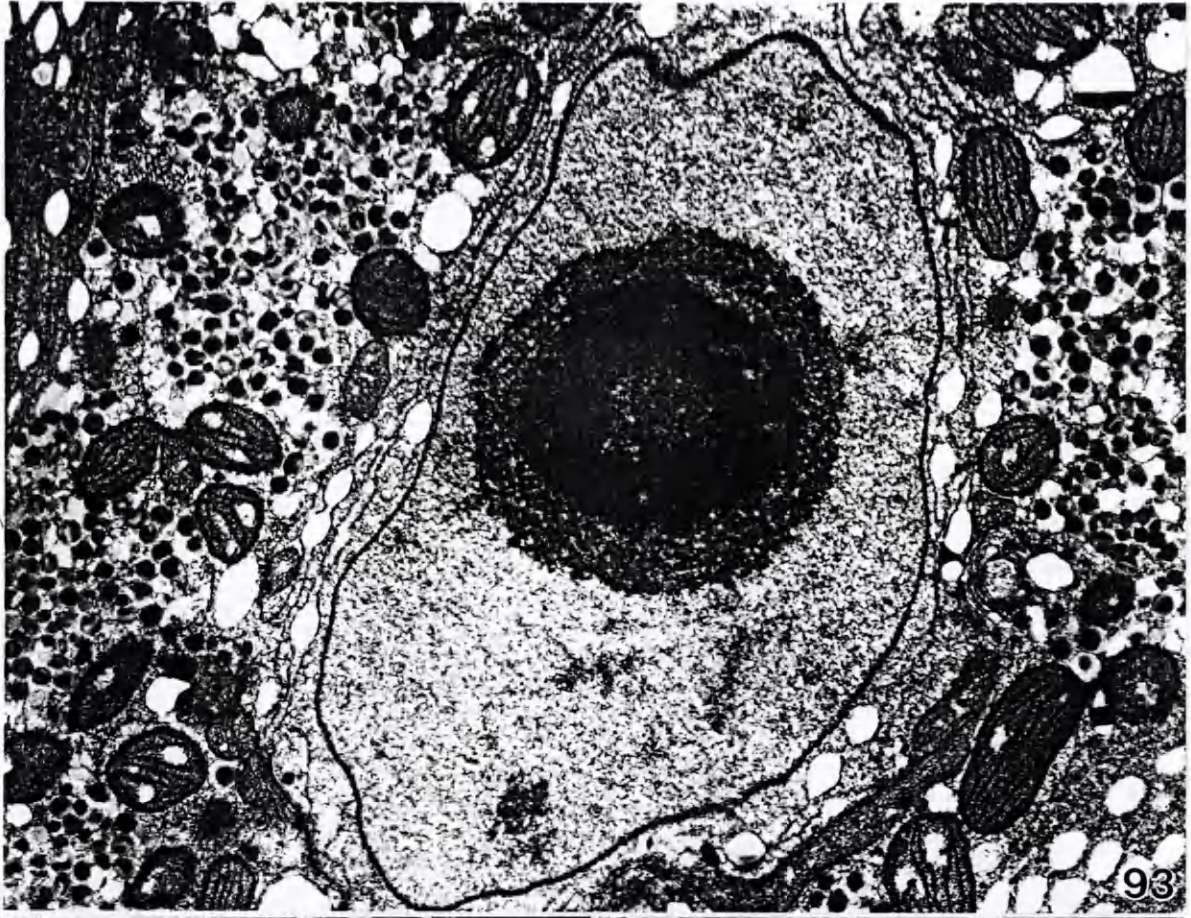


Figure 96. Titanoderma TS. Note accumulation of starch in nuclear region. x 1400.

Figure 97. Titanoderma TS nucleus. Note absence of EDM. x 19,400.

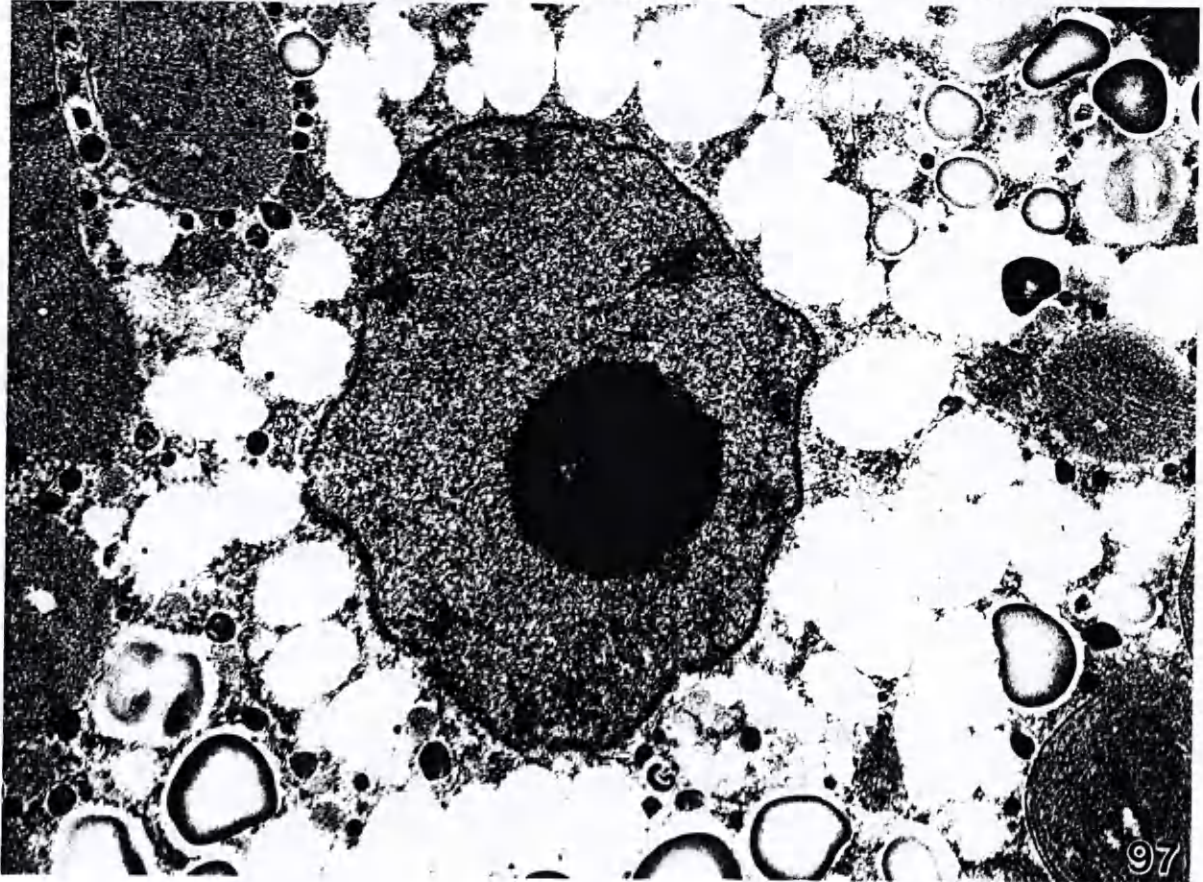


Figure 98. Fosliella TS. Note large vacuoles at sites of cleavage initiation (asterisks). x 7,800.

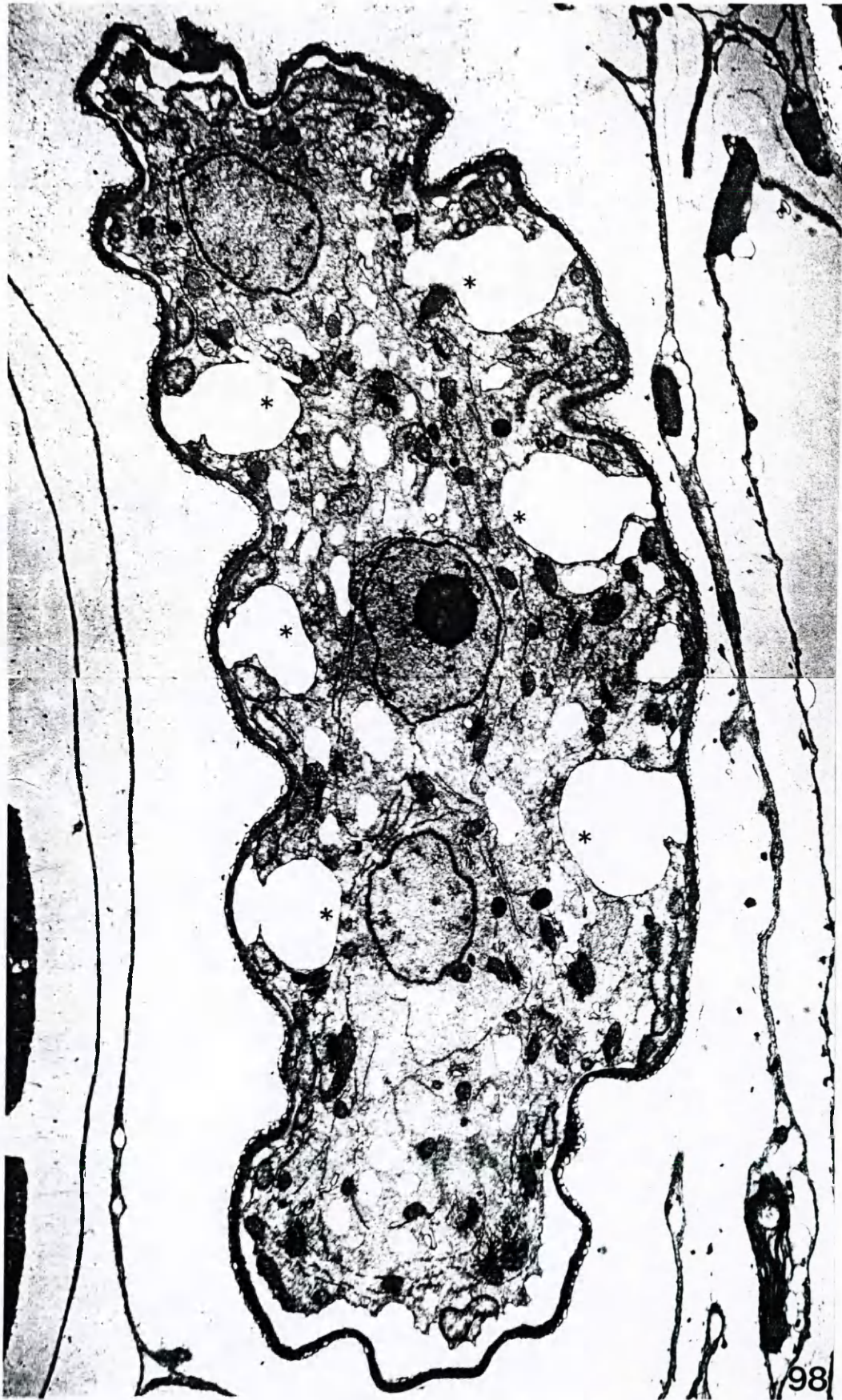


Figure 99. Early post-meiotic Fosliella TS nucleus.
x 23,500.

Figure 100. Periphery of nucleus shown in Fig. 99. Note RER
but absence of EDM. x 62,800.

Figure 101. Fosliella TS nucleus at later stage of post-
meiotic maturation. x 42,500.

Figure 102. Periphery of nucleus shown in Fig. 101. Note
extensive RER and absence of EDM. x 100,700.

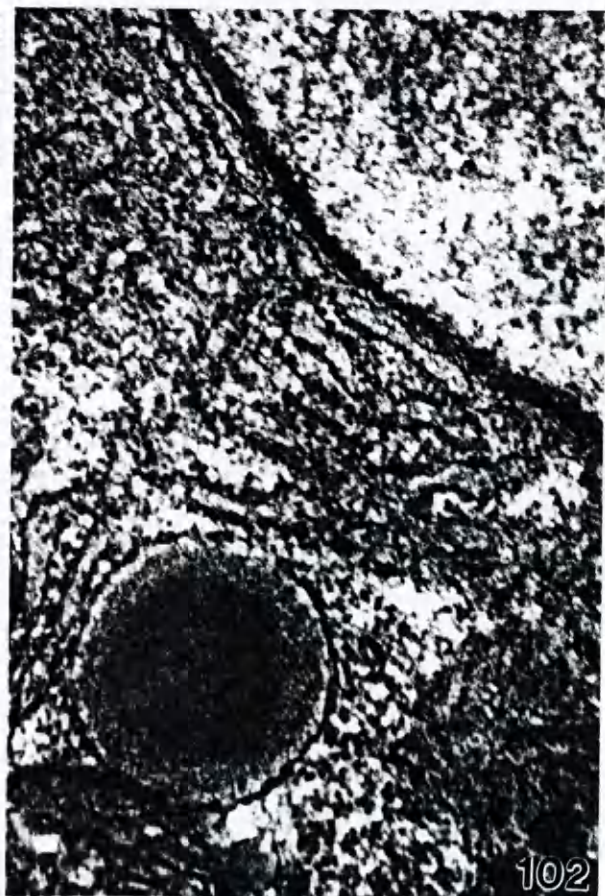
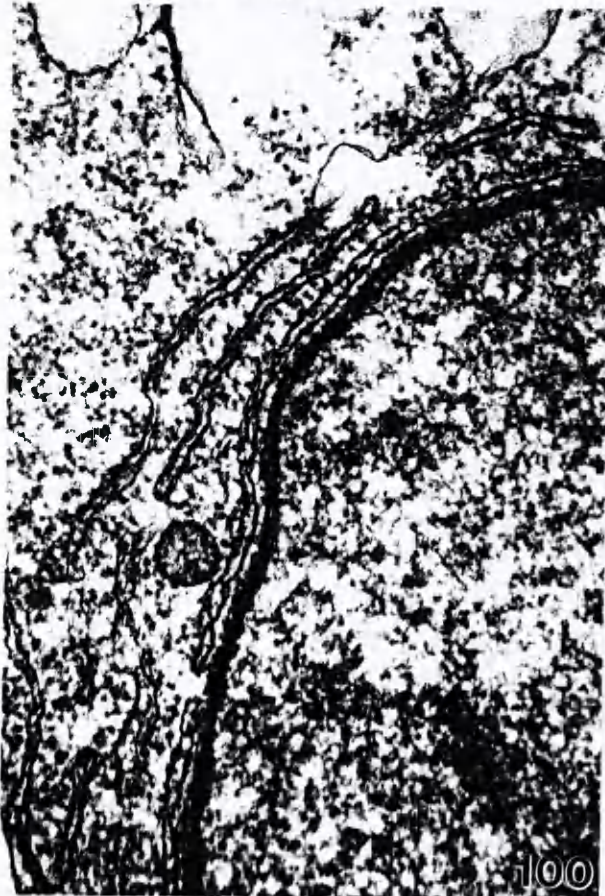
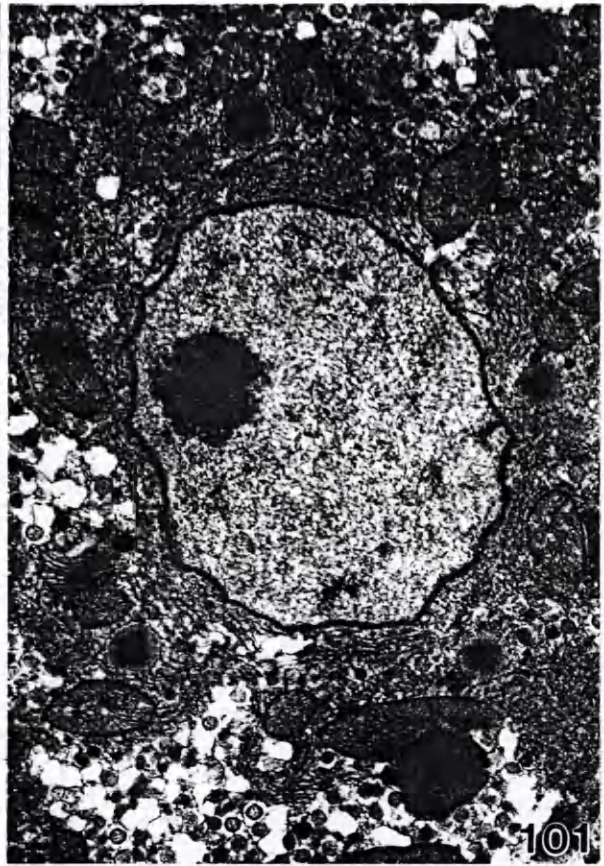
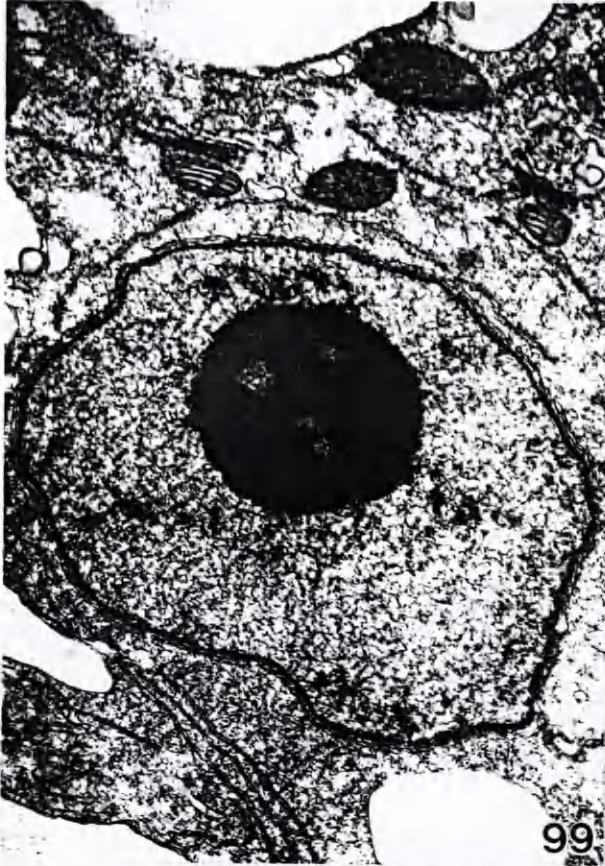


Figure 103. Metamastophora TS nucleus. x 7,800.

Figure 104. Periphery of nucleus shown in Fig. 103. Note EDM-filled NE invaginations. x 19,800.

Figure 105. Metamastophora cleavage furrow. Note thickness of TSW (asterisk). x 7,300.

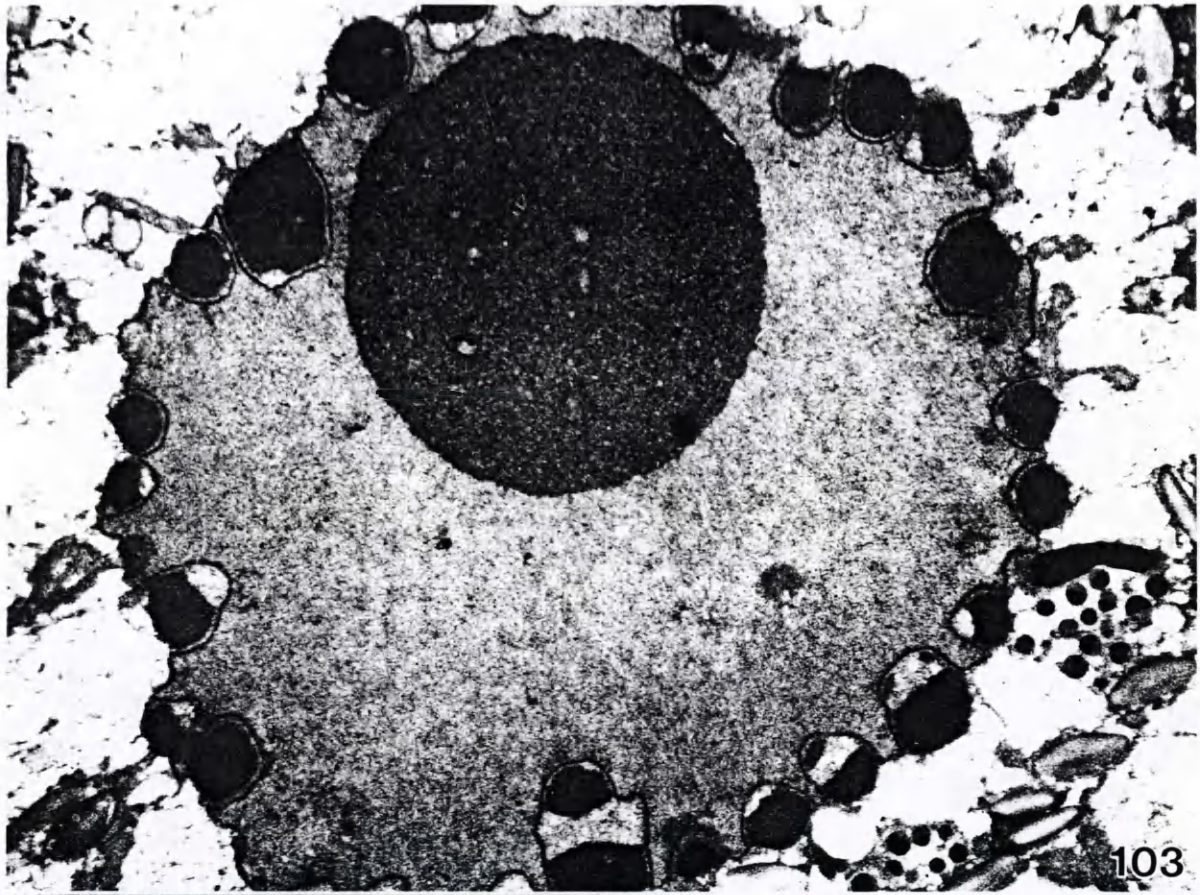
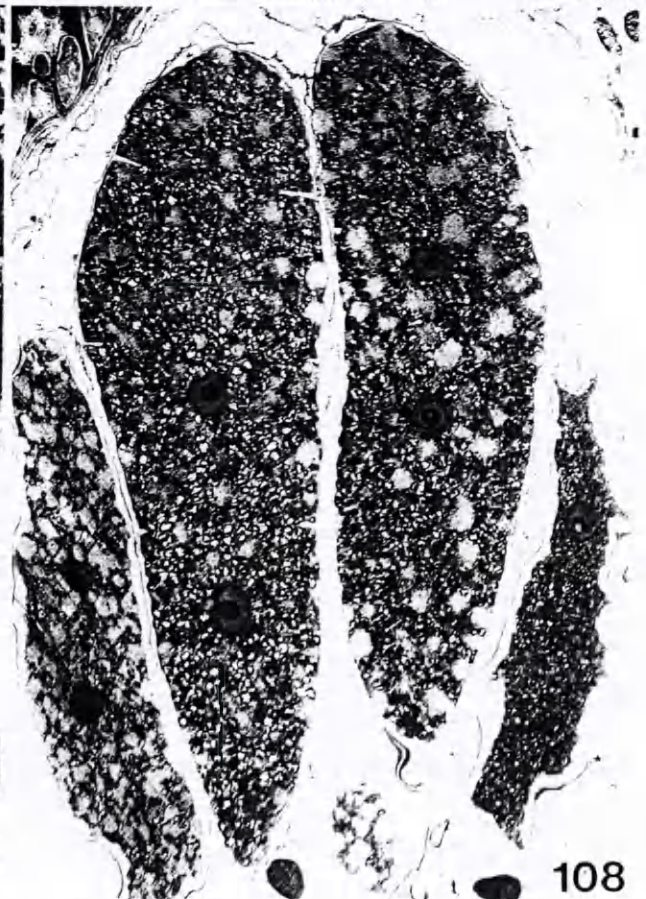
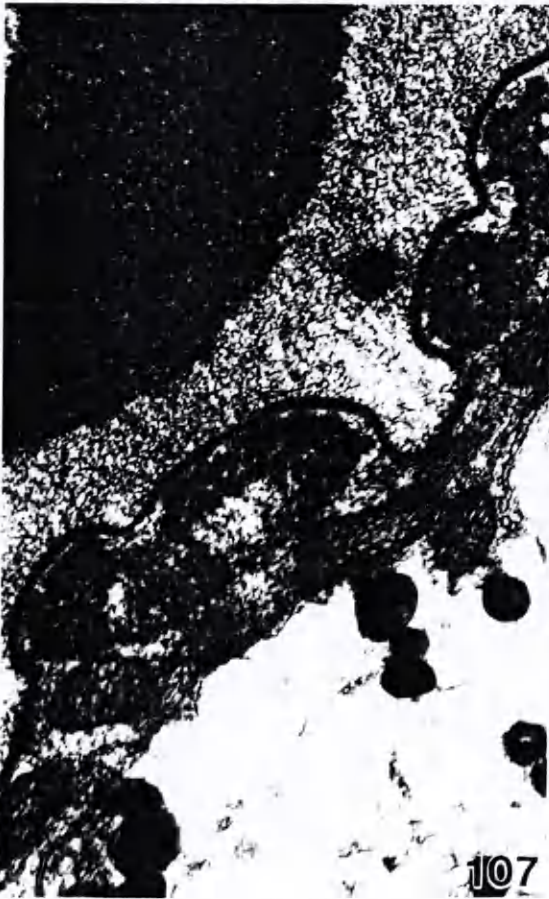
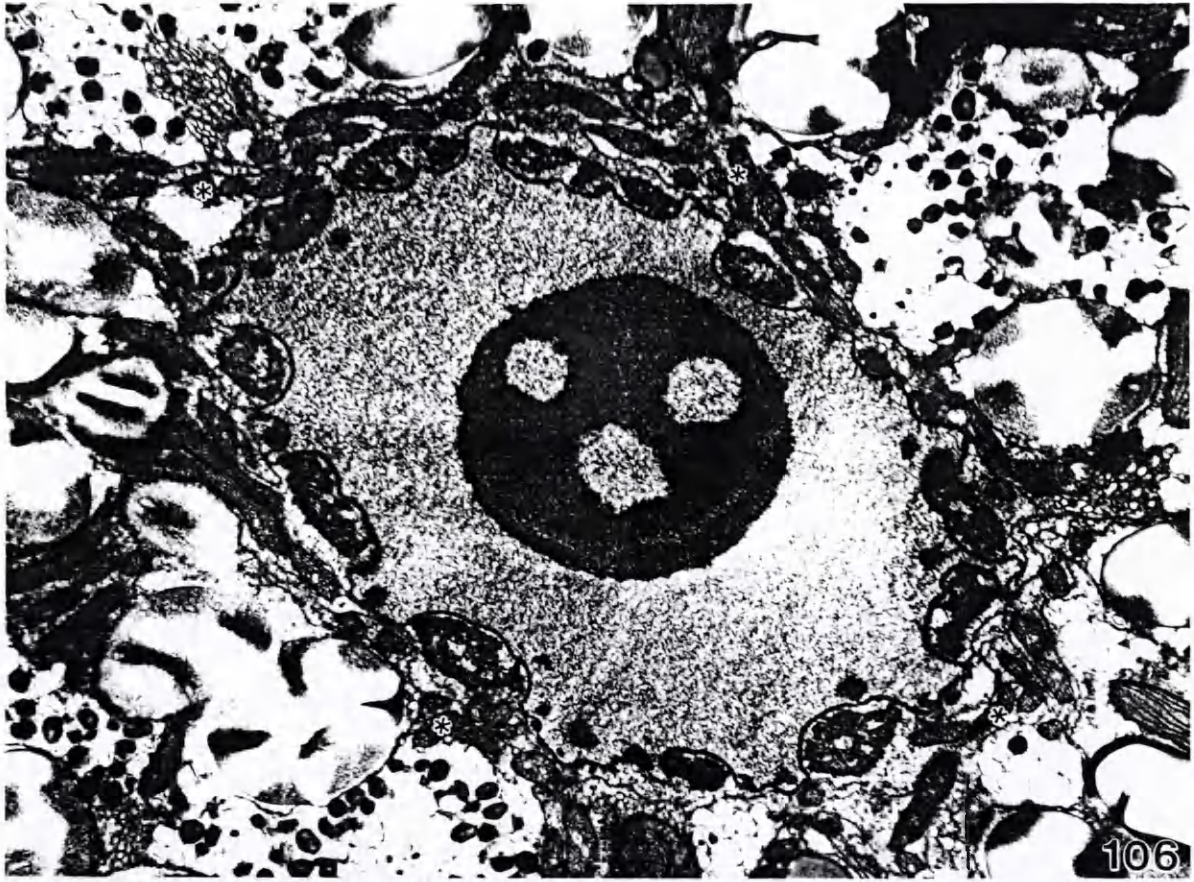


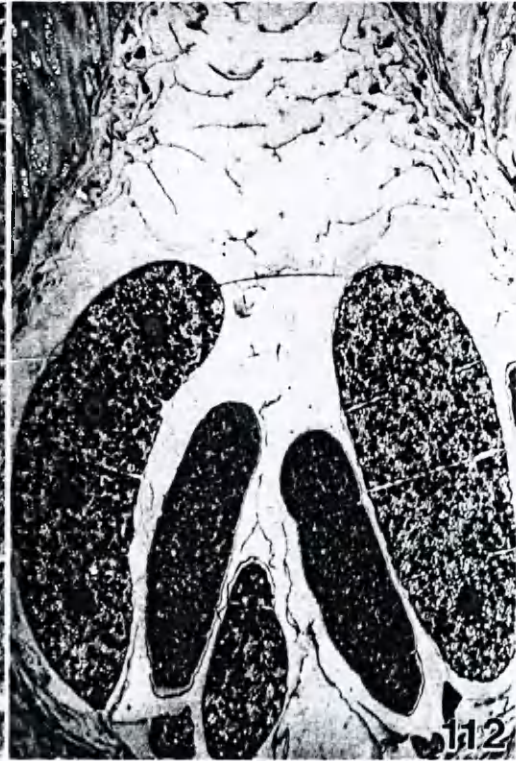
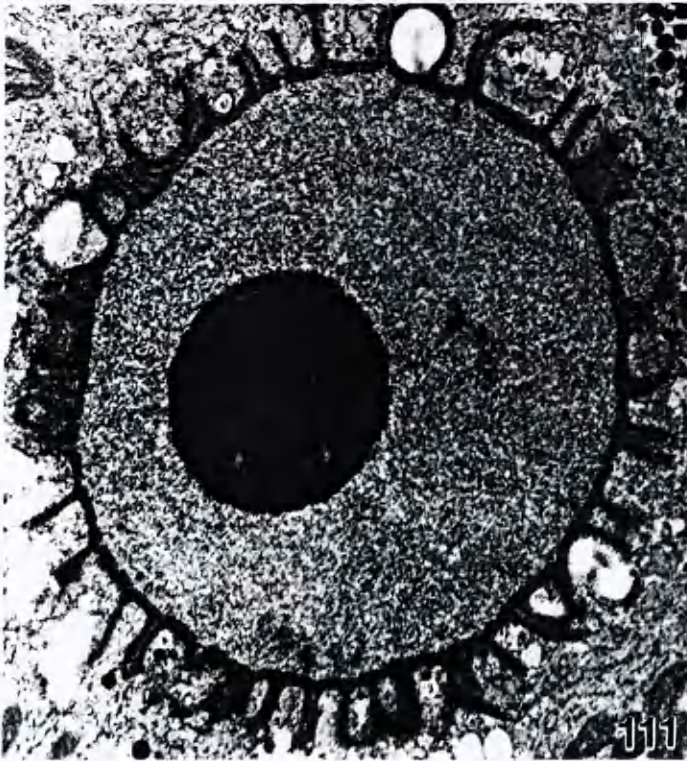
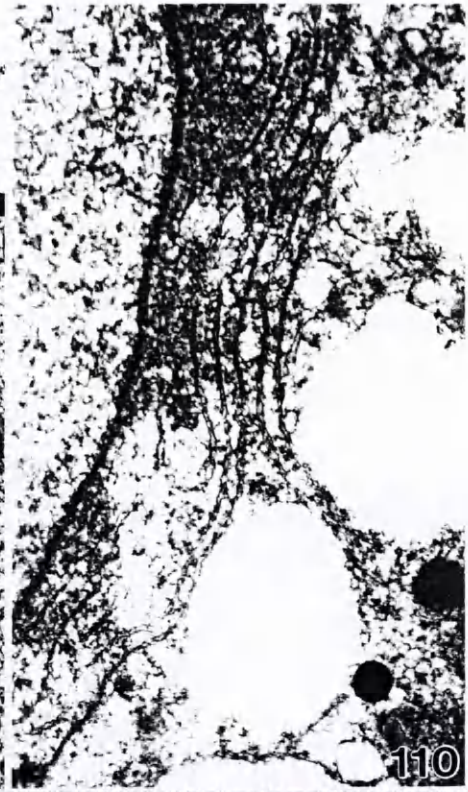
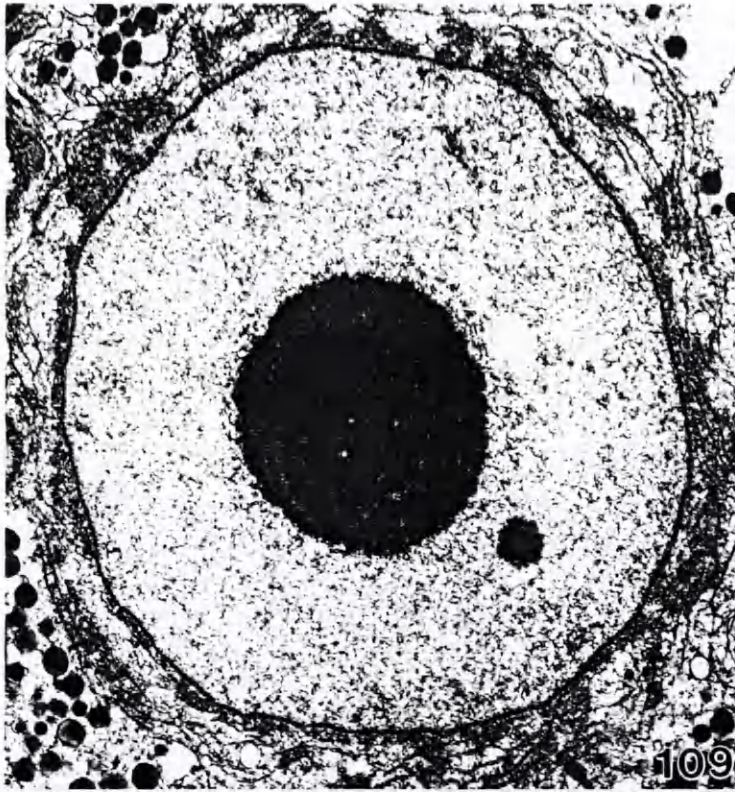
Figure 106. Haliptilon TS nucleus (asterisks). x 7,800.

Figure 107. Periphery of nucleus shown in Fig. 106. Note EDM-filled NE invaginations and adjacent mitochondria. x 18,600.

Figure 108. Haliptilon TS conceptacle. Note presence of three post-meiotic TS with EDM-filled NE invaginations. x 360.



- Figure 109. Early post-meiotic TS nucleus in Jania. Note concentric parallel arrangement of RER at NE. x 13,600.
- Figure 110. Periphery of nucleus shown in Fig. 109. Note diffuse localization of EDM coating RER cisternae. x 53,700.
- Figure 111. Later post-meiotic TS nucleus in Jania. Note perpendicular orientation of RER at NE. EDM closely appressed to NE, coating RER cisternae. x 8,700.
- Figure 112. Jania TS conceptacle. Compare size and arrangement with Halitilon conceptacle. x 380.



- Figure 113. Early Corallina post-meiotic TS nucleus. Note diffuse localization of EDM at NE. x 7,400.
- Figure 114. Periphery of nucleus shown in Fig. 113. Note diffuse organization of EDM and radiating RER. x 49,200.
- Figure 115. Later Corallina post-meiotic TS nucleus. Note tight organization of EDM in RER cisternae at the NE. This is the same organization seen in Jania (Fig. 111). x 7,400.
- Figure 116. Periphery of nucleus shown in Fig. 115. Note organization of EDM coating RER cisternae at the NE. x 49,200.

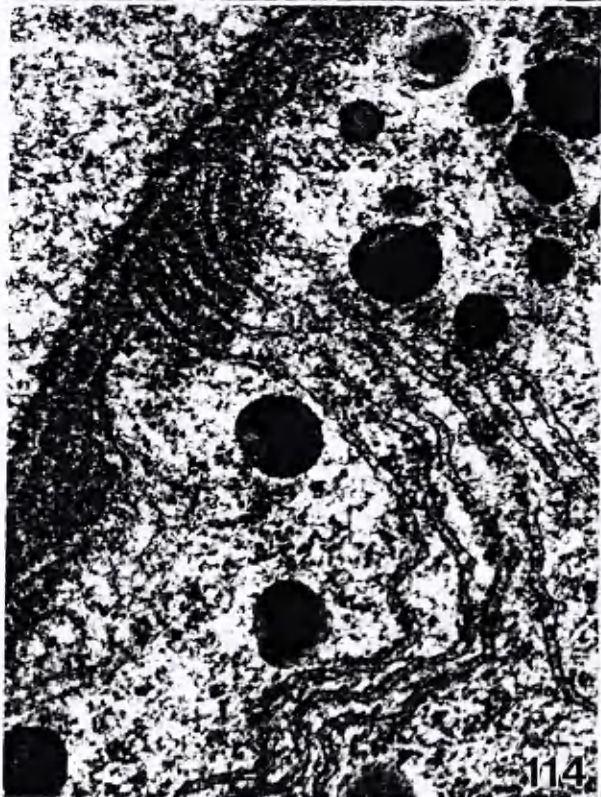
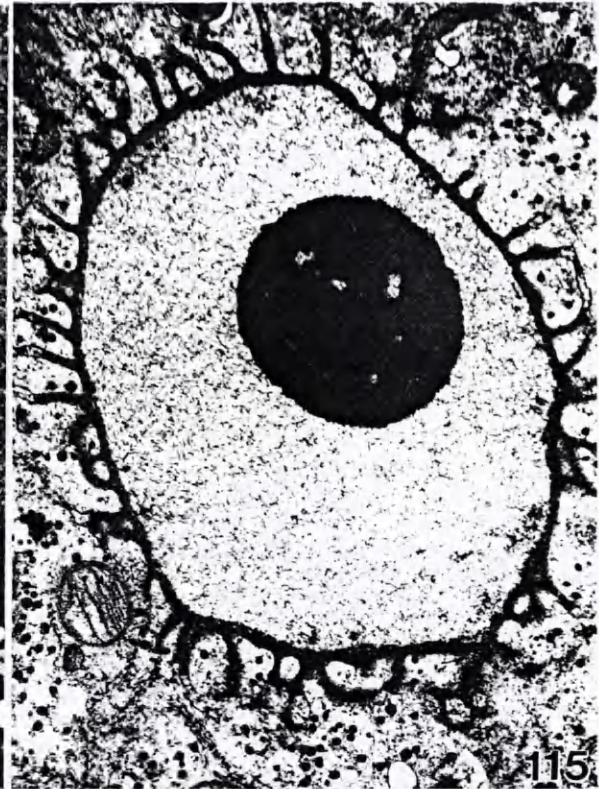
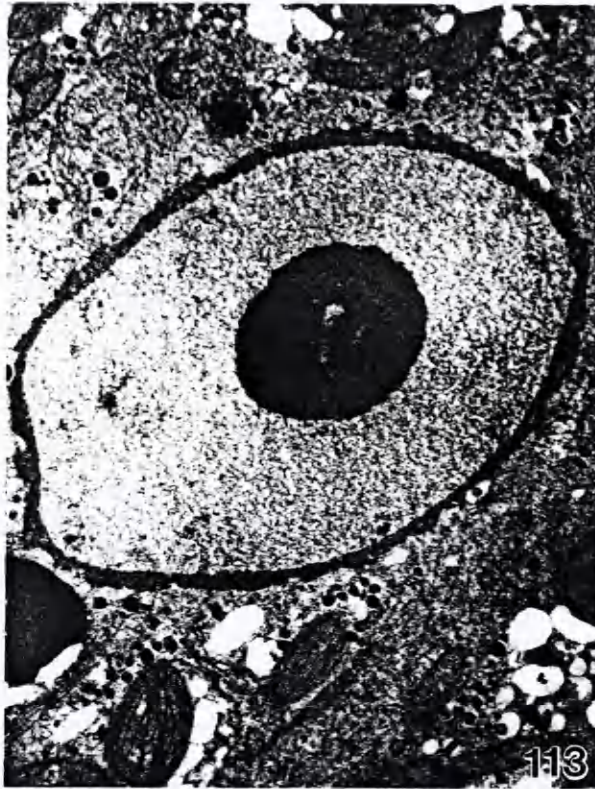
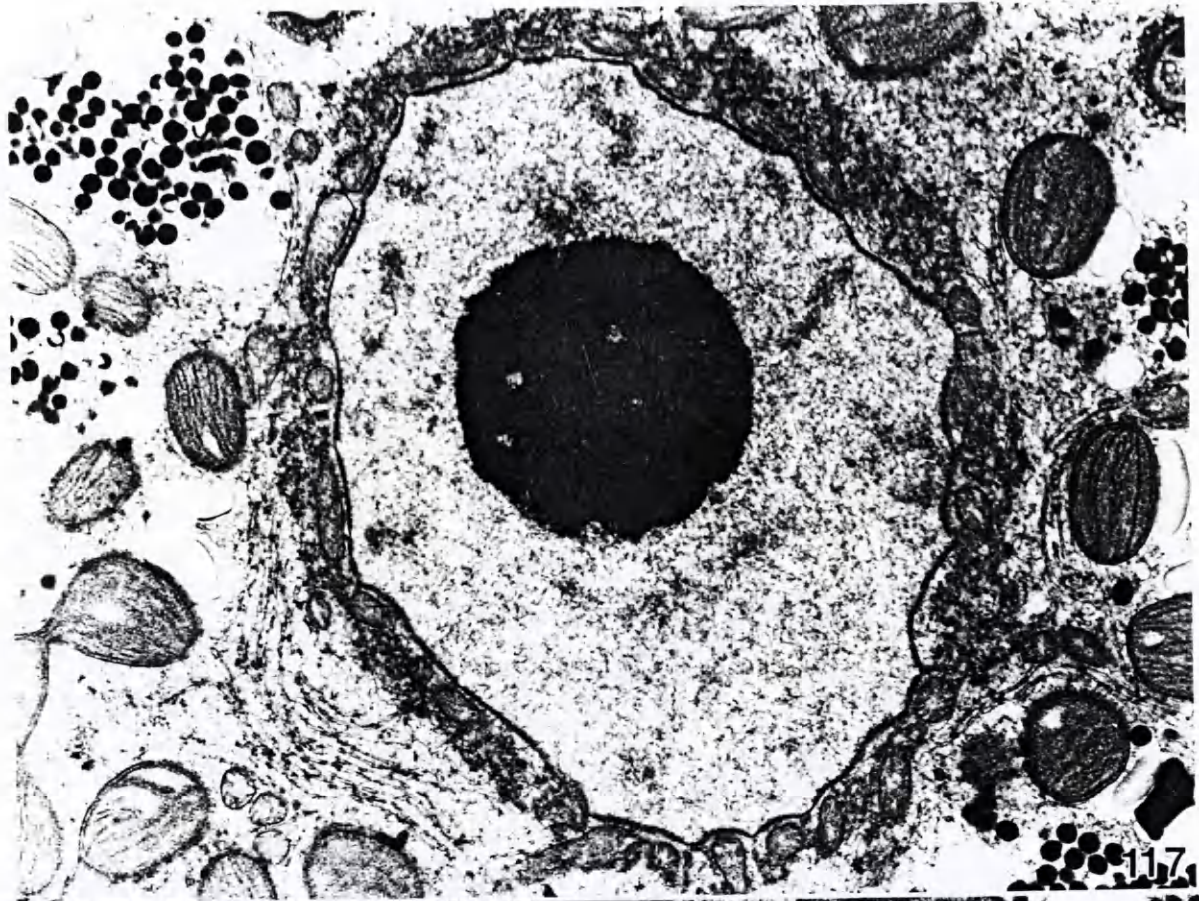
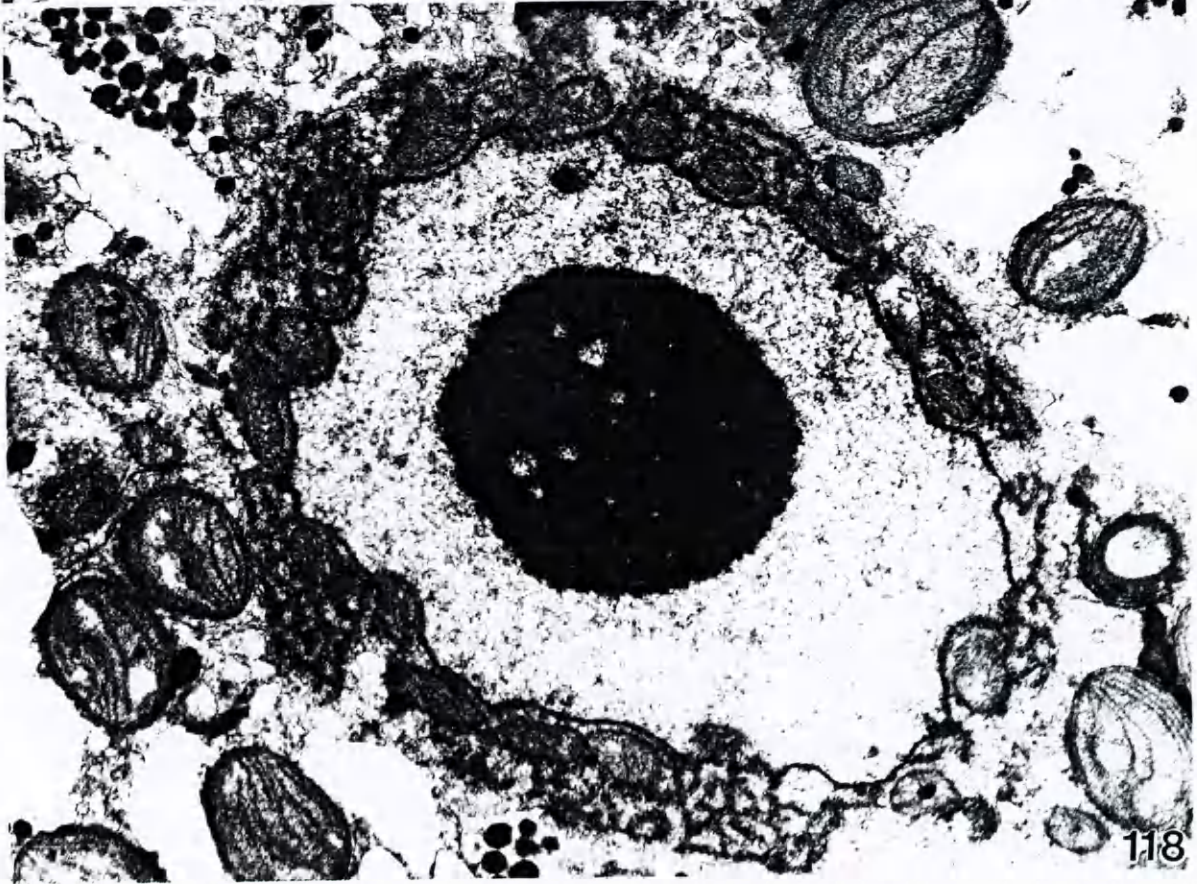


Figure 117. Calliarthron TS nucleus. Note mitochondrion-NE association and adjacent EDM-coated SM system. x 10,500.

Figure 118. Bossiella TS nucleus. Note similarity of PN EDM-coated SM and NE-mitochondrion organization to pattern seen in Calliarthron. x 17,200.



117



118

VITA**Christina Wilson**

Born in Wiesbaden, Germany, October 10, 1969. Graduated from Heidelberg American High School in Heidelberg, Germany, May 1987. Attended Bard College, in Annandale-on-Hudson, New York, on an Excellence and Equal Cost Scholarship. Awarded a Bachelor of Arts degree in Anthropology from Bard College in May 1991. Entered the graduate program in biology at the College of William and Mary in August 1991, where studies were supported with a teaching assistantship. Accepted to the University of Texas Graduate School of Biomedical Sciences at the Texas Medical Center in Houston, with a research assistantship, to pursue the Doctor of Philosophy degree in molecular microbiology, commencing Fall 1993.